SMALL SIGNAL ANALYSIS OF MICROGRID

A DISSERTATION

Submitted in partial fulfillment of the
requirements for the award of the degree
of

MASTER OF TECHNOLOGY
in
ELECTRICAL ENGINEERING
(with specialization in Power Systems)

By
AKSHAY BHARGAVA
(17529003)

DEPARTMENT OF ELECTRICAL ENGINEERING
INDIAN INSTITUTE OF TECHNOLOGY ROORKEE
ROORKEE – 247667 (INDIA)

MAY, 2019

CANDIDATE DECLARATION

I hereby certify that the work which is being presented in thesis report, entitled **"Small signal analysis of microgrid"** in partial fulfilment of the requirement for the award of the degree of **Masters Of Technology** with specialization in **"Power Systems Engineering",** submitted in **Electrical Department, Indian Institute of Technology Roorkee** is an authentic record of my own work carried out during the period from May 2018 to May 2019 under the supervision of **Dr. C.P Gupta, Associate Professor, Electrical Department, Indian Institute of Technology Roorkee India**.

The matter embodied in the dissertation report has not been submitted by me for the award of any other degree or diploma.

Dated: 21/05/2019

Place: ROORKEE

(AKSHAY BHARGAVA)

CERTIFICATE

This is to certify that the above statement made by the candidate is correct to the best of my knowledge.

Dr. C.P Gupta

Associate Professor

Electrical Department

Indian Institute of Technology

Roorkee-247667

ACKNOWLEDGEMENT

I would like to express my sincere and deep sense of gratitude and indebtedness to my supervisor **Dr. C.P Gupta, Associate Professor, Electrical Department, Indian Institute of Technology Roorkee** for guiding me to undertake this dissertation work as well as providing me all the necessary guidance and support throughout this work. He has displayed unique tolerance and understanding at every step of progress, without which this work would not have been in the present shape.

I would also be thankful to all the staff and research scholars of **Electrical Engineering Department** for their constant support and all my friends, for their help and encouragement.

Dated: 21/05/2019

AKSHAY BHARGAVA

17529003

M. Tech 2nd year

EE(PSE), IITR

TABLE OF CONTENTS

LIST OF FIGURES

CHAPTER-3

CHAPTER-4

CHAPTER-5

CHAPTER-6

LIST OF TABLES

CHAPTER-4

CHAPTER-5

ABSTRACT

The idea of microgrid is to integrate selected number of DGs with proper control strategy and loads and should have a PCC (point of common coupling) point for connection/disconnection with the grid. While connected to grid, it is called working under grid connected mode and the inverter operates in constant current mode or P/Q mode. Due to certain faults or interruptions PCC point is opened and microgrid function autonomously and hence it is referred as working under autonomous mode or islanded mode. In autonomous mode, microgrid operates in constant voltage control mode or V/f control mode.

In microgrid, selected number of distributed sources are operated in parallel to each other and interfaced via power electronic devices resulting into large number of power electronic devices, so their dynamic stability needs to be studied. Here the state space modelling of whole system is done which is used for stability analysis and designing of filters and droop gains and other major parameters. Moreover, control strategy is developed based on state space equation and simulation study is performed for verification of controller design in time domain.

This report presents systematic small signal modelling approach for grid connected mode as well as autonomous mode. DER (Distributed Energy Resource) unit is represented by a dc voltage source interfaced through power electronic devices for supplying suitable loads. Modelling is done for these elements and then control strategy is developed for proper regulation of output power in grid connected mode and regulation of voltage and frequency in autonomous mode. Each subsystem is modelled separately and then all are interfaced. All modelling and simulations are done in MATLAB. Eigen value analysis is done to observe states causing unstability and the range of their values for stable operation is determined and optimal design of LC filter, controller parameters and damping resistance is carried out. It is also shown that how fast responsive distributed energy sources can be, if interfaced with power electronic devices. Lastly, load sharing is done among DGs in autonomous mode.

LIST OF ABBREVATIONS

PCC	Point of Common Coupling
PLL	Phase Locked Loop
PI	Proportional Integrator
DG	Distributed Generation
DER	Distributed Energy Resource
MS	Microsources
KVL	Kirchhoff's Voltage Law
KCL	Kirchhoff's Current Law
P	Active power
Q	Reactive power
k_p	Proportional controller gain
k_i	Integral controller gain

CHAPTER – 1
INTRODUCTION

1.1 GENERAL

The need of reducing CO_2 emissions in electricity generation along with technological changes in this field are main factors contributing for interest in microgrid. Microgrid is a power system on small scale basis which is controllable in terms of power sharing to its loads, can be operating in grid feeding mode or grid forming mode. Distributed Generation (DGs) consist of small capacity generation units often termed as DG units, using mostly non-conventional energy resources. DGs are required due to environmental issues, limited transmission lines construction and capacity. These can supply electricity to remote areas, reduce greenhouse emissions, maintain peak loads and most importantly helps us in shifting from conventional sources. These DG units alongwith power electronic interface is termed as DER (Distributed Energy Resource) unit**[1]**.This power electronic setup improves power quality and provides fast response and many more as discussed in**[2]** but also has a drawback of low inertia, small oscillations and has to maintain stability. In microgrid, a large no of DGs are connected, in place of which if a large convention DG is connected then CO_2 emissions pose another problem apart from transmission network extension. But DGs are connected directly to distribution side which is a bidirectional network. DGs have several advantages for example they maintain reliable power supply due to small power output, impose less burden, reduce transmission losses as directly installed near customer locations and facilitate integration of renewables. However they have certain limitations **[3]** e.g. DGs have low inertia which can be enhanced by connecting batteries and capacitors on dc side.

Small generating units called microsources (MS) enhance the reliability of whole system and also lead to electricity business restructuring like investment reduction for future grid reinforcement and expansion. However, their power output very much depend on weather conditions so power electronic interface is a necessity. Therefore, control of inverter is main concern in operation of microgrid. Multiple inverters are connected to common ac system and need to operate in parallel. Microsources or DER operate at their max point and lack the inertia, so their small signal analysis is important as oscillations can occur**[4]** during their operation.

Microgrid has quite a large number of advantages **[5]** like integration of renewables, connection & disconnection from grid as and when required. The DG helps in supplying high priority loads

at grid failure times. In event of failure, apart from controlling voltage and frequency, power output of DGs is also regulated by droop equations**[6]**. Since microgrid can operate with or without support of grid, its viability is very high and DER units used does not have inertia like synchronous machine, so their analysis has an interesting side. Inverters used needed to have capacitor but those are ignored here. Such system can only be used in autonomous mode which means we can also observe dynamic response during black start operation meaning that initially synchronous generator is run and generate references for voltage and frequency, resulting which DER are connected one by one using grid connected controller and later switched to droop mode**[7]**.

In grid connected mode the magnitude and frequency of the microgrid terminal voltages are imposed by the grid whereas current controller is designed to provide constant current output during grid connected operation **[8**. The inverter AC output current is transformed into DC quantity in synchronous rotating frame by Park's transformation. The direct and quadrature components are compared with the reference quantities and the error signal is passed to the PI controller to generate the voltage references **[9]**. The inverter terminal voltage is considered as a disturbance and hence fed forward to compensate it. The inverter is fitted with a coupling impedance and possibly further passive filter elements to attenuate the switching frequency components of voltage and this inverter is phase locked through PLL. Inverters are sometimes modelled in a space-state formulation with the power devices in the inverter represented as ideal switches **[10]**. State space modelling is well explained in textbook **[11]**. A common simplification is to linearise the switching circuit by creating a small-signal model and to consider the average behaviour of the switched circuit over a period.

In standalone systems, entire power is supplied by inverters, no synchronous alternators are there and hence no reference for voltage and frequency is provided. For stable operation of microgrid we need to control P and Q which are decoupled, as P depend on power angle and Q on voltage magnitude. This dependency of P on load angle and of Q on voltage is expressed through the droop method**[12]**. Therefore both voltage and frequency are controlled in islanded mode but only voltage is controlled in grid connected mode due to negligible effect of frequency change. Therefore for the grid connected mode of operation of microgrid, voltage is local variable and frequency is a global variable. Furthermore, for removing harmonics and increasing damping LCL filter is designed **[13]**.

The dynamic model including power and control stages of every subsystem, usually leads to a large number of state variables, which is difficult to manage and can necessitate significant

redesign if the control scheme or microgrid configuration is modified. In this modelling approach, the first stage is to develop systematic models of each microgrid subsystem in its local d-q frame. Then, each model is schematically interfaced in a global d-frame. Under grid-connected mode, the global d-q frame frequency is imposed by the main grid but in isolated mode one DG is considered as reference and all other variables are converted to its frame. These variables includes the PLL, the abc–dq transformations, the controllers for current, voltage, power and any low-pass filters applied to feedback or control signals. A complete model should also include the control system associated with the converter circuit **[14]**.

This report represent model of three phase inverter alongwith its complete sub-models needed for interfacing in both grid connected mode and islanded mode. If a microgrid is islanding, then switching in control strategy should be studied **[15]**. The mathematical model of microgrid applicable in both the modes is formulated which helps in determining eigen values. Here small signal model of inverter is developed for designing control loop and analyse system stability using eigen value analysis. The mathematical model equations formed are linearized around an operating point and small signal state space model is formed. Stability margin of microgrid is found out by varying one of the filter parameters at a time and observing eigen values but in isolated mode droop gains are also varied. Higher droop gains result in proper sharing of power among DGs but they often lead to instability**[4].** In this report only resistive load is considered both locally and globally of a DG. Also the control strategy explained here can only be used if a microgrid is either in grid connected mode or in islanded mode from the start. For autonomous mode, where microgrid is first operating in grid connected mode and later switched to islanded, different control strategy or switch among proposed strategy needs to be studied. Since load is resistive so sharing is done by varying power frequency droop coefficient only and voltage- reactive power coefficient is kept constant. In chapter III, small signal model is made with chosen current and voltages as state variables. In chapter IV, control strategy is presented and frequency domain characteristic of system is analysed. In chapter V, simulation is done in time domain to verify the model and chosen strategy**[16]**. In chapter VI, load sharing is explained among DGs in autonomous mode.

1.2 EIGEN VALUE AND STABILITY OF MICROGRID

The fundamental property of a system which facilitate it to persist in the condition of stability and to recapture its original equilibrium point even after being exposed to any disturbances is System Stability. Operating conditions and configuration affect stability. Stability, conventionally is capability of power system to remain in synchronism but that's not entirely

true. Inertia of inverters used is very less and hence any small disturbance affect output to great extent. For determining stability of system, determination of eigen value is widely acceptable. Hence state space equations are formed and initial values are found out. When plotted in frequency domain the close loop poles will change their locations which may lead to oscillations. For stability analysis, we need to change a particular parameter while maintaining others as constant at their nominal values.

1.2.1Eigen value

Filter parameters and droop variables of individual inverters play an important role in deciding stability of the microgrid so we need to observe their variation for stability analysis. A state space model of microgrid is formed considering droop equations and droop gains. Eigen value is used to determine small signal stability, damping margin and sensitivity. Eigen value is traced after varying a parameter and it is observed whether system is moving towards unstability i.e. on RHS of complex plane and that point is obtained where it is crossing imaginary axes which is upper limit of parameter. Hence root locus is plotted by varying open loop gain observing its effect **[17]**. Therefore there is direct correlation between stability and parameter **[18]**. The time dependent characteristic of a mode corresponding to an eigen value λ is given by $e^{\lambda t}$. So stability of the system is determined as follows:

a) A real eigenvalue corresponds to a non-oscillatory mode.
b) A negative real eigenvalue represent decaying mode.
c) A positive real eigenvalue represent aperiodic instability.
d) Complex eigenvalue occur in conjugate pair and each corresponds to oscillatory mode and is of the form:

$$(a + jb)e^{(\sigma - j\omega)t} + (a - jb)e^{(\sigma + j\omega)t} \quad \textbf{(1.1)}$$

Where a and b are coefficients of complex equation, (1.1) further converts to (1.2).

$$e^{\sigma t}\sin(\omega t + \theta) \quad \textbf{(1.2)}$$

$$\lambda = \sigma + j\omega \quad \textbf{(1.3)}$$

The real component of eigen value (σ) gives damping and imaginary part (ω) gives oscillation frequency. The oscillation frequency is given by:

$$f = \frac{\omega}{2\pi} \quad \textbf{(1.4)}$$

The damping ratio is given by:

$$\xi = -\sigma/\sqrt{(\sigma^2 + \omega^2)} \quad \textbf{(1.5)}$$

So if eigen value is known then frequency of oscillation and damping ratio can be calculated.

1.2.2 Small Signal Stability

System's ability to maintain synchronism under small disturbances which occur due to small variation in load and generation is called small signal stability. These disturbances are sufficiently small for linearization of system equations for analysis purposes. The system is said to be stable about an operating point if subjected to small perturbation, it remains within small region around equilibrium point. Small signal stability in a microgrid is related to feedback controller and bandwidth of controller designed, continuous load switching, power limit of microsources. Therefore, if we only talk about stability of fundamental component of voltage and frequency, then we are not doing fair analysis and we need thorough research of small signal stability of microgrid. Small signal analysis can be done by varying load, step changes in load, varying droop parameters**[19]**.

Small signal analysis allows us to select control and system parameters through frequency domain analysis by knowing eigen values. If power system oscillations caused by small disturbances can be suppressed, such that the deviations of system state variables remain small for a long time, the power system is stable. Since it is inevitable that power system operation is subject to small disturbances, any power system that is unstable in terms of small-signal stability cannot operate in practice. Hence a power system that is able to operate normally must first be stable in terms of small-signal stability. Hence, one of the principal tasks in power system analysis is to carry out small-signal stability analysis to assess the power system under the specified operating conditions. Since microgrid comprises of large no of power electronic devices, hence their dynamic stability is more prominent. Through small signal analysis, we can know the response of system to a large no of parameter variations. Small signal analysis is done at an operating point and often investigate the interactions among several converters and also done for stability issues of whole system**[16]**.Small signal analysis also allows us to select control and system parameters through frequency domain analysis by knowing eigen values.

In this report, small signal model of VSI has been developed, control loop is designed and stability of system is studied. When the power system is subject to any such disturbance, state variables of the linearized system model vary over a very small range. Hence, asymptotic stability of the linearized system can guarantee a certain type of asymptotic stability of the actual nonlinear system**[20]**.

CHAPTER – 2
LITERATURE SURVEY

Yazdani [1] developed a control strategy for regulation of voltage and frequency in islanded mode. Unlike the conventional droop characteristics which depend on load configuration and characteristics, a new feedforward strategy is proposed where stability and performance of system does not largely depend on load.

Pogaku, Green and Prodanović [4] modelled and analysed isolated microgrid. In this work a control strategy has been established based on state space approach and each submodel has been modelled in state space form. Finally, all submodels are combined to give complete model of inverter and eigen values are found out. Futher, model reduction technique has also been done based on damping and sensitivity calculations. The switching states of inverter are neglected. The method of conversion from individual reference frame to common reference frame is shown clearly and droop equations are also defined so as to mimic the synchronous generator's governor characteristics. Through modelling of controllers, stability improvement has also been done and experimental verification of the same model has been done. Sensitive states are found out through calculations. It was stated that eigen values are subjected to change, if a parameter has been varied. Finally it was shown and verified experimentally, that low frequency modes are affected by parameters of power controller block and high frequency modes by inner loop and load dynamics.

Mueller and Kimball [21] introduced a method in which two inverters are working as DER and whole microgrid is in isolated mode. The controllers used has been designed in dq reference frame and non-linear equations are developed, which are further linearized around an operating point. LCL filter has also been designed and included in equations. The linearized equations are now used for forming state space equations from which eigen values are calculated. In addition, a unique model of forming voltage controller by comparing ω with ω_{PLL} has been developed. Conversion from local reference frame to global reference frame has clearly been specified. Assessment of developed model is done by comparing it with experimental results. The equations developed, clearly give eigen values which can be used for stability analysis, sensitivity calculations and for designing parameters of LCL filter and droop coefficients.

Leitner, Yazdanian, Sani and Muetze [22] analysed small signal model of isolated microgrid, using internal model based current and voltage controllers based approach. The proposed approach is compared with PI based current and voltage controller approach. Eigen values and sensitivity analysis has been done. Simulation has been done to point out that overshoots are less in case of IMC based approach and transient response is better in IMC based approach. It has been concluded that IMC based approach is more robust.

Pogaku, Prodanovic and Green [23] formulated state space equation alongwith necessary conversion from local to global reference frame. Taking all the network and line into consideration, overall model of microgrid has been developed. Stability parameters and trajectory of modes has been analysed. Furthermore, it has been shown that developed model can analyse operation in low and high frequency range.

Hassan and Abido [24] developed non-linear models of microgrid which are converted to linearized form and analysed. Through these analysis optimal design of LCL filter and controller parameters were found out. Additionally damping resistor was also included in study and by tracing locus of eigen values, power sharing coefficients were calculated. Operation of inverters in both the modes has clearly been explained in this alongwith function of each controller. Additionally, power electronic interface was quick enough for sudden changes in load has also been shown.

Katiraei, Iravani and Lehn [25] simulated a microgrid model having two DGs in autonomous mode, one being synchronous generator and other an inverter. Based on modelling, controllers were designed for both sources and their optimization for fast response and reliable system has been done. Frequency control was also explained in dq reference frame and frequency deviations were discussed in autonomous mode. Thereafter, small signal stability of whole system was analysed by linearizing developed equations. It was stated that fast response of electronically interfaced DG unit, can be used for frequency regulation and reactive power balancing.

M.A. Hassan and M.A. Abido [24] investigated microgrid in grid connected mode. Models of controllers namely power controller, current controller, PLL and LCL filter have been developed alongwith state space equations. The power controller gave reference value of inductor current which were passed through PI controllers for error minimization. Since PI controllers are used only for stationary systems, so a strategy was proposed where modelling is done in dq stationary frame. PLL generates a reference angle required for conversion from local rotating frame to global frame. The developed model also included current controller for

power quality improvement. Due to high switching frequency, the states were not affected by inverter action, so inverter was represented by voltage gain only. It has also been shown that filter designing plays a crucial role in deciding stability. With the step changes in load, inverter's performance was studies and observed.

N. Kroutikova, C.A. Hernandez-Aramburo and T.C. Green [26] developed models of inverter-interfaced DGs in grid connected mode. These individual models were combined and detailed analysis of whole system has been done. Stability of these inverters models was studied through eigen value analysis. State space equations of all individual models i.e. current controller, PLL, LCL filter, power controller were developed, clearly stating their state variables and inputs. Then state space equation of whole model was developed with the overall state space equation of system. The developed non-linear state space equation, then linearized around an operating point for analysis of eigen value. Finally, the developed system's response was analysed by the step change in the reference power and results were proposed.

F.katiraei, M.R. Iravani, P.W. Lehn [25] analysed eigen values through state space equation of developed overall model. Small signal analysis was done in dq0 frame with validation. Control strategy for various modes of operation of microgrid has been proposed. Linearized model was shown and eigen value plot was also analysed for validation of small signal model.

K. H. Ahmed, S. J. Finney, and B. W. Williams [27] investigated LCL filter design. Parameters were calculated by considering harmonics injection, resonant frequency and damping of the resonant effects. Formulation of PR controller in single phase inverter system analysis has also been done.

Tusar Kumar Dash and B. ChittiBabu [28] developed a model to linearize state space equation. Model for inverters has also been developed alongwith state space equations. These equations are linearized and whole system stability is analysed

Lasseter [29] defined the microgrid as an aggregation of loads and microsources operating like single system providing both power and heat.

Barnes [30] presented the microgrid concept to integrate large amounts of microgeneration without disrupting the operation of the utility network.

The Microgrid concept assumes a cluster of loads and microsources operating as a single controllable system that provides power. This concept provides a new paradigm for defining the operation of distributed generation. When the customers are too far from the main grid,

small power sources (typically diesel generators or renewable power sources) are used to produce the local needed energy. Generally, such small-scale electrical grid can operate isolated or interconnected with a main grid and is called microgrid (MG). It is mainly composed by one or several micro-sources, multiple loads and potential energy storage systems connected together **[20]**.Today there is much interest in microgrid due to the environment protection and energy sustainable development. B. Lasseter., first put forward a review of the microgrid example in 2001. Then CERTS (Consortium for Electric Reliability Technology Solutions) **[31]**and European Commission Project Micro grids respectively proposed the concept of microgrid. Now the concept of microgrid has been accepted in many organizations and laboratories **[32]**. In a typical microgrid, the microsources may be rotating generators or Distributed Energy Resources (DER) interfaced by power electronic inverters **[33]**. The installed DERs may be biomass, fuel cells, geothermal, solar, wind, steam or gas turbines and reciprocation internal combustion engines.

The real world microgrids are **American Microgrid**s (AEPCERTS, Mad River, BC Hydro Boston Bar, and GE Microgrid), **Asian Microgrids**(Shimizu's Microgrid, Hachinohe Project, Kyoto Eco-Energy Project, Aichi Project, Sendai Project, Hsinchiang in China), and **European Microgrids**(Kythnos, Labein Experimental Centre, EDP Feeder, CESI, Continuon Holiday Park, Demotec, MVV Energie Projects) **[34].**

CHAPTER – 3
MICROGRID

The idea of microgrid is to integrate selected number of DG with proper control strategy and loads having a PCC point for its connection/disconnection with the grid. A broadly cited definition, developed for the U.S. Department of Energy by the Microgrid Exchange Group, an ad hoc group of research and deployment experts, reads as follows:

‘‘A microgrid is a group of interconnected loads and distributed energy resources within clearly defined electrical boundaries that acts as a single controllable entity with respect to the grid. A microgrid can connect and disconnect from the grid to enable it to operate in both grid-connected or island mode **[35]**.”This description includes three requirements:

1) Local generation sources and loads.
2) It should control voltage and frequency.
3) It should have PCC point

IEEE Std 1547.4-2011 states microgrids as electric power systems (EPS) that:

(1) Include DR and load
(2) Include the ability to disconnect from and parallel with the area EPS
(3) Include the local EPS and may include portions of the area EPS

Microgrid is a subsystem of generation and its associated loads where a vast number of renewable sources are connected as main power source. However, each one is operated in parallel via power electronic devices having various controllers with each one having fix role**[16]**. In a typical microgrid, the microsources may be rotating generators or Distributed Energy Resources (DER) interfaced by power electronic inverters **[36]**. The installed DERs may be biomass, fuel cells, geothermal, solar, wind, steam or gas turbines and reciprocation internal combustion engines. DER unit is represented by a dc voltage source interfaced through power electronic devices for supplying suitable loads. Modelling is done for them and then control strategy is developed for regulation of voltage and frequency **[1]**.

3.1 MODES OF MICROGRID

Microgrids can be operated in both autonomous and grid-connected modes.

- When the grid is connected and the utility is fully functional, power flows to and fro.

- If, however, the utility experiences energy interruptions due to faults, with pre-planned switching, the microgrid disconnects from the grid and self-supplies its loads. These microgrids are in autonomous mode. Once the microgrid senses that the utility grid is stable, it reconnects to the utility.
- Some microgrids are in remote locations and not connected to the utility grid i.e. they do not have PCC connection and therefore, always operates under autonomous mode.

With interconnection of microgrid with main grid, microgrid operation is highly flexible, allowing it to operate freely in the grid-connected or islanded mode of operation. For the grid connected mode, each microgrid source can be operated like a current source with maximum power transferred to the grid. In grid connected mode, inverter operate in constant P/Q mode which has set-points maintained by grid which itself control voltage and frequency. However for islanded mode or autonomous mode, each microgrid operate as constant voltage source regulating frequency as grid is disconnected. Without a strong grid and a firm system voltage, each microgrid source must now regulate its own terminal voltage within an allowed range determined by its internally generated reference. The microsource thus appears like a controlled voltage source, whose output should rightfully share the load demand with the other sources. So far, this can only be met by the droop control method, where virtual inertia is intentionally added to each microsource.

3.2CONTROL OF MICROGRID

Micro-grid operating in the grid-connected mode, can separate itself from the main grid whenever a power quality event or malfunction occurs in the main grid and this mode is called islanded mode. After the malfunction is eliminated, the micro-grid is connected to the main grid again. Connection to main grid should be at such an instant, where voltage difference between terminal voltages of microgrid and main grid is 0. Grid connected mode of microgrid consist of PLL. LCL filter, current controller as shown in figure 3.1. In the grid-connected mode, P/Q control is adopted in the micro-grid **[38]**.

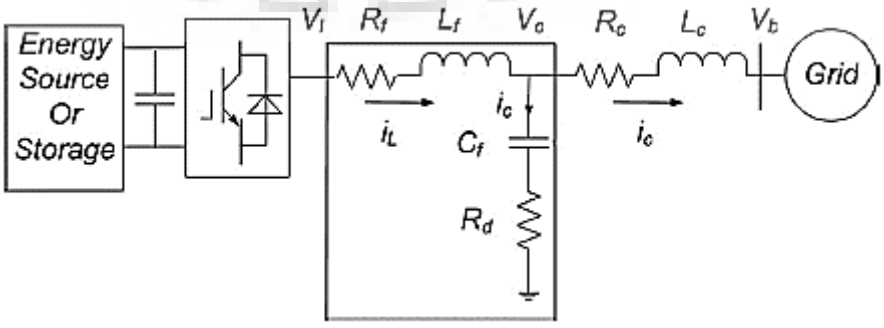

Figure 3. 1: Grid connected mode of microgrid

An inverter based isolated microgrid is shown in figure 3.2, consisting of PLL, LCL filter, current controller, voltage controller, power controller which are combined and shown in subsequent section.

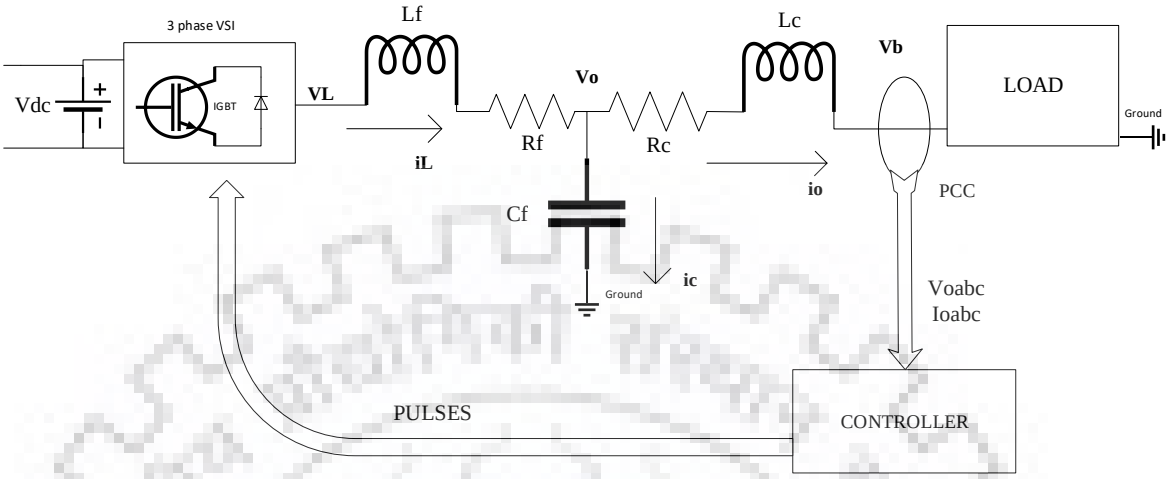

Figure 3. 2: Isolated mode of microgrid

Power electronic interface brings challenging issue and huge scale of possibilities as follows:

1) Allowing microsources to operate in islanded mode.
2) Provide high reliability and fast operation.
3) Incorporating "frequency droop" methods for proper load sharing between microsources in islanded mode.

So we need proper control of inverters and for that there are 2 types of control in microgrid:

1) P/Q control mode or constant current mode:
   In this mode, inverter is made to operate such that it delivers fix amount of P and Q to grid and no regulation in terms of voltage and frequency is required. This control is used in grid connected mode and power is delivered to grid. For delivering power to the grid, inverter voltage must in synchronism with grid voltage and frequency.
2) Voltage control mode or V/f control mode or P/V control mode:
   In this mode inverter operates with reference values of voltage and frequency. As load demand changes, so does voltage and frequency. This control is used in isolated mode of operation as P/Q control would fail, due to non-availability of P and Q references. During islanded mode, inverters need to control voltage and provide required active power which is done by power-frequency droop**[39]**.

3.2.1 Control Techniques for inverter:

The difference in control strategy in both modes lie in the available reference values. In grid connected mode, active power and reactive power reference values are available

($P_{ref}$and Q_{ref}) and other quantities like voltage and frequency are controlled by main-grid. Therefore, inverter need to supply required P and Q, and it is said to be operating in constant current mode. However in islanded mode, the microgrid has been disconnected, so voltage and frequency are no longer regulated by grid. In such case, reference values of voltage and frequency are to be provided, and inverter is operated in voltage control mode.

Modelling of grid connected mode is done by considering only one DG and based on developed model, multiple DGs can be connected. DG variables are converted to common reference frame and in this case PCC point or main grid is considered as common reference frame and all DGs are converted to this common frame. Similarly, in the islanded mode, modelling is done by considering single DG and inverter is modelled on its own reference frame. In later section, where multiple DG interfacing is done, conversion to common reference frame is done. The frequency of reference frame is decided by the power controller. In later section, models of voltage controller, current controller, LCL filter, loads are shown. Droop equation is also considered for power sharing among DGs. In the case of multiple DGs, for transformation to common reference frame, (3.1) is used where δ is defined as angle between d axis of local reference frame and global reference frame.

$$\delta = \int \omega - \omega_{ref} \qquad \textbf{(3.1)}$$

Inputs and outputs of an inverter are transformed to global reference frame. The output of an inverter is output currents (i_o) and input to inverter is the bus voltage (v_b). Also we need to make sure that reference inverter's change in frequency (Δω) needs to be supplied to other inverters and is termed as ($\Delta\omega_{com}$)**[40]**.

Now each inverter can be modelled into state space equation with 13 state variables, 3inputs (bus voltages in dq frame and common frame frequency) and 2 ouputs (output current in dq frame). Then whole microgrid model considering all the inverters is modelled in**[4]**. The power and current control loop has been implemented by using PI controllers in the d-q synchronous reference frame. AC quantities are converted in to DC synchronous reference frame by Parks Transformation, hence all reference quantities become DC in nature, so that simple PI controllers would be sufficient to yield zero steady state error. Moreover every block diagram is mentioned and state space equations are derived which combines to give state space model of whole system along with state space equations.

3.2.2 DROOP

To make inverter interfaced DG behave as synchronous generator, droop is used. In synchronous generator, if load is increased then it is compensated from mechanical power of

the rotor. Therefore, as power increases correspondingly frequency decreases and same relationship goes with voltage and reactive power. In figure 3.3, it can be seen that power is flowing through inductor as per current direction, induced voltage (E) should lead terminal voltage (V) by an angle δ.

Figure 3. 3: Phasor vectors of applied voltage and induced voltage

$$P = \frac{EV}{X}\sin\delta \tag{3.2}$$

$$Q = \frac{V^2}{X} - \frac{VE}{X}\cos\delta \tag{3.3}$$

From above equations we can see that P depends on δ, and Q on V which helps in developing droop equations. Hence, change in load directly affect f and changes in V directly affect Q on a generator. Droop characteristics states that as the load changes, generation should also change for proper sharing of power among multiple DGs.

a) VOLTAGE VS REACTIVE POWER DROOP:

Since voltage directly affects reactive power so it is controlled as depicted in figure 3.4. The relationship of V and Q is shown in (3.4), where d axis voltage is considered depending on reactive power and no unbalancing is considered, so q axis component is zero. If reference value of voltage is changed by a small amount then circulating currents are affected. This is main reason of using droop but it also serve the purpose of power sharing.

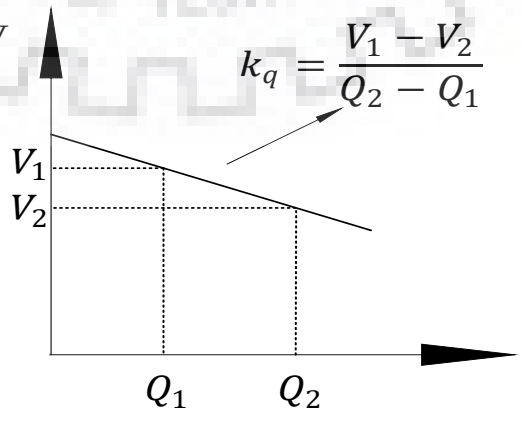

Figure 3. 4: Reactive power vs frequency droop

$$V_{od}{}^{*} = V_{od_{ref}} - k_q \quad \textbf{(3.4)}$$

$$V_{oq}{}^{*} = 0 \quad \textbf{(3.5)}$$

b) POWER VS FREQUENCY DROOP:

There is always a little error in selecting operating point, sometimes the error lies in frequency generation and sometimes in matching load requirements. Let us consider a grid connected having a load, supplied partly by grid and by microsources. Now microgrid goes into islanding and phase angle of voltage at microsources are changed alongwith reduction in frequency, leading to mismatch in generation and load. So we introduce droop where the drop in frequency results increase in active power so that inverter can provide its share of power as given by (3.6). This droop characteristic is shown in figure 3.5. Droop dampens the changes occurring due to load variation**[41]** and explained in **[5]**.

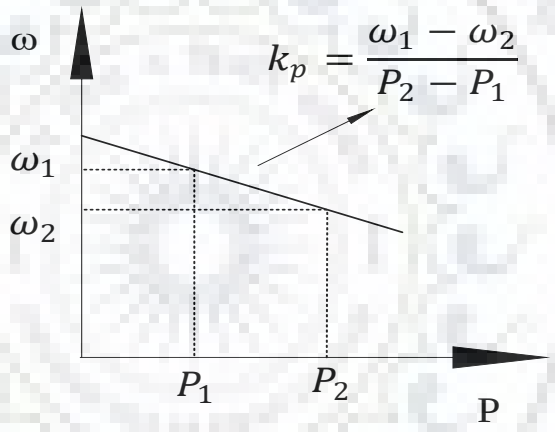

Figure 3. 5: Active power vs frequency droop

$$\omega = \omega_{ref} - k_p P \quad \textbf{(3.6)}$$

3.2.3 REFERENCE FRAME TRANSFORMATION

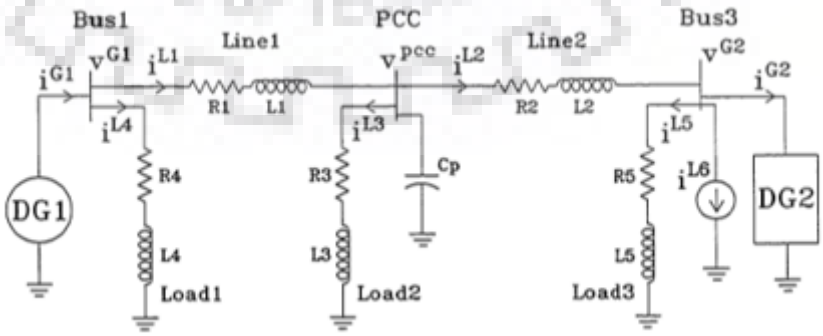

Figure 3. 6: Single-Line diagram of the microgrid used for small signal analysis

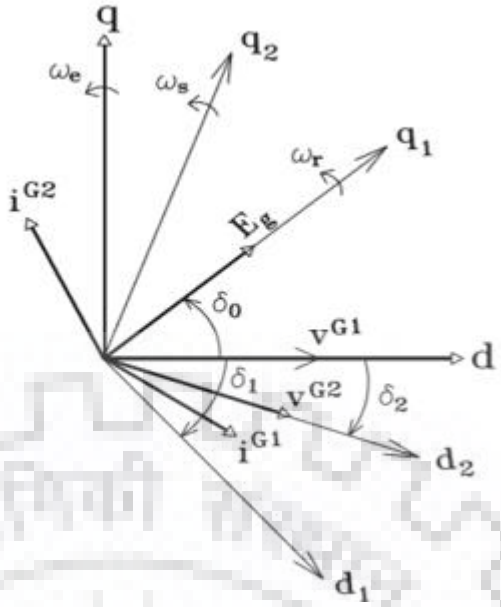

Figure 3. 7: Global and local rotating reference frames of the study

Let us consider the system shown in figure 3.6 having 2 DGs are there. Now both DGs have their d-q frame at certain angle from reference, DG-1 has transformation angle of δ_1 and DG-2 has angle of δ_2 as shown in figure 3.7. Assuming DG-1 as reference, d axis terminal voltage of DG-1 is forced to be align in direction of reference frame resulting in decoupling of dq quantities. D axis terminal voltage of DG-2 lies along d2 local frame and q axis along q2 frame. Let us assume local reference frame of DG1 rotates at speed ω_r. It is common standard that d axis align along applied voltage (V) and q axis along internal rotor voltage (E). The power angle of DG1 is δ_0, these are further described in**[42]**and shown through (3.7)-(3.8).

$$\delta_0 = \frac{\pi}{2} + \delta_1 \tag{3.7}$$

$$\omega_r = \frac{\partial \delta_1}{\partial u} \tag{3.8}$$

For further analysis each subsystem is transformed to dq reference frame.

$$X^g = T_n X^n \tag{3.9}$$

$$X^g = [X_d{}^g X_q{}^g] \tag{3.10}$$

X^n is any variable defined in dn-qn reference frame and X^g is reference frame and this conversion is shown in (3.9)-(3.11).

$$T_n = \begin{bmatrix} \cos\delta_n & \sin\delta_n \\ -\sin\delta_n & \cos\delta_n \end{bmatrix} \tag{3.11}$$

δ_n is the angle between d axis reference frame and d axis of dn local frame.

3.2.4 SMALL SIGNAL STABILITY ANALYSIS METHOD

With power electronically interfaced microgrid, most appropriate method of small signal stability is eigen value analysis but there are other methods like impedance analysis based models (load unbalance create problem and it is difficult to model it into dq frame), other non-linear analysis methods namely bifurcation theory and probabilistic analysis methods (require certain hypothesis and also consider uncertainties).

3.2.4.1 Eigen value analysis methods using state space modelling

State space model of whole system is developed and then system is linearized around an operating point which is a steady state point. Obtained small signal model is used for eigen value analysis. Linearization is done by applying taylor series to differential equations formed. After system is linearized and state space equations are formed **[16]** as shown in (3.12)-(3.15), where x is state variable, u is input to system.

$$\dot{x} = f(x(t), u(t), t) \tag{3.12}$$

$$\Delta\dot{x}(t) = \dot{x}_0 + \Delta\dot{x}(t) \tag{3.13}$$

$$\dot{x}(t) = f(x_0(t), u_0(t), t) + A\Delta x(t) + B\Delta u(t) \tag{3.14}$$

$$A = \frac{\partial f}{\partial x}\left(x_0(t), u_0(t)\right), B = \frac{\partial f}{\partial u}\left(x_0(t), u_0(t)\right) \tag{3.15}$$

$$\dot{x} = Ax + Bu \tag{3.16}$$

$$\dot{x} = Ax + B(u, v) + F(w) \tag{3.17}$$

$$sX(s) = AX(s) + BU(s) + F(W(s)) \tag{3.18}$$

State space equations and process of converting it into s domain for finding eigen values is shown through (3.16)-(3.18). Most of the development of models is done in in d-q axis frame**[17]**.

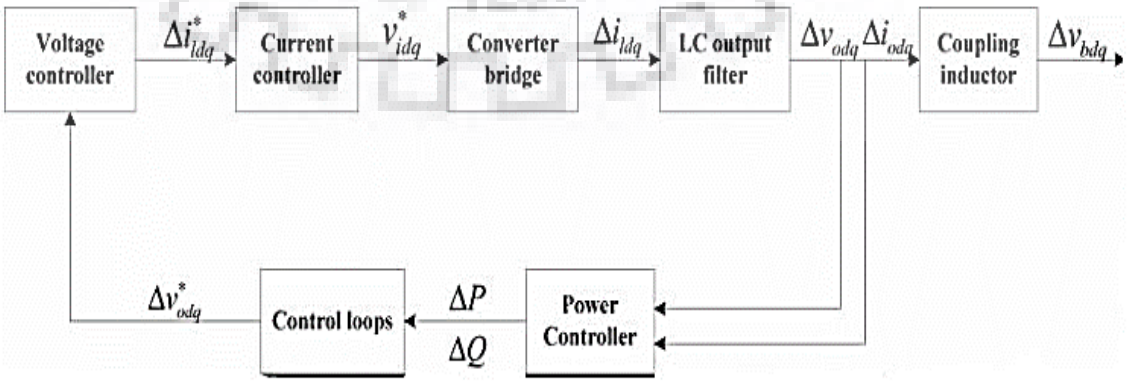

Figure 3. 8: Small signal model of inverter in isolated mode

In figure 3.8, P is real power, Q is reactive power, v_o is voltage at pcc point, v_o^* is output voltage reference, v_l^* is modulating voltage of inverter and v_b is bus voltage. Inverters are modelled in their own reference frame and their state space equations are found out. Each subsystem's equation is combined to form system's state space equation**.** In system where multiple inverters are there, each inverter is modelled in own reference frame but certain values like inputs and outputs are find out in common d-q reference frame.

3.2.4.2 Working of PLL

For decoupling and conversion to common reference frame, an angle of transformation is obtained from PLL. The PLL form adopted in this study is shown in figure 3.9. PLL will fix voltage such that v_q=0, and is said to be in locked state. It has VCO, integrator and phase detector. When angle after integrator equals that of VCO, that angle is noted and d axis voltage directly gives magnitude of voltage **[43]**. Input of PLL is PCC voltage in dq frame, with angle in feedback from output of PLL. PLL also measures frequency of system and lock the phase when Θ generated by oscillator approximates to $\hat{\Theta}$. The value of V_d will become V (magnitude of voltage) i.e. at the instant locking is done **[44]**. The state space equations are mentioned below:

$$\dot{\Phi}_{PLL} = V_{oq,f} \quad \textbf{(3.19)}$$

$$\dot{\theta} = \omega_{PLL} \quad \textbf{(3.20)}$$

$$\omega_{PLL} = k_{p,PLL} v_{oq,f} + k_{i,PLL} \Phi_{PLL} \quad \textbf{(3.21)}$$

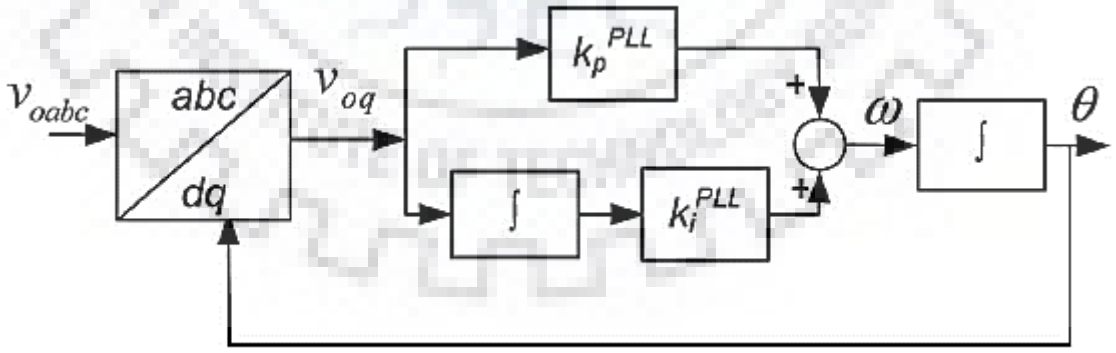

Figure 3. 9: PLL model

3.3 Controller blocks of both modes

3.3.1 Grid connected mode

In grid connected mode P_{ref} and Q_{ref} are available, so inverter needs to regulate its P and Q, and voltage and frequency are controlled by the grid and inverter is said to be operating in current control mode.

a) Current controller:

In grid connected mode the magnitude and frequency of the microgrid terminal voltages are imposed by the grid voltage. Current controller used in grid connected mode is essential for power quality improvement. LCL filter shown in figure 3.10, improves system response by increasing damping and filtering.

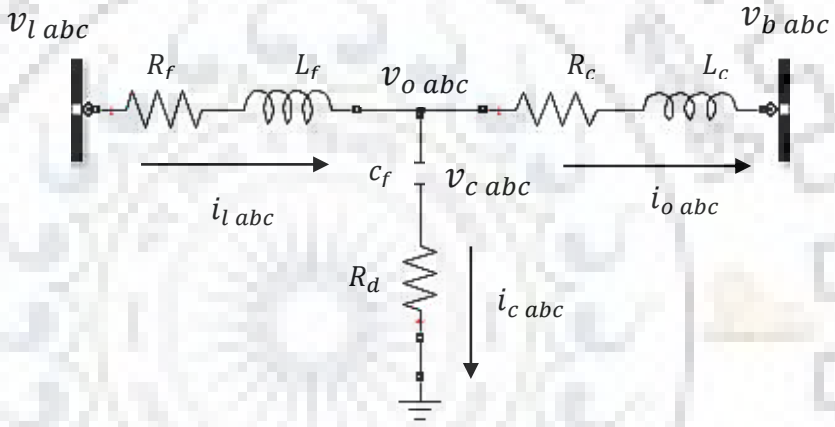

Figure 3. 10: LCL filter model

$$v_{l\,abc} = v_{0\,abc} + (j\omega L_f)i_{l\,abc} + (i_{l\,abc})r_f \quad \textbf{(3.22)}$$

The inverter AC output current is transformed in to DC quantity in synchronous rotating frame by Park's transformation. By applying KVL in figure 3.10, we get (3.22) and applying small signal (3.23)-(3.24) are developed.

$$v_{l\,dq} = v_{0\,dq} + (j\omega L_f)i_{l\,dq} + (i_{l\,dq})r_f + \Delta(i_{l\,dq}) \quad \textbf{(3.23)}$$

$$v_{ld} = v_{0d} + (\omega L_f)(ji_{ld}) + (i_{ld})r_f + \Delta(i_{ldref} - i_{ld}) \quad \textbf{(3.24)}$$

The direct and quadrature components are compared with the reference quantities and the error signal is passed to the PI controller to generate the voltage references **[24]**. The inverter terminal voltage is considered as a disturbance and hence fed forward to compensate it. This equation is converted into model as shown in figure 3.11.

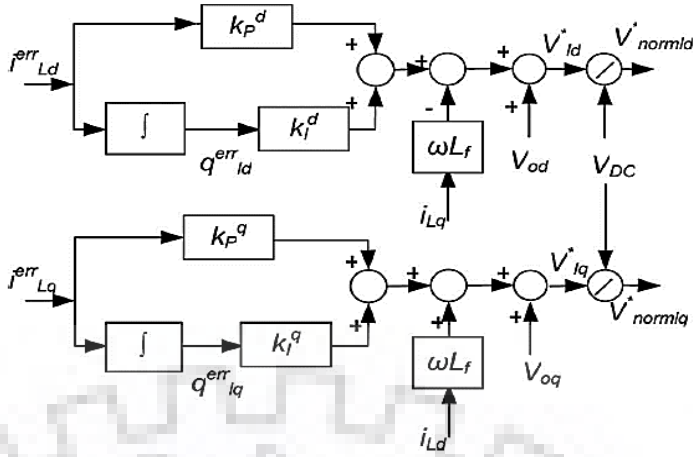

Figure 3. 11: Current controller in grid connected mode

The model in figure 3.12 is developed as per (3.25)-(3.26).

$$v_{ld}{}^{ref} = v_{od} - \omega L_f i_{lq} + (i_{ld}) r_f + K_p{}^{d,cc} i_{ld}{}^{err} + K_i{}^{d,cc} \int i_{ld}{}^{err}\, dt \quad \textbf{(3.25)}$$

$$v_{lq}{}^{ref} = v_{oq} + \omega L_f i_{ld} + (i_{lq}) r_f + K_p{}^{q,cc} i_{lq}{}^{err} + K_i{}^{q,cc} \int i_{lq}{}^{err}\, dt \quad \textbf{(3.26)}$$

ω is taken from PLL, charge on inductor is taken as state variable and is defined as $q_{dq}{}^{err}$ with equation shown in (3.27)-(3.29) so that state space equations can be derived.

$$q_{dq}{}^{err} = \int i_{l\,dq}{}^{err}\, dt \quad \textbf{(3.27)}$$

$$\dot{q_d}{}^{err} = i_{ld}{}^{err} \quad \textbf{(3.28)}$$

$$\dot{q_q}{}^{err} = i_{lq}{}^{err} \quad \textbf{(3.29)}$$

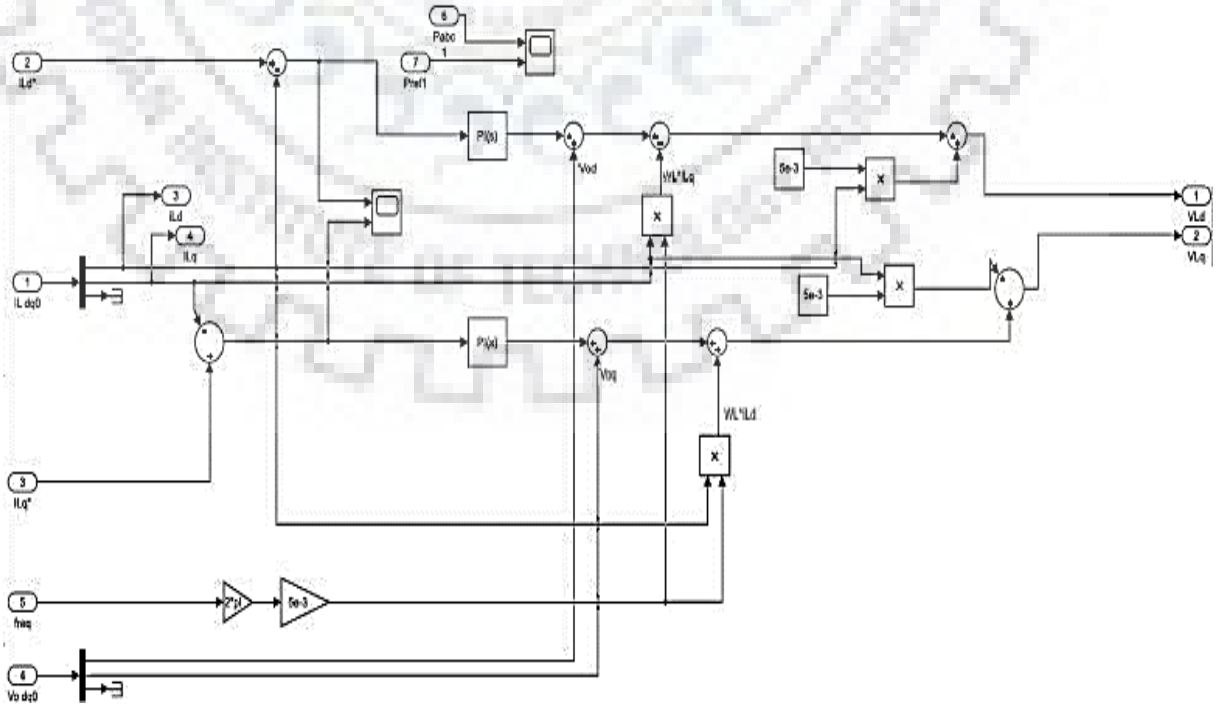

Figure 3. 12: Developed model of current controller in simulink

b) Power controller

The power controller is used to calculate current references in dq form, when active and reactive reference powers are fed as input. Power controller block is shown in figure 3.13 and the developed model is also shown in figure 3.14. The d-q axis output voltage and current measurements, used to calculate the instantaneous active power (p) and reactive power (q) generated by the inverter is shown through (3.30) and (3.31).

$$p = \frac{3}{2}\left(v_{od}i_{od} + v_{oq}i_{oq}\right) \quad \textbf{(3.30)}$$

$$q = \frac{3}{2}\left(v_{oq}i_{od} - v_{od}i_{oq}\right) \quad \textbf{(3.31)}$$

Instantaneous powers are then passed through low pass filters with the corner frequency $\omega_c$to obtain the filtered output power as shown in (3.32) and (3.33).

$$P = \frac{\omega_c}{s+\omega_c}p \quad \textbf{(3.32)}$$

$$Q = \frac{\omega_c}{s+\omega_c}q \quad \textbf{(3.33)}$$

Since $v_{oq} = 0$, (3.30) is now converted to (3.34) and (3.31) to (3.35).

$$P = \frac{3}{2}\left(v_{od}i_{od}\right) \quad \textbf{(3.34)}$$

$$Q = \frac{3}{2}\left(-v_{od}i_{oq}\right) \quad \textbf{(3.35)}$$

With the reference active power (P_{ref}) and reactive power (Q_{ref}), current reference values ($i_{d,ref}$) and ($i_{q,ref}$) are calculated, as shown in (3.36) and (3.37).

$$i_{d,ref} = \frac{2}{3}\left(P_{ref}/v_{od}\right) \quad \textbf{(3.36)}$$

$$i_{q,ref} = -\frac{2}{3}\left(Q_{ref}/v_{od}\right) \quad \textbf{(3.37)}$$

(3.38) can be derived from figure 3.10.

$$i_l = i_o + i_c \quad \textbf{(3.38)}$$

(3.38) can be converted to (3.39) which further can be modified to (3.40).

$$i_l^{\,*} = i_o^{\,*} + i_c^{\,*} \quad \textbf{(3.39)}$$

$$i_l^{\,\Sigma} = i_o^{\,*} + (i_l - i_o) \quad \textbf{(3.40)}$$

(3.40) denote reference values converted to d-q namely $i_d{}^{\Sigma}$ and $i_q{}^{\Sigma}$. In order to remove harmonics, it is passed through low pass filter of second order and is shown through (3.41) and (3.42). For better results butterworth filter of cut off frequency ω_c is used.

$$i_d{}^{\Sigma} = i_{od}{}^{*} + (i_{ld} - i_{od})$$

$$i_d{}^{\Sigma} = \frac{v_{od}{}^{*}P_{ref} - v_{oq}{}^{*}Q_{ref}}{v_{od}{}^{2} + v_{oq}{}^{2}} + (i_{ld} - i_{od})$$

$$i_q{}^{\Sigma} = i_{oq}{}^{*} + (i_{lq} - i_{oq})$$

$$i_q{}^{\Sigma} = \frac{v_{oq}{}^{*}P_{ref} + v_{od}{}^{*}Q_{ref}}{v_{od}{}^{2} + v_{oq}{}^{2}} + (i_{ld} - i_{od})$$

$$i_{ld}{}^{*} = \frac{\omega_c{}^{2}}{s^2 + \sqrt{2}s\omega_c + \omega_c{}^{2}} i_d{}^{\Sigma} \quad \textbf{(3.41)}$$

$$i_{lq}{}^{*} = \frac{\omega_c{}^{2}}{s^2 + \sqrt{2}s\omega_c + \omega_c{}^{2}} i_q{}^{\Sigma} \quad \textbf{(3.42)}$$

Solving (3.41) and (3.42), (3.43)-(3.46) can be formulated.

$$\dot{i_{ld}}{}^{*} = \omega_c{}^{2} q_{3d} - \omega_c\sqrt{2} i_{ld}{}^{*} \quad \textbf{(3.43)}$$

$$\dot{i_{lq}}{}^{*} = \omega_c{}^{2} q_{3q} - \omega_c\sqrt{2} i_{lq}{}^{*} \quad \textbf{(3.44)}$$

$$\dot{q_{3d}} = i_d{}^{\Sigma} - i_{ld}{}^{*} \quad \textbf{(3.45)}$$

$$\dot{q_{3q}} = i_q{}^{\Sigma} - i_{lq}{}^{*} \quad \textbf{(3.46)}$$

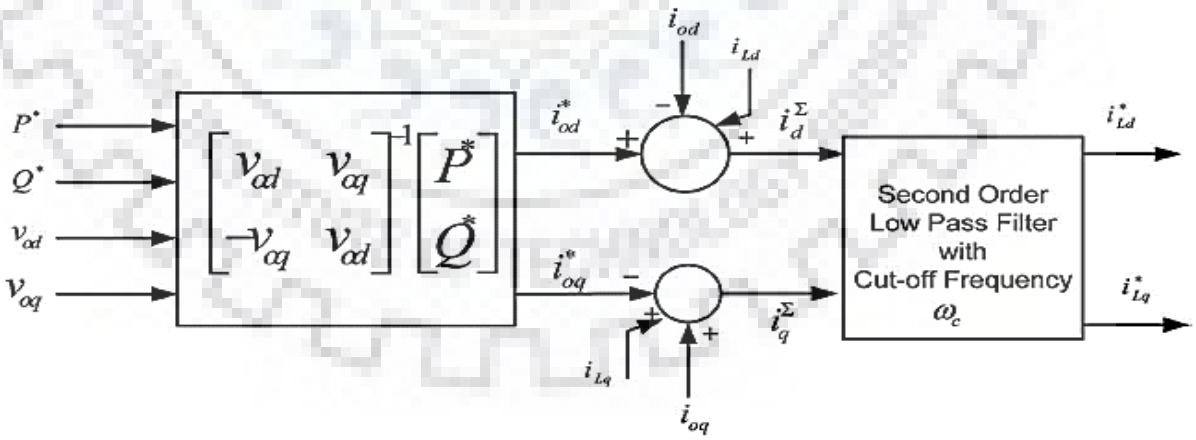

Figure 3. 13: Power controller block

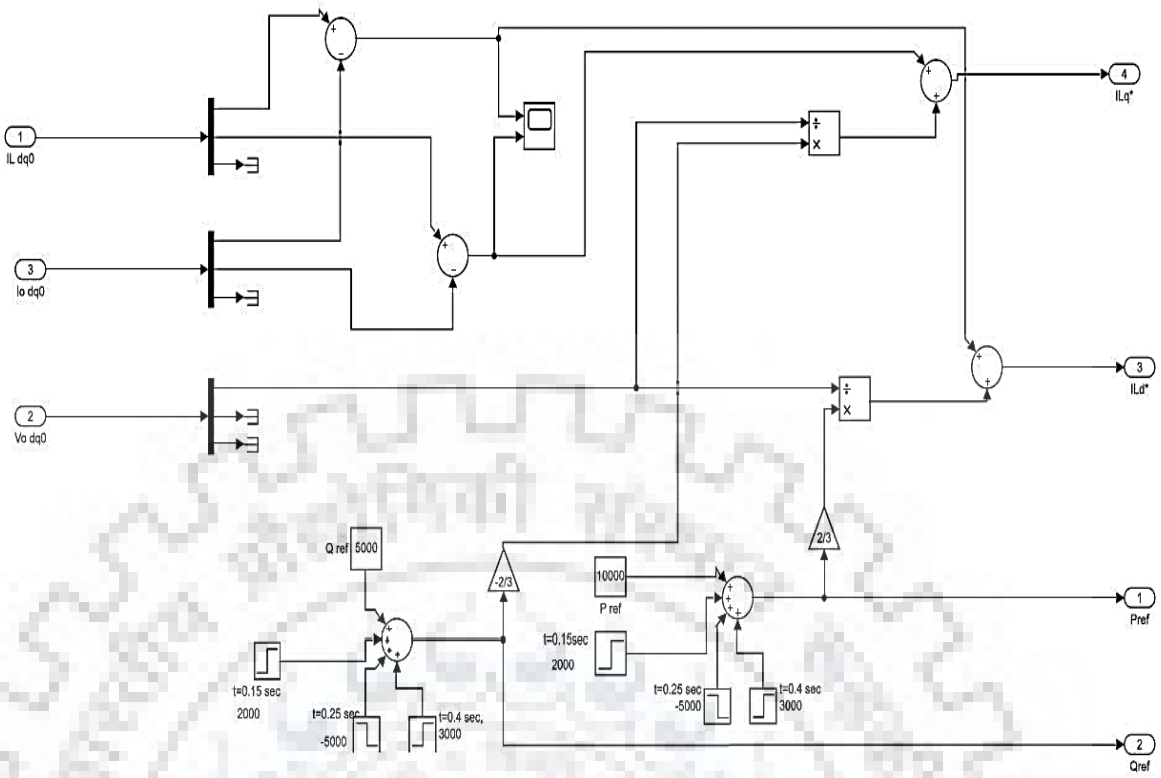

Figure 3. 14: Developed model of power controller block in Simulink

3.3.2 Islanded mode

In isolated mode, voltage and power controller are used to control voltage and frequency. Droop characteristics are incorporated in power controller for load sharing. Current controller is required to maintain flow of required amount of current.

a) Voltage controller:

With the given reference value of voltage, it is used to generate reference values for current controller. The error in voltage is passed through PI controller for reducing steady state error to zero. Feedforward and feedback signals are also used. LCL filter shown in figure 3.10, is used for developing (3.47).

$$i_{c_{abc}} = c_f \frac{\partial v_{o_{abc}}}{\partial t} \tag{3.47}$$

Converting (3.47) in dq frame by multiplying both sides by T_{dq0} and it convert to (3.48)

$$T_{dq0} * (i_{c_{abc}}) = T_{dq0} * (c_f \frac{\partial v_{o_{abc}}}{\partial t})$$

$$i_{c_{dq0}} = T_{dq0} * (c_f \frac{\partial}{\partial t}\left\{{T_{dq0}}^{-1} v_{0_{dq0}}\right\}) \tag{3.48}$$

Further solving (3.48) by variable separation method of integration we get (3.49)

$$i_{c_{dq0}} = T_{dq0} * \left(c_f {T_{dq0}}^{-1} \frac{\partial}{\partial t}\left\{v_{0_{dq0}}\right\}\right) + T_{dq0} * \left(c_f v_{0_{dq0}} \frac{\partial}{\partial t}\left\{{T_{dq0}}^{-1}\right\}\right)$$

$$i_{c_{dq0}} = T_{dq0} * \left(c_f {T_{dq0}}^{-1} \frac{\partial}{\partial t}\left\{v_{0_{dq0}}\right\}\right) + \left(c_f v_{0_{dq0}} T_{dq0} \frac{\partial}{\partial t}\left\{{T_{dq0}}^{-1}\right\}\right) \quad \textbf{(3.49)}$$

Now simplifying (3.49) we get (3.50)

$$i_{c_{dq0}} = \left(c_f \frac{\partial}{\partial t}\left\{v_{0_{dq0}}\right\}\right) + \left(c_f v_{0_{dq0}} * (-\omega) \begin{bmatrix} 0 & 1 & 0 \\ -1 & 0 & 0 \\ 0 & 0 & 0 \end{bmatrix}\right) \quad \textbf{(3.50)}$$

$v_{o_{dq0}}$ is constant as voltage controller will regulate voltage, so under its operation voltage remain same. Also $v_{o_d} = rated\ voltage$ and$v_{o_d} = 0$ and with this (3.50) converges to (3.51).

$$i_{c_{dq0}} = 0 + \left(c_f \begin{bmatrix} v_{od} \\ v_{oq} \\ v_{o0} \end{bmatrix} * (-\omega) \begin{bmatrix} 0 & 1 & 0 \\ -1 & 0 & 0 \\ 0 & 0 & 0 \end{bmatrix}\right)$$

Now we have assumed balanced load, so zero component of v_o is zero and with this (3.50) converts to (3.51)

$$i_{c_{dq}} = \left(c_f \begin{bmatrix} v_{od} \\ v_{oq} \end{bmatrix} * (-\omega) \begin{bmatrix} 0 & -1 \\ 1 & 0 \end{bmatrix}\right)$$

$$i_{c_{dq}} = \left(c_f * (-\omega) \begin{bmatrix} -v_{oq} \\ v_{od} \end{bmatrix}\right)$$

$$i_{c_{dq}} = \begin{bmatrix} -\omega C_f v_{oq} \\ \omega C_f v_{od} \end{bmatrix} \quad \textbf{(3.51)}$$

Further from Fig. 3.10, (3.52) can be deduced

$$i_l = i_o + i_c \quad \textbf{(3.52)}$$

Now applying small signal on (3.51) and (3.52) we get (3.53) and (3.54) respectively.

$$\Delta i_{l_{dq}} = \Delta i_{o_{dq}} + \Delta i_{c_{dq}} + error_{dq} \quad \textbf{(3.53)}$$

$$\Delta i_{c_{dq}} = \begin{bmatrix} -\omega C_{f\Delta} v_{oq} \\ \omega C_f \Delta v_{od} \end{bmatrix} \quad \textbf{(3.54)}$$

For small signal model, we need a small signal called as disturbance or error from which system stability can be analysed. This small signal modify equation as shown in (3.53). The value of this error is given in (3.55)-(3.58).

$$error\ in\ d\ axis = \Delta v_{od}{}^{*} - \Delta v_{od} = \frac{\partial \Delta \varphi_d}{\partial t} \quad \textbf{(3.55)}$$

$$\frac{1}{s}(\Delta v_{od}{}^{*} - \Delta v_{od}) = \frac{1}{s}\left(\frac{\partial \Delta \varphi_d}{\partial t}\right) = \Delta \varphi_d \quad \textbf{(3.56)}$$

$$error\ in\ q\ axis = \Delta v_{oq}{}^{*} - \Delta v_{oq} = \frac{\partial \Delta \varphi_q}{\partial t} \quad \textbf{(3.57)}$$

$$\frac{1}{s}(\Delta v_{oq}{}^{*} - \Delta v_{oq}) = \frac{1}{s}\left(\frac{\partial \Delta \varphi_q}{\partial t}\right) = \Delta \varphi_q \quad \textbf{(3.58)}$$

Rewriting (3.53) after applying small signal and using (3.55)-(3.58) we get (3.59)

$$\Delta i_{ldq}{}^{*} = \Delta i_{o\,dq} + \Delta i_{c\,dq} + error_{dq} \quad \textbf{(3.59)}$$

Further, a feedforward term (F) has been added to $i_{o\,dq}$ for stability reasons and the error now developed, has been passed to PI controllers. So applying all of this we obtain (3.60).

$$\Delta i_{ldq}{}^{*} = F\Delta i_{o\,dq} + \begin{bmatrix} -\omega C_{f\Delta} v_{oq} \\ \omega C_f \Delta v_{od} \end{bmatrix} + (k_{pv} + \frac{k_{iv}}{s}) * \begin{bmatrix} \Delta v_{od}{}^{*} - \Delta v_{od} \\ \Delta v_{oq}{}^{*} - \Delta v_{oq} \end{bmatrix} \quad \textbf{(3.60)}$$

$$\begin{bmatrix} \Delta i_{ld}{}^{*} \\ \Delta i_{lq}{}^{*} \end{bmatrix} = F \begin{bmatrix} \Delta i_{od} \\ \Delta i_{oq} \end{bmatrix} + \begin{bmatrix} -\omega C_{f\Delta} v_{oq} \\ \omega C_f \Delta v_{od} \end{bmatrix} + (k_{pv} + \frac{k_{iv}}{s}) * \begin{bmatrix} \Delta v_{od}{}^{*} - \Delta v_{od} \\ \Delta v_{oq}{}^{*} - \Delta v_{oq} \end{bmatrix} \quad \textbf{(3.61)}$$

$$\begin{bmatrix} \Delta i_{ld}{}^{*} \\ \Delta i_{lq}{}^{*} \end{bmatrix} = F \begin{bmatrix} \Delta i_{od} \\ \Delta i_{oq} \end{bmatrix} + \begin{bmatrix} -\omega C_{f\Delta} v_{oq} \\ \omega C_f \Delta v_{od} \end{bmatrix} + \begin{bmatrix} k_{pv_d} \\ k_{pv_q} \end{bmatrix} \begin{bmatrix} \Delta v_{od}{}^{*} - \Delta v_{od} \\ \Delta v_{oq}{}^{*} - \Delta v_{oq} \end{bmatrix} + \begin{bmatrix} k_{iv_d} \\ k_{iv_q} \end{bmatrix} \begin{bmatrix} \Delta \varphi_d \\ \Delta \varphi_q \end{bmatrix} \quad \textbf{(3.62)}$$

Using (3.56) and (3.58) alongwith (3.62) we get (3.63) and (3.64)

$$\begin{bmatrix} \Delta i_{ld}{}^{*} \\ \Delta i_{lq}{}^{*} \end{bmatrix} = \begin{bmatrix} \mathrm{F}\Delta i_{od} - \omega C_{f\Delta} v_{oq} + k_{pv_d} \Delta v_{od}{}^{*} - k_{pv_d} \Delta v_{od} + k_{iv_d} \Delta \varphi_d \\ \mathrm{F}\Delta i_{oq} + \omega C_{f\Delta} v_{od} + k_{pv_q} \Delta v_{oq}{}^{*} - k_{pv_q} \Delta v_{oq} + k_{iv_q} \Delta \varphi_q \end{bmatrix} \quad \textbf{(3.63)}$$

$$\begin{bmatrix} \Delta \dot{\varphi}_d \\ \Delta \dot{\varphi}_q \end{bmatrix} = \begin{bmatrix} \Delta v_{od}{}^{*} - \Delta v_{od} \\ \Delta v_{oq}{}^{*} - \Delta v_{oq} \end{bmatrix} \quad \textbf{(3.64)}$$

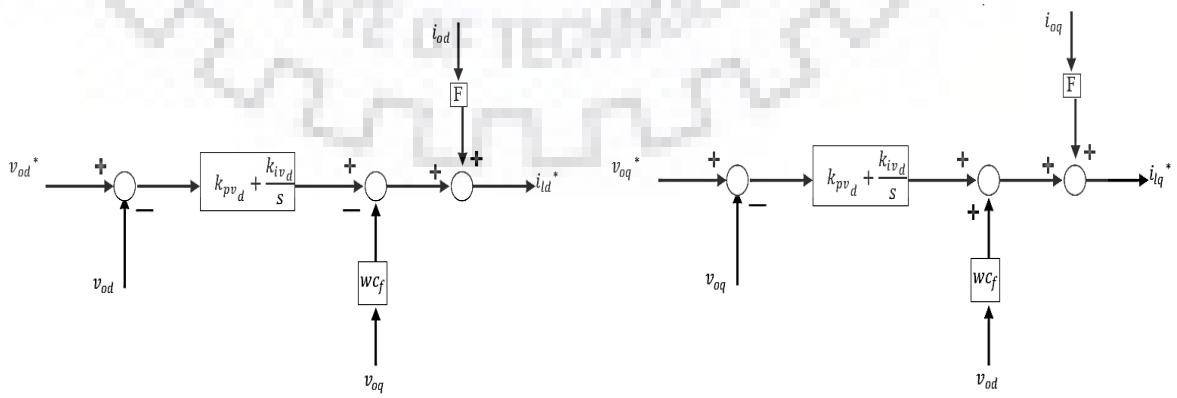

Figure 3. 15: Small signal model of voltage controller for autonomous mode in d-q frame

Voltage controller model has been shown in figure 3.15 based on developed equation. Voltage controller model has been developed in Simulink, shown in figure 3.16.

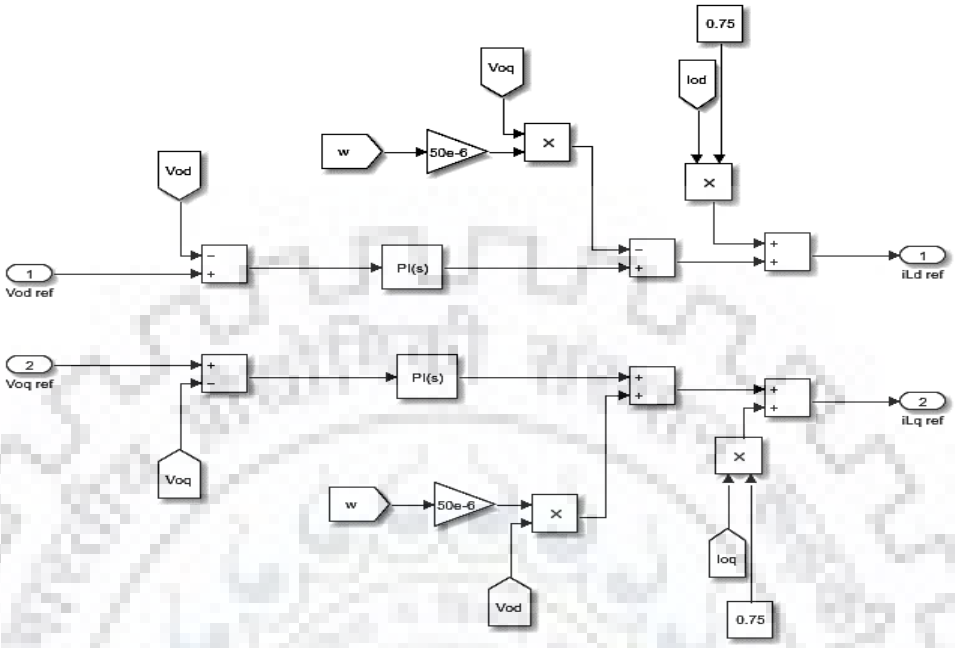

Figure 3. 16: Developed model of voltage controller for autonomous mode in Simulink

b) Current control:

Current controller is used to achieve required current in system in order to match load. It also houses PI controller for reduction in error. In case of isolated mode, feedforward signal is not used as PI is not available in next stage for error reduction. It also generate voltage references used in PWM. Moreover current controller used in isolated mode, is essential for power quality improvement. Applying KVL equation on Fig. 3.10, (3.65) is obtained which is used for current controller design.

$$\begin{bmatrix} v_{l_d} \\ v_{l_q} \\ v_{l_0} \end{bmatrix} = \begin{bmatrix} i_{l_a} * r_f \\ i_{l_b} * r_f \\ i_{l_c} * r_f \end{bmatrix} + L_f \frac{d}{dt} \begin{bmatrix} i_{la} \\ i_{lb} \\ i_{lc} \end{bmatrix} + \begin{bmatrix} v_{o_d} \\ v_{o_q} \\ v_{o_0} \end{bmatrix} \quad \textbf{(3.65)}$$

Multiplying both sides by T_{dq0} for conversion from abc to dq0 frame we get (3.66)-(3.68).

$$T_{dq0} * \begin{bmatrix} v_{l_a} \\ v_{l_b} \\ v_{l_c} \end{bmatrix} = T_{dq0} \begin{bmatrix} i_{l_a} * r_f \\ i_{l_b} * r_f \\ i_{l_c} * r_f \end{bmatrix} + T_{dq0} * L_f \frac{d}{dt} \begin{bmatrix} i_{la} \\ i_{lb} \\ i_{lc} \end{bmatrix} + T_{dq0} \begin{bmatrix} v_{o_a} \\ v_{o_b} \\ v_{o_c} \end{bmatrix} \quad \textbf{(3.66)}$$

$$\begin{bmatrix} v_{l_d} \\ v_{l_q} \\ v_{l_0} \end{bmatrix} = \begin{bmatrix} i_{l_d} * r_f \\ i_{l_q} * r_f \\ i_{l_0} * r_f \end{bmatrix} + T_{dq0} * L_f \frac{d}{dt} \left\{ {T_{dq0}}^{-1} \begin{bmatrix} i_{l_d} \\ i_{l_q} \\ i_{l_0} \end{bmatrix} \right\} + \begin{bmatrix} v_{o_d} \\ v_{o_q} \\ v_{o_0} \end{bmatrix} \quad \textbf{(3.67)}$$

$$\begin{bmatrix} v_{l_d} \\ v_{l_q} \\ v_{l_0} \end{bmatrix} = \begin{bmatrix} i_{l_d} * r_f \\ i_{l_q} * r_f \\ i_{l_0} * r_f \end{bmatrix} + T_{dq0} * L_f * {T_{dq0}}^{-1} \frac{d}{dt} \begin{bmatrix} i_{l_d} \\ i_{l_q} \\ i_{l_0} \end{bmatrix} + T_{dq0} * L_f \begin{bmatrix} i_{l_d} \\ i_{l_q} \\ i_{l_0} \end{bmatrix} \frac{d}{dt} ({T_{dq0}}^{-1}) + \begin{bmatrix} v_{o_d} \\ v_{o_q} \\ v_{o_0} \end{bmatrix}$$

$$\begin{bmatrix} v_{l_d} \\ v_{l_q} \\ v_{l_0} \end{bmatrix} = \begin{bmatrix} i_{l_d} * r_f \\ i_{l_q} * r_f \\ i_{l_0} * r_f \end{bmatrix} + \frac{d}{dt} \begin{bmatrix} i_{l_d} \\ i_{l_q} \\ i_{l_0} \end{bmatrix} + L_f \begin{bmatrix} i_{l_d} \\ i_{l_q} \\ i_{l_0} \end{bmatrix} T_{dq0} * \frac{d}{dt} ({T_{dq0}}^{-1}) + \begin{bmatrix} v_{o_d} \\ v_{o_q} \\ v_{o_0} \end{bmatrix} \quad \textbf{(3.68)}$$

Now current controller helps in maintaining constant current, so $i_{l_{dq0}}$ is constant and hence its differentiation is zero. After simplifying (3.68), (3.69) can be deduced.

$$\begin{bmatrix} v_{l_d} \\ v_{l_q} \\ v_{l_0} \end{bmatrix} = \begin{bmatrix} i_{l_d} * r_f \\ i_{l_q} * r_f \\ i_{l_0} * r_f \end{bmatrix} + L_f \begin{bmatrix} i_{l_d} \\ i_{l_q} \\ i_{l_0} \end{bmatrix} * (-\omega) \begin{bmatrix} 0 & 1 & 0 \\ -1 & 0 & 0 \\ 0 & 0 & 0 \end{bmatrix} + \begin{bmatrix} v_{o_d} \\ v_{o_q} \\ v_{o_0} \end{bmatrix} \quad \textbf{(3.69)}$$

Load is assumed to be balanced, so zero component is neglected. Further on applying small signal analysis (3.70) and (3.71) are deduced.

$$\begin{bmatrix} \Delta {v_{l_d}}^* \\ \Delta {v_{l_q}}^* \end{bmatrix} = \begin{bmatrix} i_{l_d} * r_f \\ i_{l_q} * r_f \end{bmatrix} + L_f \begin{bmatrix} i_{l_d} \\ i_{l_q} \end{bmatrix} * \begin{bmatrix} 0 & -\omega \\ \omega & 0 \end{bmatrix} + \begin{bmatrix} v_{o_d} \\ v_{o_q} \end{bmatrix} \quad \textbf{(3.70)}$$

$$\begin{bmatrix} \Delta {v_{l_d}}^* \\ \Delta {v_{l_q}}^* \end{bmatrix} = \begin{bmatrix} \Delta i_{l_d} * r_f \\ \Delta i_{l_q} * r_f \end{bmatrix} + L_f \begin{bmatrix} \Delta i_{l_d} \\ \Delta i_{l_q} \end{bmatrix} * \begin{bmatrix} 0 & -\omega \\ \omega & 0 \end{bmatrix} + \begin{bmatrix} \Delta v_{o_d} \\ \Delta v_{o_q} \end{bmatrix} + error_{dq} \quad \textbf{(3.71)}$$

Now error in d frame and q frame are expressed in (3.72)-(3.75).

$$error\ in\ d\ axis = \Delta {i_{ld}}^* - \Delta i_{ld} = \frac{\partial \Delta Y_d}{\partial t} \quad \textbf{(3.72)}$$

$$\frac{1}{s} (\Delta {i_{ld}}^* - \Delta i_{ld}) = \Delta Y_d \quad \textbf{(3.73)}$$

$$error\ in\ q\ axis = \Delta {i_{lq}}^* - \Delta i_{lq} = \frac{\partial \Delta Y_q}{\partial t} \quad \textbf{(3.74)}$$

$$\frac{1}{s} \left(\Delta {i_{lq}}^* - \Delta i_{lq}\right) = \Delta Y_q \quad \textbf{(3.75)}$$

Error is now passed through PI controller and equation is changed as shown below.

$$\begin{bmatrix} \Delta {v_{l_d}}^* \\ \Delta {v_{l_q}}^* \end{bmatrix} = \begin{bmatrix} \Delta i_{l_d} * r_f \\ \Delta i_{l_q} * r_f \end{bmatrix} + L_f \begin{bmatrix} \Delta i_{l_d} \\ \Delta i_{l_q} \end{bmatrix} * \begin{bmatrix} 0 & -\omega \\ \omega & 0 \end{bmatrix} + \begin{bmatrix} \Delta v_{o_d} \\ \Delta v_{o_q} \end{bmatrix} + (k_{pv_{dq}} + \frac{k_{iv_{dq}}}{s}) * \begin{bmatrix} \Delta {i_{ld}}^* - \Delta i_{ld} \\ \Delta {i_{lq}}^* - \Delta i_{lq} \end{bmatrix}$$

$$\begin{bmatrix} \Delta {v_{l_d}}^* \\ \Delta {v_{l_q}}^* \end{bmatrix} = \begin{bmatrix} \Delta i_{l_d} * r_f \\ \Delta i_{l_q} * r_f \end{bmatrix} + L_f \begin{bmatrix} \Delta i_{l_d} \\ \Delta i_{l_q} \end{bmatrix} * \begin{bmatrix} 0 & -\omega \\ \omega & 0 \end{bmatrix} + \begin{bmatrix} \Delta v_{o_d} \\ \Delta v_{o_q} \end{bmatrix} + (k_{pv_{dq}} + \frac{k_{iv_{dq}}}{s}) * \begin{bmatrix} \Delta {i_{ld}}^* - \Delta i_{ld} \\ \Delta {i_{lq}}^* - \Delta i_{lq} \end{bmatrix}$$

$$\begin{bmatrix}\Delta \mathrm{v}_{\mathrm{l}_d}{}^* \\ \Delta \mathrm{v}_{\mathrm{l}_q}{}^*\end{bmatrix} = \begin{bmatrix}\Delta \mathrm{i}_{\mathrm{l}_d} * \mathrm{r_f} \\ \Delta \mathrm{i}_{\mathrm{l}_q} * \mathrm{r_f}\end{bmatrix} + \begin{bmatrix}-\omega \mathrm{L_f} \Delta \mathrm{i}_{\mathrm{l}_q} \\ \omega \mathrm{L_f} \Delta \mathrm{i}_{\mathrm{l}_d}\end{bmatrix} + \begin{bmatrix}\Delta \mathrm{v}_{0_d} \\ \Delta \mathrm{v}_{0_q}\end{bmatrix} + k_{pv_{dq}} \begin{bmatrix}\Delta i_{ld}{}^* - \Delta i_{ld} \\ \Delta i_{lq}{}^* - \Delta i_{lq}\end{bmatrix} + k_{iv_{dq}} \begin{bmatrix}\Delta \Upsilon_d \\ \Delta \Upsilon_q\end{bmatrix}$$

Here we don't use $\mathrm{v}_{0_{dq}}$ as they are feedforward terms but there is no PI controller after current controller block, so if we use this then there would be a lot of disturbance so we neglect it.

$$\begin{bmatrix}\Delta \mathrm{v}_{\mathrm{l}_d}{}^* \\ \Delta \mathrm{v}_{\mathrm{l}_q}{}^*\end{bmatrix} = \begin{bmatrix}\Delta \mathrm{i}_{\mathrm{l}_d} * \mathrm{r_f} \\ \Delta \mathrm{i}_{\mathrm{l}_q} * \mathrm{r_f}\end{bmatrix} + \begin{bmatrix}-\omega \mathrm{L_f} \Delta \mathrm{i}_{\mathrm{l}_q} \\ \omega \mathrm{L_f} \Delta \mathrm{i}_{\mathrm{l}_d}\end{bmatrix} + k_{pv_{dq}} \begin{bmatrix}\Delta i_{ld}{}^* - \Delta i_{ld} \\ \Delta i_{lq}{}^* - \Delta i_{lq}\end{bmatrix} + k_{iv_{dq}} \begin{bmatrix}\Delta \Upsilon_d \\ \Delta \Upsilon_q\end{bmatrix}$$

Now combining all equations, (3.76) and (3.77) are obtained.

$$\begin{bmatrix}\Delta \mathrm{v}_{\mathrm{l}_d}{}^* \\ \Delta \mathrm{v}_{\mathrm{l}_q}{}^*\end{bmatrix} = \begin{bmatrix}\Delta \mathrm{i}_{\mathrm{l}_d} * \mathrm{r_f} - \omega \mathrm{L_f} \Delta \mathrm{i}_{\mathrm{l}_q} + k_{pv_d} \Delta i_{ld}{}^* - k_{pv_d} \Delta i_{ld} + k_{iv_d} \Delta \Upsilon_d \\ \Delta \mathrm{i}_{\mathrm{l}_q} * \mathrm{r_f} + \omega \mathrm{L_f} \Delta \mathrm{i}_{\mathrm{l}_d} + k_{pv_q} \Delta i_{lq}{}^* - k_{pv_q} \Delta i_{lq} + k_{iv_q} \Delta \Upsilon_q\end{bmatrix} \quad \textbf{(3.76)}$$

$$\begin{bmatrix}\Delta \dot{\Upsilon}_d \\ \Delta \dot{\Upsilon}_q\end{bmatrix} = \begin{bmatrix}\Delta i_{ld}{}^* - \Delta i_{ld} \\ \Delta i_{lq}{}^* - \Delta i_{lq}\end{bmatrix} \quad \textbf{(3.77)}$$

The inverter AC output current is transformed in to DC quantity in synchronous rotating frame by Park's transformation. The direct and quadrature components are compared with the reference quantities and the error signal is passed to the PI controller to generate the voltage references **[24]**. Current controller model has been shown in figure 3.17 based on developed equation. Current controller model shown in figure 3.18, has been developed in Simulink.

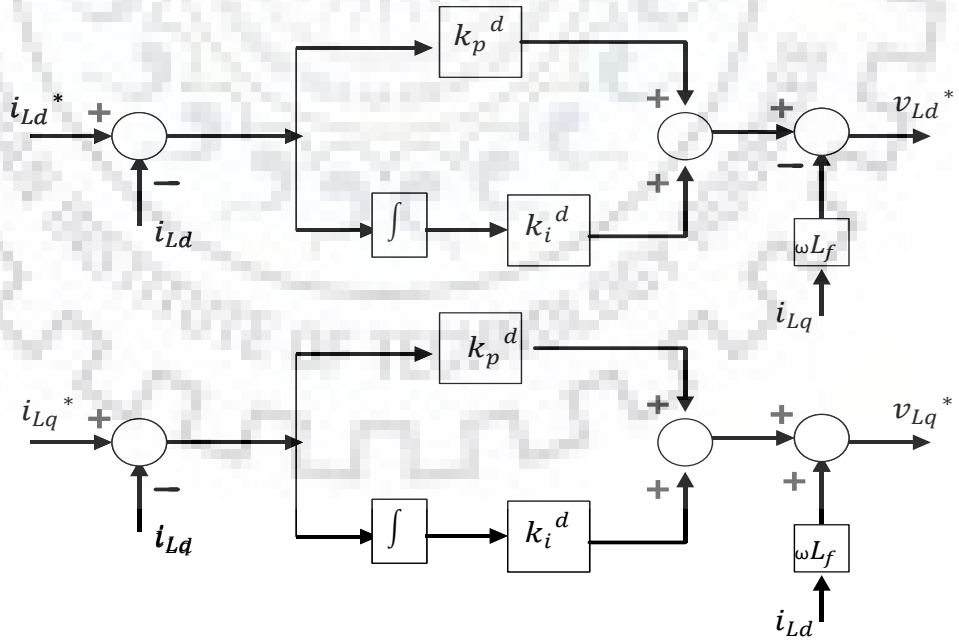

Figure 3. 17: Current controller in d-q frame for autonomous mode

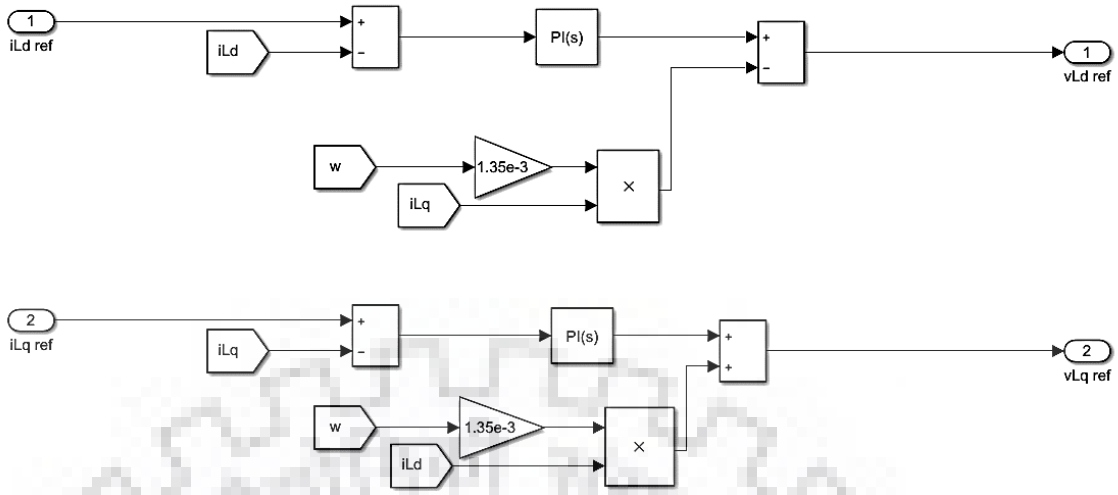

Figure 3. 18: Developed model of current controller for autonomous mode in Simulink.

c) Power controller

Power controller houses the droop characteristics **[45]**. One of its output is the angle needed for conversion from abc or dq0 to either one. Another output is the voltage magnitude, used for reactive power balancing. The d-q axis output voltage and current measurements are used to calculate the instantaneous active power (p) and reactive power (q) generated by the inverter as shown in (3.30)-(3.35) and using them (3.78) is obtained.

$$sP + \omega_c P = \omega_c(v_{od}i_{od} + v_{oq}i_{oq}) \quad \textbf{(3.78)}$$

Applying small signal, assuming frequency to be constant in (3.78) we get (3.79). Similarly doing so on (3.81) and (3.83) we get (3.80).

$$s\Delta P + \omega_c \Delta P = \omega_c(\Delta v_{od}i_{od} + v_{od}\Delta i_{od} + \Delta v_{oq}i_{oq} + v_{oq}\Delta i_{oq})$$

$$\Delta \dot{P} = -\omega_c \Delta P + \omega_c(\Delta v_{od}i_{od} + v_{od}\Delta i_{od} + \Delta v_{oq}i_{oq} + v_{oq}\Delta i_{oq}) \quad \textbf{(3.79)}$$

$$\Delta \dot{Q} = -\omega_c \Delta Q + \omega_c(\Delta v_{od}i_{oq} + v_{od}\Delta i_{oq} - i_{od}\Delta v_{oq} - v_{oq}\Delta i_{od}) \quad \textbf{(3.80)}$$

Using (3.6) and converting it into state space form we get (3.81)

$$\Delta\omega = -k_p \Delta P \quad \textbf{(3.81)}$$

Now finding θ through (3.81), necessary for active power flow and for conversion abc/dq0 frame.

$$\theta = \int \omega \, dt \quad \textbf{(3.82)}$$

Using variable of (3.82) and merging with (3.6) we get (3.83)

$$\theta = \omega_{ref} t - k_p \int P \, dt \tag{3.83}$$

Small signal is applied on (3.1) and (3.84) is obtained and is converted to state space form shown in (3.85) using (3.6).

$$\Delta\delta = \int \Delta\omega - \Delta\omega_{com} \tag{3.84}$$

$$\dot{\Delta\delta} = \Delta\omega - \Delta\omega_{com}$$

$$\dot{\Delta\delta} = (\Delta\omega_{ref} - k_p \Delta P) - \Delta\omega_{com}$$

$$\dot{\Delta\delta} = -k_p \Delta P - \Delta\omega_{com} \tag{3.85}$$

Now applying small signal to (3.4), (3.86) is obtained

$$V_{od}{}^{*} = V_{od_{ref}} - k_q Q$$

$$\Delta V_{od}{}^{*} = -k_q \Delta Q \tag{3.86}$$

$$V_{oq}{}^{*} = 0$$

Combining all equations of state variables and arranging into state space form we get (3.87) and (3.88) and model shown in figure 3.19, is developed.

$$\begin{bmatrix} \dot{\Delta\delta} \\ \dot{\Delta P} \\ \dot{\Delta Q} \end{bmatrix} = \begin{bmatrix} -k_p \Delta P - \Delta\omega_{com} \\ -\omega_c \Delta P + \omega_c(\Delta v_{od} i_{od} + v_{od} \Delta i_{od} + \Delta v_{oq} i_{oq} + v_{oq} \Delta i_{oq}) \\ -\omega_c \Delta Q + \omega_c(\Delta v_{od} i_{oq} + v_{od} \Delta i_{oq} - i_{od} \Delta v_{oq} - v_{oq} \Delta i_{od}) \end{bmatrix} \tag{3.87}$$

$$\begin{bmatrix} \Delta\omega \\ \Delta V_{od}{}^{*} \\ \Delta V_{oq}{}^{*} \end{bmatrix} = \begin{bmatrix} -k_p \Delta P \\ -k_q \Delta Q \\ 0 \end{bmatrix} \tag{3.88}$$

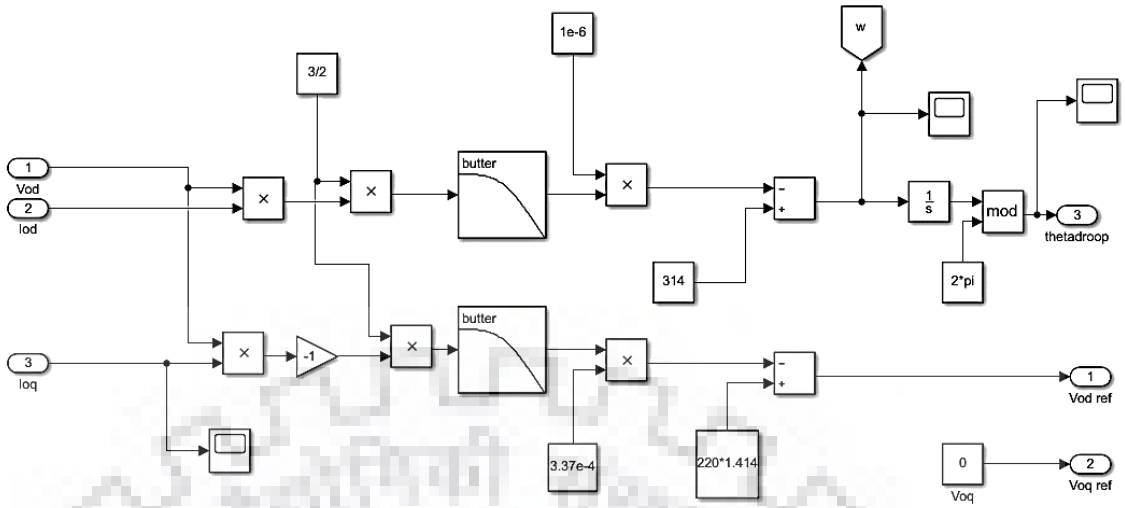

Figure 3. 19: Developed model of power controller block in Simulink for autonomous mode

d) LCL filter

LCL filter is used to increase damping and filtering harmonics. The resistors r_c and $r_f$are the parasitic resistances of the inductors. By applying KVL and KCL equations of current and voltages in figure 3.10, LCL filter can be expressed through equations shown below. These nonlinear equations are linearized about an operating point calculated from Simulink. Assumption has been made that, $v_{ldq} = v_{ldq}{}^{*}$. The state space equations of filter dynamics are presented below. (3.50) is rewritten here.

$$i_{c_{dq0}} = \left(c_f \frac{\partial}{\partial t}\left\{v_{0_{dq0}}\right\}\right) + \left(c_f v_{0_{dq0}} * (-\omega)\begin{bmatrix} 0 & 1 & 0 \\ -1 & 0 & 0 \\ 0 & 0 & 0 \end{bmatrix}\right)$$

From Fig. 3.10, we can deduce (3.89).

$$i_{c_{dq0}} = i_{l_{dq0}} - i_{o_{dq0}} \tag{3.89}$$

Combining (3.50) and (3.89) we get (3.90)

$$i_{l_{dq0}} - i_{o_{dq0}} = \left(c_f \frac{\partial}{\partial t}\left\{v_{0_{dq0}}\right\}\right) + \left(c_f \begin{bmatrix} \mathrm{v}_{o_d} \\ \mathrm{v}_{o_q} \\ \mathrm{v}_{o_0} \end{bmatrix} * \begin{bmatrix} 0 & -\omega & 0 \\ \omega & 0 & 0 \\ 0 & 0 & 0 \end{bmatrix}\right) \tag{3.90}$$

Arranging (3.90) into state space form we get (3.91)

$$\begin{bmatrix} \dot{\mathrm{v}}_{o_d} \\ \dot{\mathrm{v}}_{o_q} \\ \dot{\mathrm{v}}_{o_0} \end{bmatrix} = \frac{1}{c_f}\begin{bmatrix} i_{l_d} - i_{o_d} \\ i_{l_q} - i_{o_q} \\ i_{l_0} - i_{o_0} \end{bmatrix} + \begin{bmatrix} 0 & \omega \mathrm{v}_{o_q} & 0 \\ -\omega \mathrm{v}_{o_d} & 0 & 0 \\ 0 & 0 & 0 \end{bmatrix} \tag{3.91}$$

Neglecting zero component by assuming balanced load (3.91) is modified into (3.92).

$$\begin{bmatrix} \dot{v_{o_d}} \\ \dot{v_{o_q}} \end{bmatrix} = \begin{bmatrix} \frac{1}{c_f}\left(i_{l_d} - i_{o_d}\right) + \omega v_{o_q} \\ \frac{1}{c_f}\left(i_{l_q} - i_{o_q}\right) - \omega v_{o_d} \end{bmatrix} \tag{3.92}$$

Applying KVL on Fig. 3.22 (3.93) can be obtained.

$$\begin{bmatrix} v_{la} \\ v_{lb} \\ v_{lc} \end{bmatrix} = \begin{bmatrix} i_{la} * r_f \\ i_{lb} * r_f \\ i_{lc} * r_f \end{bmatrix} + L_f \frac{d}{dt}\begin{bmatrix} i_{la} \\ i_{lb} \\ i_{lc} \end{bmatrix} + \begin{bmatrix} v_{oa} \\ v_{ob} \\ v_{oc} \end{bmatrix} \tag{3.93}$$

Now converting abc frame into dq0 frame we get (3.94).

$$T_{dq0} * \begin{bmatrix} v_{l_a} \\ v_{l_b} \\ v_{l_c} \end{bmatrix} = T_{dq0} \begin{bmatrix} i_{l_a} * r_f \\ i_{l_b} * r_f \\ i_{l_c} * r_f \end{bmatrix} + T_{dq0} * L_f \frac{d}{dt}\begin{bmatrix} i_{la} \\ i_{lb} \\ i_{lc} \end{bmatrix} + T_{dq0} \begin{bmatrix} v_{o_a} \\ v_{o_b} \\ v_{o_c} \end{bmatrix}$$

$$\begin{bmatrix} v_{l_d} \\ v_{l_q} \\ v_{l_0} \end{bmatrix} = \begin{bmatrix} i_{l_d} * r_f \\ i_{l_q} * r_f \\ i_{l_0} * r_f \end{bmatrix} + T_{dq0} * L_f \frac{d}{dt}\left\{ {T_{dq0}}^{-1} \begin{bmatrix} i_{l_d} \\ i_{l_q} \\ i_{l_0} \end{bmatrix} \right\} + \begin{bmatrix} v_{o_d} \\ v_{o_q} \\ v_{o_0} \end{bmatrix}$$

$$\begin{bmatrix} v_{l_d} \\ v_{l_q} \\ v_{l_0} \end{bmatrix} = \begin{bmatrix} i_{l_d} * r_f \\ i_{l_q} * r_f \\ i_{l_0} * r_f \end{bmatrix} + T_{dq0} * L_f * {T_{dq0}}^{-1} \frac{d}{dt}\begin{bmatrix} i_{l_d} \\ i_{l_q} \\ i_{l_0} \end{bmatrix} + T_{dq0} * L_f \begin{bmatrix} i_{l_d} \\ i_{l_q} \\ i_{l_0} \end{bmatrix} \frac{d}{dt}\left({T_{dq0}}^{-1}\right) + \begin{bmatrix} v_{o_d} \\ v_{o_q} \\ v_{o_0} \end{bmatrix}$$

$$\begin{bmatrix} v_{l_d} \\ v_{l_q} \\ v_{l_0} \end{bmatrix} = \begin{bmatrix} i_{l_d} * r_f \\ i_{l_q} * r_f \\ i_{l_0} * r_f \end{bmatrix} + L_f \frac{d}{dt}\begin{bmatrix} i_{l_d} \\ i_{l_q} \\ i_{l_0} \end{bmatrix} + L_f \begin{bmatrix} i_{l_d} \\ i_{l_q} \\ i_{l_0} \end{bmatrix} * (-\omega) \begin{bmatrix} 0 & 1 & 0 \\ -1 & 0 & 0 \\ 0 & 0 & 0 \end{bmatrix} + \begin{bmatrix} v_{o_d} \\ v_{o_q} \\ v_{o_0} \end{bmatrix}$$

$$\begin{bmatrix} v_{l_d} \\ v_{l_q} \\ v_{l_0} \end{bmatrix} = \begin{bmatrix} i_{l_d} * r_f \\ i_{l_q} * r_f \\ i_{l_0} * r_f \end{bmatrix} + L_f \frac{d}{dt}\begin{bmatrix} i_{l_d} \\ i_{l_q} \\ i_{l_0} \end{bmatrix} + \begin{bmatrix} 0 & -\omega L_f i_{l_d} & 0 \\ \omega L_f i_{l_q} & 0 & 0 \\ 0 & 0 & 0 \end{bmatrix} + \begin{bmatrix} v_{o_d} \\ v_{o_q} \\ v_{o_0} \end{bmatrix} \tag{3.94}$$

Arranging (3.94) into state space form we get (3.95).

$$\begin{bmatrix} \dot{i_{l_d}} \\ \dot{i_{l_q}} \\ \dot{i_{l_0}} \end{bmatrix} = \begin{bmatrix} \frac{1}{L_f}(v_{l_d} - v_{o_d}) + \omega i_{l_q} - \frac{r_f}{L_f} i_{l_d} \\ \frac{1}{L_f}(v_{l_q} - v_{o_q}) - \omega i_{l_d} - \frac{r_f}{L_f} i_{l_q} \\ \frac{1}{L_f}(v_{l_0} - v_{o_0}) \end{bmatrix} \tag{3.95}$$

Now neglecting zero component on (3.95), (3.96) can be obtained.

$$\begin{bmatrix} \dot{\mathrm{i}}_{\mathrm{l}_d} \\ \dot{\mathrm{i}}_{\mathrm{l}_q} \end{bmatrix} = \begin{bmatrix} \frac{1}{\mathrm{L_f}}(\mathrm{v}_{\mathrm{l}_d} - \mathrm{v}_{\mathrm{o}_d}) + \omega \mathrm{i}_{\mathrm{l}_q} - \frac{\mathrm{r_f}}{\mathrm{L_f}} \mathrm{i}_{\mathrm{l}_d} \\ \frac{1}{\mathrm{L_f}}(\mathrm{v}_{\mathrm{l}_q} - \mathrm{v}_{\mathrm{o}_q}) - \omega \mathrm{i}_{\mathrm{l}_d} - \frac{\mathrm{r_f}}{\mathrm{L_f}} \mathrm{i}_{\mathrm{l}_q} \end{bmatrix} \quad \textbf{(3.96)}$$

Applying KVL on Fig. 3.24, (3.97) can be deduced.

$$\begin{bmatrix} \mathrm{v}_{\mathrm{o}a} \\ \mathrm{v}_{\mathrm{o}b} \\ \mathrm{v}_{\mathrm{o}c} \end{bmatrix} = \begin{bmatrix} \mathrm{i}_{\mathrm{o}a} * \mathrm{r_c} \\ \mathrm{i}_{\mathrm{o}b} * \mathrm{r_c} \\ \mathrm{i}_{\mathrm{o}c} * \mathrm{r_c} \end{bmatrix} + \mathrm{L_c} \frac{\mathrm{d}}{\mathrm{dt}} \begin{bmatrix} \mathrm{i}_{\mathrm{o}a} \\ \mathrm{i}_{\mathrm{o}b} \\ \mathrm{i}_{\mathrm{o}c} \end{bmatrix} + \begin{bmatrix} \mathrm{v}_{\mathrm{b}a} \\ \mathrm{v}_{\mathrm{b}b} \\ \mathrm{v}_{\mathrm{b}c} \end{bmatrix} \quad \textbf{(3.97)}$$

Converting (3.97) into dq0 frame and arranging it into state space form we get (3.98)

$$T_{dq0} * \begin{bmatrix} \mathrm{v}_{\mathrm{o}a} \\ \mathrm{v}_{\mathrm{o}b} \\ \mathrm{v}_{\mathrm{o}c} \end{bmatrix} = T_{dq0} \begin{bmatrix} \mathrm{i}_{\mathrm{o}a} * \mathrm{r_c} \\ \mathrm{i}_{\mathrm{o}b} * \mathrm{r_c} \\ \mathrm{i}_{\mathrm{o}c} * \mathrm{r_c} \end{bmatrix} + T_{dq0} * \mathrm{L_c} \frac{\mathrm{d}}{\mathrm{dt}} \begin{bmatrix} \mathrm{i}_{\mathrm{o}a} \\ \mathrm{i}_{\mathrm{o}b} \\ \mathrm{i}_{\mathrm{o}c} \end{bmatrix} + T_{dq0} \begin{bmatrix} \mathrm{v}_{\mathrm{b}a} \\ \mathrm{v}_{\mathrm{b}b} \\ \mathrm{v}_{\mathrm{b}c} \end{bmatrix}$$

$$\begin{bmatrix} \mathrm{v}_{\mathrm{o}_d} \\ \mathrm{v}_{\mathrm{o}_q} \\ \mathrm{v}_{\mathrm{o}_0} \end{bmatrix} = \begin{bmatrix} \mathrm{i}_{\mathrm{o}_d} * \mathrm{r_c} \\ \mathrm{i}_{\mathrm{o}_q} * \mathrm{r_c} \\ \mathrm{i}_{\mathrm{o}_0} * \mathrm{r_c} \end{bmatrix} + T_{dq0} * \mathrm{L_f} \frac{\mathrm{d}}{\mathrm{dt}} \left\{ {T_{dq0}}^{-1} \begin{bmatrix} \mathrm{i}_{\mathrm{o}_d} \\ \mathrm{i}_{\mathrm{o}_q} \\ \mathrm{i}_{o_0} \end{bmatrix} \right\} + \begin{bmatrix} \mathrm{v}_{\mathrm{b}_d} \\ \mathrm{v}_{\mathrm{b}_q} \\ \mathrm{v}_{\mathrm{b}_0} \end{bmatrix}$$

$$\begin{bmatrix} \mathrm{v}_{\mathrm{o}_d} \\ \mathrm{v}_{\mathrm{o}_q} \\ \mathrm{v}_{\mathrm{o}_0} \end{bmatrix} = \begin{bmatrix} \mathrm{i}_{\mathrm{o}_d} * \mathrm{r_c} \\ \mathrm{i}_{\mathrm{o}_q} * \mathrm{r_c} \\ \mathrm{i}_{\mathrm{o}_0} * \mathrm{r_c} \end{bmatrix} + T_{dq0} * \mathrm{L_f} * {T_{dq0}}^{-1} \frac{\mathrm{d}}{\mathrm{dt}} \begin{bmatrix} \mathrm{i}_{\mathrm{o}_d} \\ \mathrm{i}_{\mathrm{o}_q} \\ \mathrm{i}_{o_0} \end{bmatrix} + \mathrm{L_f} \begin{bmatrix} \mathrm{i}_{\mathrm{o}_d} \\ \mathrm{i}_{\mathrm{o}_q} \\ \mathrm{i}_{o_0} \end{bmatrix} T_{dq0} * \frac{\mathrm{d}}{\mathrm{dt}} ({T_{dq0}}^{-1}) + \begin{bmatrix} \mathrm{v}_{\mathrm{b}_d} \\ \mathrm{v}_{\mathrm{b}_q} \\ \mathrm{v}_{\mathrm{b}_0} \end{bmatrix}$$

$$\begin{bmatrix} \mathrm{v}_{\mathrm{o}_d} \\ \mathrm{v}_{\mathrm{o}_q} \\ \mathrm{v}_{\mathrm{o}_0} \end{bmatrix} = \begin{bmatrix} \mathrm{i}_{\mathrm{o}_d} * \mathrm{r_c} \\ \mathrm{i}_{\mathrm{o}_q} * \mathrm{r_c} \\ \mathrm{i}_{\mathrm{o}_0} * \mathrm{r_c} \end{bmatrix} + \mathrm{L_f} \frac{\mathrm{d}}{\mathrm{dt}} \begin{bmatrix} \mathrm{i}_{\mathrm{o}_d} \\ \mathrm{i}_{\mathrm{o}_q} \\ \mathrm{i}_{o_0} \end{bmatrix} + \mathrm{L_f} \begin{bmatrix} \mathrm{i}_{\mathrm{o}_d} \\ \mathrm{i}_{\mathrm{o}_q} \\ \mathrm{i}_{o_0} \end{bmatrix} * (-\omega) \begin{bmatrix} 0 & 1 & 0 \\ -1 & 0 & 0 \\ 0 & 0 & 0 \end{bmatrix} + \begin{bmatrix} \mathrm{v}_{\mathrm{b}_d} \\ \mathrm{v}_{\mathrm{b}_q} \\ \mathrm{v}_{\mathrm{b}_0} \end{bmatrix}$$

$$\begin{bmatrix} \mathrm{v}_{\mathrm{o}_d} \\ \mathrm{v}_{\mathrm{o}_q} \\ \mathrm{v}_{\mathrm{o}_0} \end{bmatrix} = \begin{bmatrix} \mathrm{i}_{\mathrm{o}_d} * \mathrm{r_c} \\ \mathrm{i}_{\mathrm{o}_q} * \mathrm{r_c} \\ \mathrm{i}_{\mathrm{o}_0} * \mathrm{r_c} \end{bmatrix} + \mathrm{L_f} \frac{\mathrm{d}}{\mathrm{dt}} \begin{bmatrix} \mathrm{i}_{\mathrm{o}_d} \\ \mathrm{i}_{\mathrm{o}_q} \\ \mathrm{i}_{o_0} \end{bmatrix} + \begin{bmatrix} 0 & -\omega \mathrm{L_f} \mathrm{i}_{\mathrm{o}_q} & 0 \\ \omega \mathrm{L_f} \mathrm{i}_{\mathrm{o}_d} & 0 & 0 \\ 0 & 0 & 0 \end{bmatrix} + \begin{bmatrix} \mathrm{v}_{\mathrm{b}_d} \\ \mathrm{v}_{\mathrm{b}_q} \\ \mathrm{v}_{\mathrm{b}_0} \end{bmatrix}$$

$$\begin{bmatrix} \dot{\mathrm{i}}_{\mathrm{o}_d} \\ \dot{\mathrm{i}}_{\mathrm{o}_q} \\ \dot{\mathrm{i}}_{\mathrm{o}_0} \end{bmatrix} = \begin{bmatrix} \frac{1}{\mathrm{L_f}}(\mathrm{v}_{\mathrm{o}_d} - \mathrm{v}_{\mathrm{b}_d}) + \omega \mathrm{i}_{\mathrm{o}_q} - \frac{\mathrm{r_c}}{\mathrm{L_c}} \mathrm{i}_{\mathrm{o}_d} \\ \frac{1}{\mathrm{L_f}}(\mathrm{v}_{\mathrm{o}_q} - \mathrm{v}_{\mathrm{b}_q}) - \omega \mathrm{i}_{\mathrm{o}_d} - \frac{\mathrm{r_c}}{\mathrm{L_c}} \mathrm{i}_{\mathrm{o}_q} \\ \frac{1}{\mathrm{L_f}}(\mathrm{v}_{\mathrm{l}_0} - \mathrm{v}_{\mathrm{o}_0}) \end{bmatrix} \quad \textbf{(3.98)}$$

Now neglecting zero component assuming all balancing is there so (3.98) is converted to (3.99).

$$\begin{bmatrix} \dot{\mathrm{i}}_{\mathrm{o}_d} \\ \dot{\mathrm{i}}_{\mathrm{o}_q} \end{bmatrix} = \begin{bmatrix} \frac{1}{\mathrm{L_f}}(\mathrm{v}_{\mathrm{o}_d} - \mathrm{v}_{\mathrm{b}_d}) + \omega \mathrm{i}_{\mathrm{o}_q} - \frac{\mathrm{r_c}}{\mathrm{L_c}} \mathrm{i}_{\mathrm{o}_d} \\ \frac{1}{\mathrm{L_f}}(\mathrm{v}_{\mathrm{o}_q} - \mathrm{v}_{\mathrm{b}_q}) - \omega \mathrm{i}_{\mathrm{o}_d} - \frac{\mathrm{r_c}}{\mathrm{L_c}} \mathrm{i}_{\mathrm{o}_q} \end{bmatrix} \quad \textbf{(3.99)}$$

From figure 3.10, (3.100) can be deduced.

$$v_{o\,abc} = v_{c\,abc} = \frac{1}{C_f}\int (i_{l\,abc} - i_{o\,abc})dt \qquad \textbf{(3.100)}$$

Using (3.92), (3.96), (3.98) and (3.100) can be obtained and used to develop state space model of LCL filter. Applying small signal on (3.101) we get (3.102).

(3.101) is used in eigen value analysis and based on initial values derived from simulation, stability analysis can be performed.

$$\begin{bmatrix} \dot{i}_{l_d} \\ \dot{i}_{l_q} \\ \dot{v}_{o_d} \\ \dot{v}_{o_q} \\ \dot{i}_{o_d} \\ \dot{i}_{o_q} \end{bmatrix} = \begin{bmatrix} \frac{1}{L_f}(v_{l_d} - v_{o_d}) + \omega i_{l_q} - \frac{r_f}{L_f} i_{l_d} \\ \frac{1}{L_f}(v_{l_q} - v_{o_q}) - \omega i_{l_d} - \frac{r_f}{L_f} i_{l_q} \\ \frac{1}{c_f}\left(i_{l_d} - i_{o_d}\right) + \omega v_{o_q} \\ \frac{1}{c_f}\left(i_{l_q} - i_{o_q}\right) - \omega v_{o_d} \\ \frac{1}{L_f}(v_{o_d} - v_{b_d}) + \omega i_{o_q} - \frac{r_c}{L_c} i_{o_d} \\ \frac{1}{L_f}(v_{o_q} - v_{b_q}) - \omega i_{o_d} - \frac{r_c}{L_c} i_{o_q} \end{bmatrix} \qquad \textbf{(3.101)}$$

$$\begin{bmatrix} \Delta\dot{i}_{l_d} \\ \Delta\dot{i}_{l_q} \\ \Delta\dot{v}_{o_d} \\ \Delta\dot{v}_{o_q} \\ \Delta\dot{i}_{o_d} \\ \Delta\dot{i}_{o_q} \end{bmatrix} = \begin{bmatrix} \frac{1}{L_f}(\Delta v_{l_d} - \Delta v_{o_d}) + \Delta(\omega i_{l_q}) - \frac{r_f}{L_f}\Delta i_{l_d} \\ \frac{1}{L_f}(\Delta v_{l_q} - \Delta v_{o_q}) - \Delta(\omega i_{l_d}) - \frac{r_f}{L_f}\Delta i_{l_q} \\ \frac{1}{c_f}\left(\Delta i_{l_d} - \Delta i_{o_d}\right) + \Delta(\omega v_{o_q}) \\ \frac{1}{c_f}\left(\Delta i_{l_q} - \Delta i_{o_q}\right) - \Delta(\omega v_{o_d}) \\ \frac{1}{L_f}(\Delta v_{o_d} - \Delta v_{b_d}) + \Delta(\omega i_{o_q}) - \frac{r_c}{L_c}\Delta i_{o_d} \\ \frac{1}{L_f}(\Delta v_{o_q} - \Delta v_{b_q}) - \Delta(\omega i_{o_d}) - \frac{r_c}{L_c}\Delta i_{o_q} \end{bmatrix}$$

$$\begin{bmatrix} \Delta\dot{\mathrm{i}}_{\mathrm{l}_d} \\ \Delta\dot{\mathrm{i}}_{\mathrm{l}_q} \\ \Delta\dot{\mathrm{v}}_{\mathrm{o}_d} \\ \Delta\dot{\mathrm{v}}_{\mathrm{o}_q} \\ \Delta\dot{\mathrm{i}}_{\mathrm{o}_d} \\ \Delta\dot{\mathrm{i}}_{\mathrm{o}_q} \end{bmatrix} = \begin{bmatrix} \frac{1}{\mathrm{L_f}}(\Delta\mathrm{v}_{\mathrm{l}_d} - \Delta\mathrm{v}_{\mathrm{o}_d}) + \mathrm{I}_{\mathrm{l}_q}\Delta\omega + \omega\Delta\mathrm{i}_{\mathrm{l}_q} - \frac{\mathrm{r_f}}{\mathrm{L_f}}\Delta\mathrm{i}_{\mathrm{l}_d} \\ \frac{1}{\mathrm{L_f}}(\Delta\mathrm{v}_{\mathrm{l}_q} - \Delta\mathrm{v}_{\mathrm{o}_q}) - \mathrm{I}_{\mathrm{l}_d}\Delta\omega - \omega\Delta\mathrm{i}_{\mathrm{l}_d} - \frac{\mathrm{r_f}}{\mathrm{L_f}}\Delta\mathrm{i}_{\mathrm{l}_q} \\ \frac{1}{c_f}\left(\Delta i_{l_d} - \Delta i_{o_d}\right) + \mathrm{V}_{\mathrm{o}_q}\Delta\omega + \omega\Delta\mathrm{v}_{\mathrm{o}_q} \\ \frac{1}{c_f}\left(\Delta i_{l_q} - \Delta i_{o_q}\right) - \mathrm{V}_{\mathrm{o}_d}\Delta\omega - \omega\Delta\mathrm{v}_{\mathrm{o}_d} \\ \frac{1}{\mathrm{L_f}}(\Delta\mathrm{v}_{\mathrm{o}_d} - \Delta\mathrm{v}_{\mathrm{b}_d}) + \mathrm{I}_{\mathrm{o}_q}\Delta\omega + \omega\Delta\mathrm{i}_{\mathrm{o}_q} - \frac{\mathrm{r_c}}{\mathrm{L_c}}\Delta\mathrm{i}_{\mathrm{o}_d} \\ \frac{1}{\mathrm{L_f}}(\Delta\mathrm{v}_{\mathrm{o}_q} - \Delta\mathrm{v}_{\mathrm{b}_q}) - \mathrm{I}_{\mathrm{o}_d}\Delta\omega - \omega\Delta\mathrm{i}_{\mathrm{o}_d} - \frac{\mathrm{r_c}}{\mathrm{L_c}}\Delta\mathrm{i}_{\mathrm{o}_q} \end{bmatrix} \quad \textbf{(3.102)}$$

3.4 MICROGRID STRATEGY

During grid connected mode, the controller has to supply pre-set power to the main grid with the inverters using the signal of main grid as reference. Thus in grid connected mode the system operates in stiff synchronization with main grid in current control mode **[33]**.The microgrid configuration with the control strategy is shown in figure 3.20. When the microgrid is isolated from the main grid, the controller is designed as shown in figure 3.21 so as to supply constant voltage to the local sensitive loads.

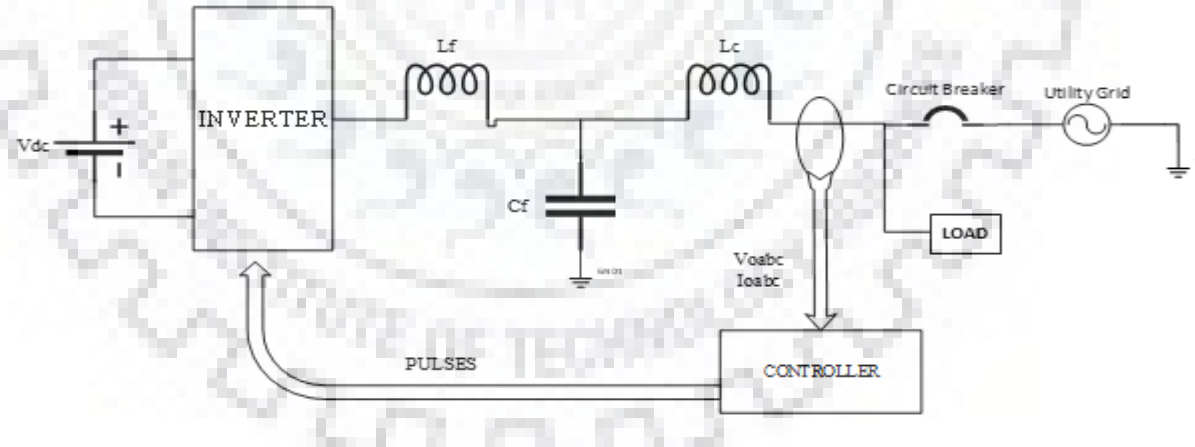

Figure 3. 20: Grid connected mode of microgrid configuration

In absence of grid, voltage and frequency references are lost. Moreover local P and Q must match to those supplied by DER unit. Widely accepted voltage and frequency control strategy is discussed in **[37]** and **[5]**. Frequency after islanding depends on the condition before islanding, if total power generated by DG before islanding is less than their demand then frequency after islanding will decrease in order to increase power output. Now real power can be balanced by i_d component and reactive power by i_q component.

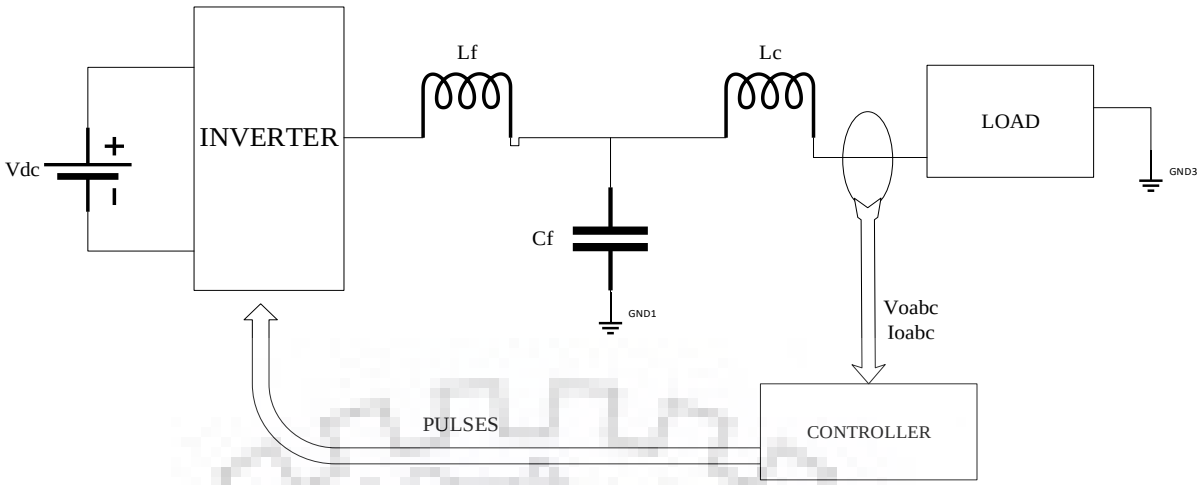

Figure 3. 21: Islanded Microgrid configuration with controller

3.4.1P/Q control:

PQ control schematic for the three-phase grid-interfacing inverter having various components is shown in figure 3.22 and discussed further.

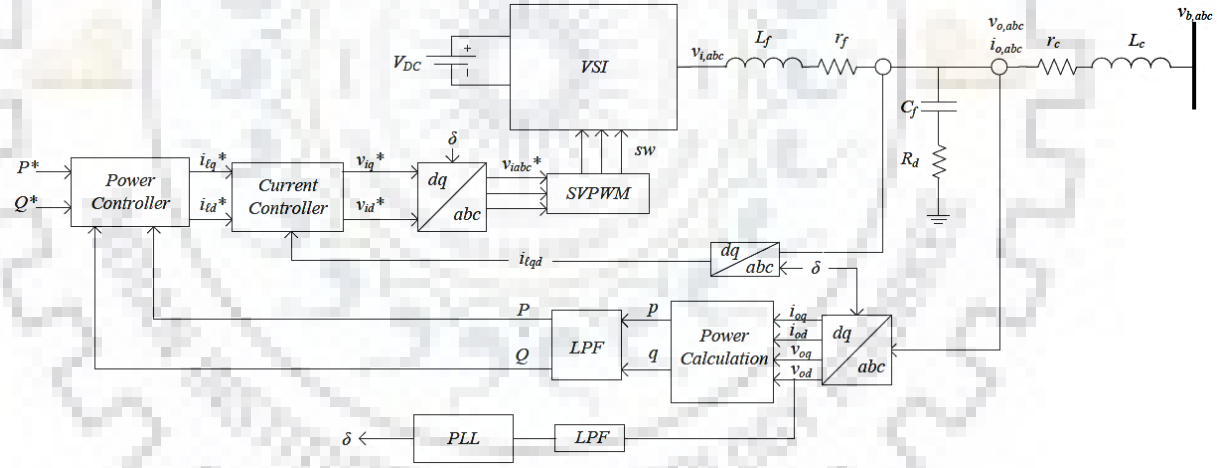

Figure 3. 22: Model of current control VSI in grid connected mode

In this mode, the output of the DGs in the micro-grid is kept to be constant, even if the frequency and voltage of the micro-grid fluctuates. In the Park transformation, the output voltage of the inverter can be converted from abc axis to dq0 axis by choosing a reasonable synchronized rotation axis, and the q-axis voltage should be set to 0 **[46]**.

$$p = \frac{3}{2}\left(v_{od}i_{od} + v_{oq}i_{oq}\right)$$

$$q = \frac{3}{2}\left(v_{oq}i_{od} - v_{od}i_{oq}\right)$$

Here instantantaneous active power (p) , reactive power (q) , d-axis voltage of grid (v_{od}) , q axis voltage of grid (v_{oq}) , d axis grid current(i_{od}) and q axis grid current(i_{oq}) are mentioned in (3.30) and (3.31) are expressed. Now since $v_{oq} = 0$ and instantaneous powers previously defined in (3.32) and (3.33) are rewritten here.

$$p = \frac{3}{2}(v_{od} i_{od})$$

$$q = \frac{3}{2}(-v_{od} i_{oq})$$

Instantaneous powers are then passed through low pass filters with the corner frequency ω_c to obtain the filtered output power as described through (3.34) and (3.35) is also shown.

$$P = \frac{\omega_c}{s+\omega_c} p$$

$$Q = \frac{\omega_c}{s+\omega_c} q$$

Above values are calculated average active power (P) and reactive power (Q). Now with the constant output real power (P_{ref}) and reactive power (Q_{ref}), current reference values ($i_{d,ref}$) and ($i_{q,ref}$) are calculated as in (3.36) and (3.37) and also shown here.

$$i_{d,ref} = \frac{2}{3}(P_{ref}/v_{od})$$

$$i_{q,ref} = -\frac{2}{3}(Q_{ref}/v_{od})$$

State space equations derived above in LCL filter subsection are used in modelling block diagram and analysis.

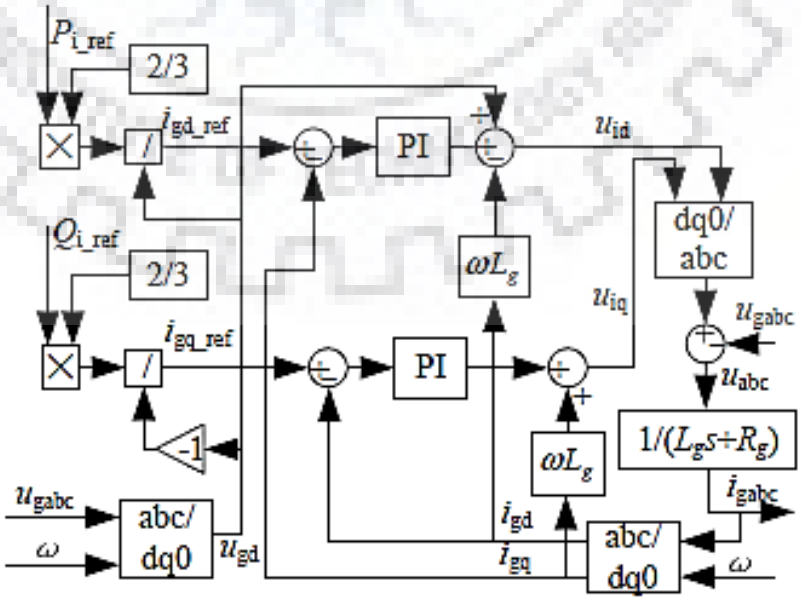

Figure 3. 23: Diagram of P/Q control

Figure 3.23 shows the structure diagram of P/Q control, which is realized by dominating the inverters directly in the micro-grid. The inverter's output power is controlled by the grid. The model shown in figure 3.24, is developed in Simulink.

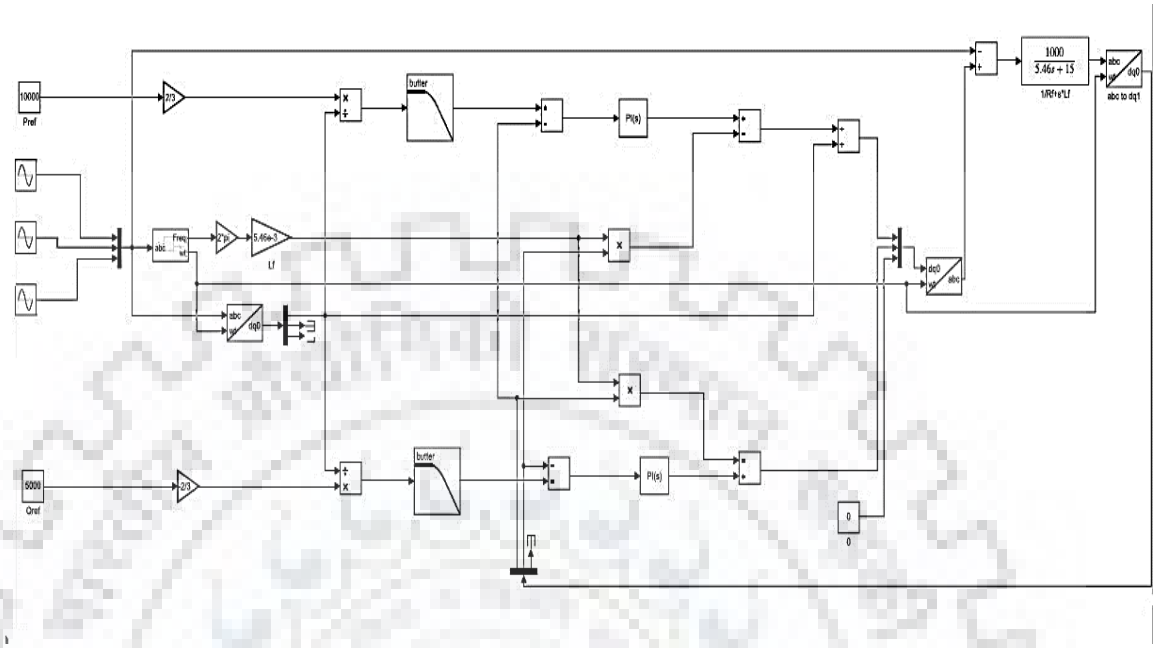

Figure 3. 24: Developed model of P/Q control in Simulink

3.4.2V/f control:

PV control schematic for the three-phase autonomous inverter having various components is shown in figure 3.25 and discussed further.

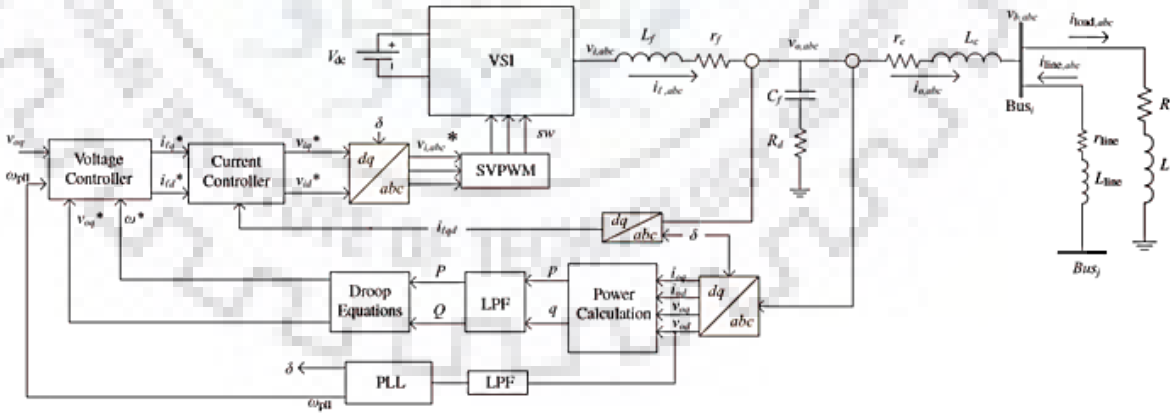

Figure 3. 25: Model of voltage control VSI in autonomous mode

The output of the DGs in this mode vary as per load, maintaining frequency and voltage of the micro-grid. In the Park transformation, the output voltage of the inverter can be converted from abc axis to dq0 axis as described in (3.30) and (3.31) and the q-axis voltage should be set to 0.

$$p = \frac{3}{2}\left(v_{od}i_{od} + v_{oq}i_{oq}\right)$$

$$q = \frac{3}{2}\left(v_{oq}i_{od} - v_{od}i_{oq}\right)$$

Here instantantaneous active power (p) , reactive power (q) , d-axis voltage of grid (v_{od}) , q axis voltage of grid (v_{oq}), d axis grid current(i_{od}) and q axis grid current(i_{oq}) are mentioned. Since $v_{oq} = 0$, instantaneous powers are modified as expressed in (3.32) and (3.33).

$$p = \frac{3}{2}\left(v_{od}i_{od}\right)$$

$$q = \frac{3}{2}\left(-v_{od}i_{oq}\right)$$

Instantaneous powers are then passed through low pass filters with the corner frequency ω_c to obtain the filtered output power as shown in (3.34) and (3.35).

$$P = \frac{\omega_c}{s + \omega_c}p$$

$$Q = \frac{\omega_c}{s + \omega_c}q$$

Above values are average active power (P) and reactive power (Q). State space equations derived above in LCL filter subsection are also used in modelling block diagram. Through power controller inverter interfaced DG behaves as a synchronous machine, controlling voltage and frequency of ac system and behaving as voltage source**[47]**.

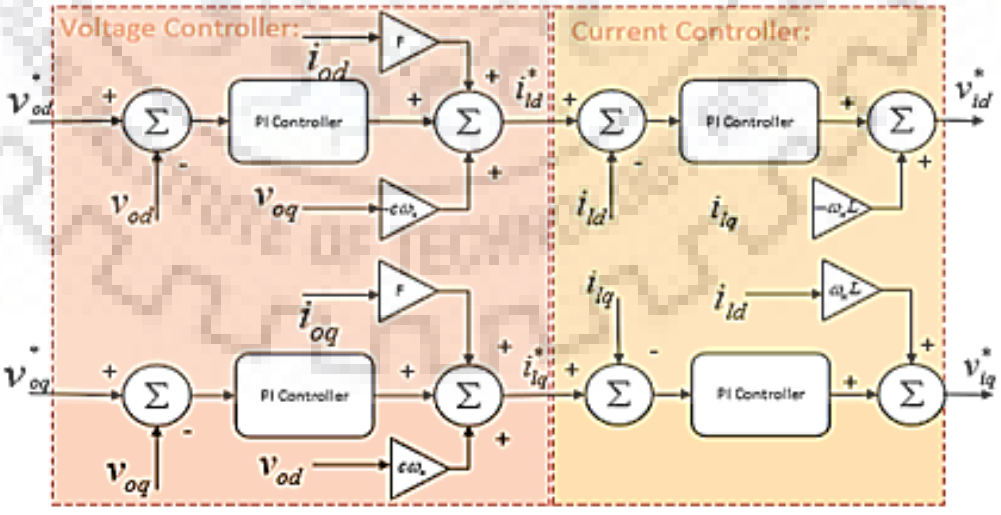

Figure 3. 26: Diagram of V/f control

Figure 3.26 shows the structure diagram of P/V control, which is realized by dominating the inventers directly in the micro-grid.

3.4 Tuning Methods

1) Zeigler Nicholas Method

   This is a very basic and fundamental tuning method. Here we firstly make k_i= 0 and keep on varying k_p such that we receive oscillations of constant amplitude and at that point we make k_p as constant and vary k_i such that error decrease. This is a very random method and approach is also not proper so it has not been used

2) Here we have 2 loops, inner and outer loop.

$$k_p = \frac{L}{\tau}, k_i = \frac{R}{\tau}$$

   Where $\tau = time\ constant$

   Firstly inner loop is designed and them same equation used for tuning outer loop**[11].**

3) Linearization Method

   With this method, whole non-linear circuit after linearizing with the help of state space equations, can easily be tuned. It is always easy to tune linear circuit. This method is inherently available in simulink but for doing so, we need to obtain bandwidth of all control loops. Switching frequency is 10 khz and basic rule states that bandwidth of current controller should be more than 1/10th of switching frequency, bandwidth of voltage controller should be more than 1/4th of current controller bandwidth and lastly resonant frequency should lie in range of current controller bandwidth. So, following values are selected.

   - Switching frequency = 10 khz
   - Bandwidth of current controller = 1600 hz
   - Bandwidth of voltage controller = 400 hz
   - Resonant frequency = 800 hz

The model used in study is shown in figure 3.27 and is developed in Simulink and based on formula, we put rise time in Simulink linearization parameters and calculate $k_p$and k_i.

$$t_{rise}(sec) = \frac{0.35}{Bandwidth\ (Hz)}$$

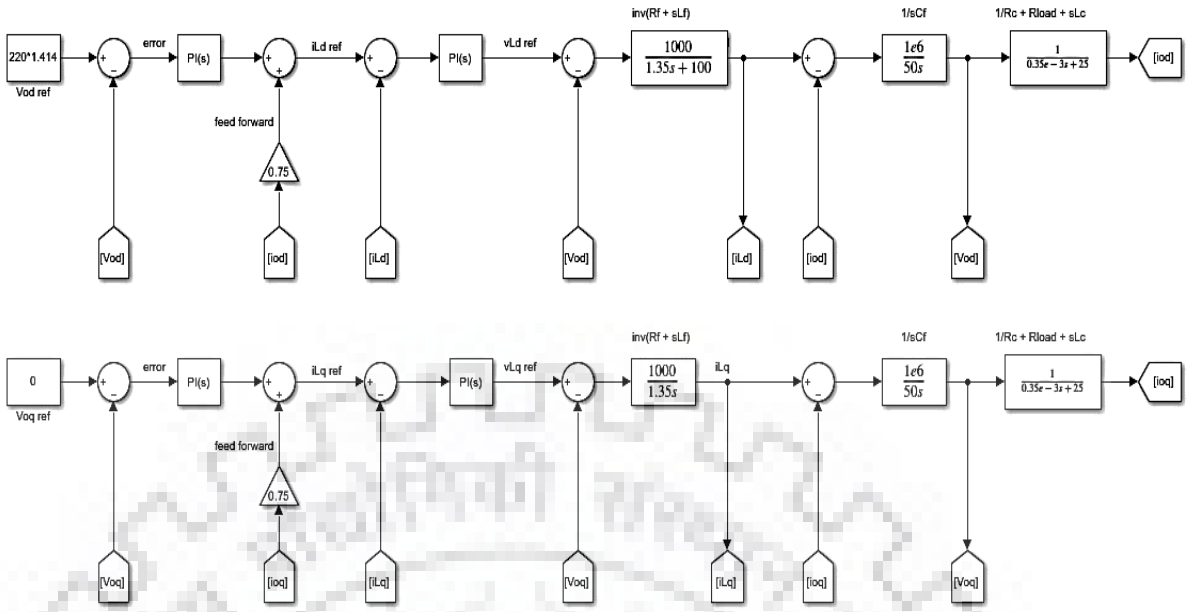

Figure 3. 27: Developed linear model of V/f control for tuning

CHAPTER – 4

LINEARIZATION OF STATE SPACE EQUATION

State space matrix of individual blocks are shown, in both grid connected and isolated mode.

4.1 Grid Connected mode:

a) PLL

(3.19) - (3.20) are used to form matrix (4.1).

$$\begin{bmatrix} \dot{\theta} \\ \dot{\Phi}_{PLL} \end{bmatrix} = \begin{bmatrix} k_{p,PLL} v_{oq} + k_{i,PLL} \Phi_{PLL} \\ V_{oq} \end{bmatrix} \quad \textbf{(4.1)}$$

$$[y] = [\theta]$$

b) Power controller

(3.43)-(3.46) are used to form (4.2), with controller block shown in figure 4.1.

$$\begin{bmatrix} \dot{\imath_{ld}}^* \\ \dot{\imath_{lq}}^* \\ \dot{q_{3d}} \\ \dot{q_{3q}} \end{bmatrix} = \begin{bmatrix} {\omega_c}^2 q_{3d} - \omega_c \sqrt{2} {i_{ld}}^* \\ {\omega_c}^2 q_{3q} - \omega_c \sqrt{2} {i_{lq}}^* \\ \dfrac{v_{od} * P_{ref} - v_{oq} * Q_{ref}}{{v_{od}}^2 + {v_{oq}}^2} + (i_{ld} - i_{od}) - {i_{ld}}^* \\ \dfrac{v_{oq} * P_{ref} + v_{od} * Q_{ref}}{{v_{od}}^2 + {v_{oq}}^2} + (i_{ld} - i_{od}) - {i_{lq}}^* \end{bmatrix} \quad \textbf{(4.2)}$$

$$[y] = \begin{bmatrix} {i_{ld}}^* \\ {i_{lq}}^* \end{bmatrix}$$

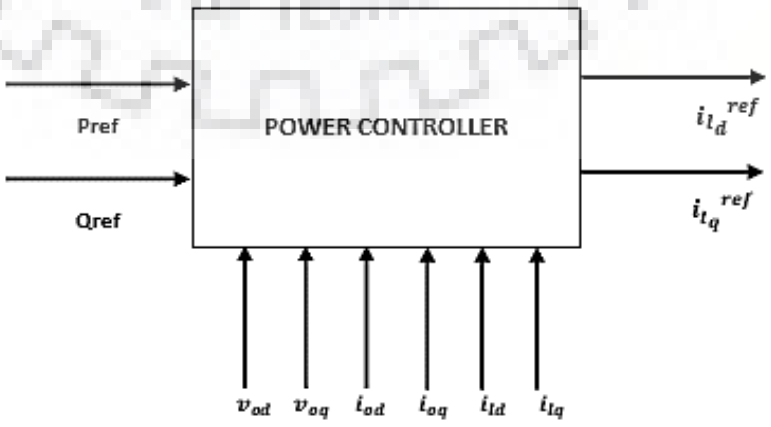

Figure 4. 1: Power controller showing inputs and outputs in grid connected mode

c) **Current controller**

Equations (3.25)-(3.29) are used to form (4.3), with controller block shown in figure 4.2.

$$\begin{bmatrix} \dot{q_d}^{err} \\ \dot{q_q}^{err} \end{bmatrix} = \begin{bmatrix} {i_{ld}}^{err} \\ {i_{lq}}^{err} \end{bmatrix} = \begin{bmatrix} {i_{ld}}^{*} - i_{ld} \\ {i_{lq}}^{*} - i_{lq} \end{bmatrix} \quad \textbf{(4.3)}$$

$$\begin{bmatrix} {v_{ld}}^{ref} \\ {v_{lq}}^{ref} \end{bmatrix} = \begin{bmatrix} v_{od} - \omega L_f i_{lq} + (i_{ld}) r_f + {K_p}^{d,cc} {i_{ld}}^{err} + {K_i}^{d,cc} {q_d}^{err} \\ v_{oq} + \omega L_f i_{ld} + (i_{lq}) r_f + {K_p}^{q,cc} {i_{lq}}^{err} + {K_i}^{q,cc} {q_q}^{err} \end{bmatrix}$$

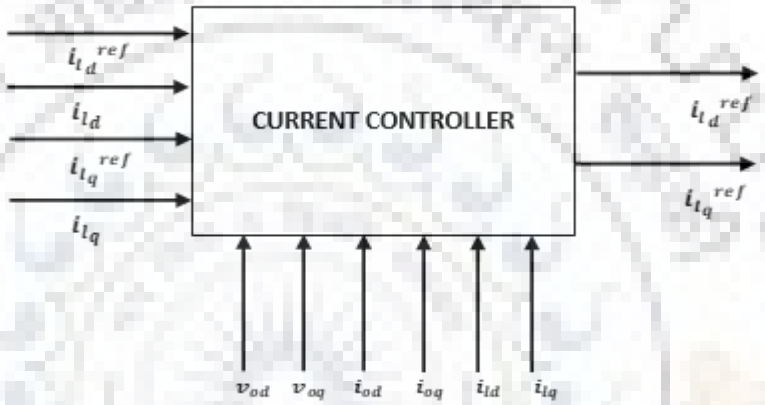

Figure 4. 2: Current controller showing inputs and outputs (along with internally generated inputs) in grid connected mode

d) **LCL filter**

Equation of LCL filter comprising of all the states was shown in (3.101) and rewritten here.

$$\begin{bmatrix} \dot{\Delta i}_{l_d} \\ \dot{\Delta i}_{l_q} \\ \dot{\Delta v}_{o_d} \\ \dot{\Delta v}_{o_q} \\ \dot{\Delta i}_{o_d} \\ \dot{\Delta i}_{o_q} \end{bmatrix} = \begin{bmatrix} \frac{1}{L_f}(\Delta v_{l_d} - \Delta v_{o_d}) + I_{l_q}\Delta\omega + \omega\Delta i_{l_q} - \frac{r_f}{L_f}\Delta i_{l_d} \\ \frac{1}{L_f}(\Delta v_{l_q} - \Delta v_{o_q}) - I_{l_d}\Delta\omega - \omega\Delta i_{l_d} - \frac{r_f}{L_f}\Delta i_{l_q} \\ \frac{1}{c_f}\left(\Delta i_{l_d} - \Delta i_{o_d}\right) + V_{o_q}\Delta\omega + \omega\Delta v_{o_q} \\ \frac{1}{c_f}\left(\Delta i_{l_q} - \Delta i_{o_q}\right) - V_{o_d}\Delta\omega - \omega\Delta v_{o_d} \\ \frac{1}{L_f}(\Delta v_{o_d} - \Delta v_{b_d}) + I_{o_q}\Delta\omega + \omega\Delta i_{o_q} - \frac{r_c}{L_c}\Delta i_{o_d} \\ \frac{1}{L_f}(\Delta v_{o_q} - \Delta v_{b_q}) - I_{o_d}\Delta\omega - \omega\Delta i_{o_d} - \frac{r_c}{L_c}\Delta i_{o_q} \end{bmatrix} \quad \textbf{(4.4)}$$

4.2 Islanded mode:

a) Power controller

Small signal state space equations (3.87) and (3.88), derived previously in section 3.3.3 are shown here. Power controller block is also shown in figure 4.3.

$$\begin{bmatrix} \Delta\dot{\delta} \\ \Delta\dot{P} \\ \Delta\dot{Q} \end{bmatrix} = \begin{bmatrix} -k_p\Delta P - \Delta\omega_{com} \\ -\omega_c\Delta P + \omega_c i_{od}\Delta v_{od} + \omega_c v_{od}\Delta i_{od} + \omega_c i_{oq}\Delta v_{oq} + \omega_c v_{oq}\Delta i_{oq}) \\ -\omega_c\Delta Q + \omega_c i_{oq}\Delta v_{od} + \omega_c v_{od}\Delta i_{oq} - \omega_c i_{od}\Delta v_{oq} - \omega_c v_{oq}\Delta i_{od}) \end{bmatrix}$$

$$\begin{bmatrix} \Delta\omega \\ \Delta {v_o}_d^{\,*} \\ \Delta {v_o}_q^{\,*} \end{bmatrix} = \begin{bmatrix} -k_p\Delta P \\ -k_q\Delta Q \\ 0 \end{bmatrix}$$

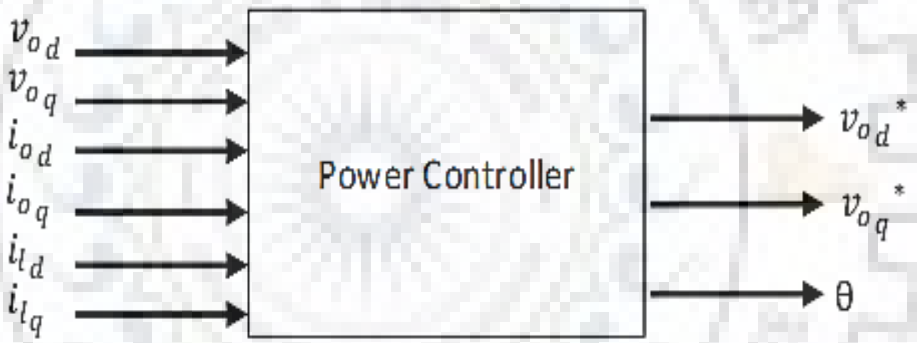

Figure 4. 3: Power controller block having input and outputs in d-q frame in isolated mode.

b) Current controller

Small signal state space equations (3.76) and (3.77) derived previously in section 3.3.3 are shown here. Current controller block is shown in figure 4.4.

$$\begin{bmatrix} \Delta\dot{\gamma}_d \\ \Delta\dot{\gamma}_q \end{bmatrix} = \begin{bmatrix} \Delta {i_{ld}}^{*} - \Delta i_{ld} \\ \Delta {i_{lq}}^{*} - \Delta i_{lq} \end{bmatrix}$$

$$\begin{bmatrix} \Delta {v_l}_d^{\,*} \\ \Delta {v_l}_q^{\,*} \end{bmatrix} = \begin{bmatrix} \Delta i_{l_d} * r_f - \omega L_f \Delta i_{l_q} + {k_{pv}}_q \Delta {i_{ld}}^{*} - {k_{pv}}_d \Delta i_{ld} + {k_{iv}}_d \Delta\gamma_d \\ \Delta i_{l_q} * r_f + \omega L_f \Delta i_{l_d} + {k_{pv}}_q \Delta {i_{lq}}^{*} - {k_{pv}}_q \Delta i_{lq} + {k_{iv}}_q \Delta\gamma_q \end{bmatrix}$$

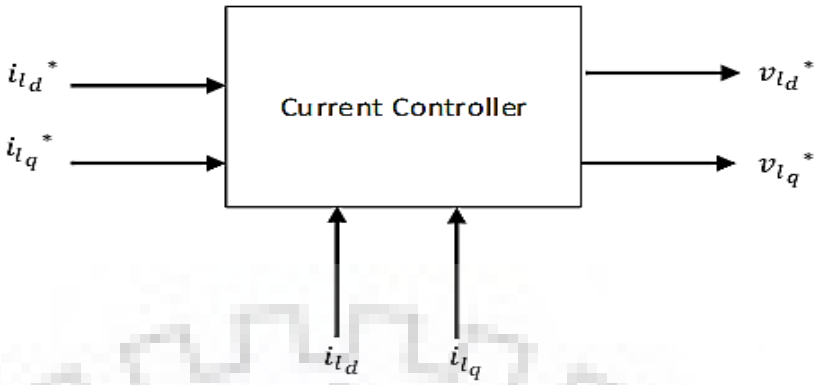

Figure 4. 4: Current controller block showing inputs and outputs (along with internally generated inputs) in d-q frame in isolated mode

c) Voltage controller

Small signal state space equations (3.13) and (3.14) derived previously in section 3.3.3, are shown here. Voltage controller block is shown in figure 4.5.

$$\begin{bmatrix}\Delta\dot{\varphi}_d\\ \Delta\dot{\varphi}_q\end{bmatrix} = \begin{bmatrix}\Delta \mathrm{v_{od}}^* - \Delta \mathrm{v_{od}}\\ \Delta \mathrm{v_{oq}}^* - \Delta \mathrm{v_{oq}}\end{bmatrix}$$

$$\begin{bmatrix}\Delta {i_{ld}}^*\\ \Delta {i_{lq}}^*\end{bmatrix} = \begin{bmatrix}F\Delta \mathrm{i}_{od} - \omega C_f \Delta v_{oq} + {k_{pv}}_d \Delta {v_{od}}^* - {k_{pv}}_d \Delta v_{od} + {k_{iv}}_d \Delta\varphi_d\\ F\Delta \mathrm{i}_{oq} + \omega C_f \Delta v_{od} + {k_{pv}}_q \Delta {v_{oq}}^* - {k_{pv}}_q \Delta v_{oq} + {k_{iv}}_q \Delta\varphi_q\end{bmatrix}$$

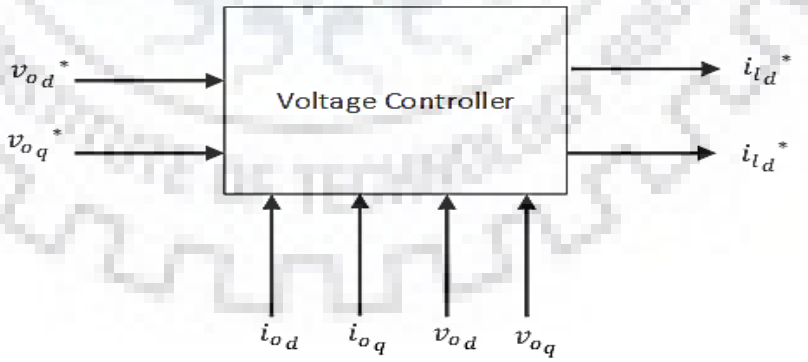

Figure 4. 5: Voltage controller block showing inputs and outputs (along with internally generated inputs) in d-q frame.

d) LCL filter

Small signal state space (3.101) derived previously in section 3.3.3, is shown here.

Equations are obtained by assuming that $v_{l_{dq}} = v_{l_{dq}}{}^{*}$and arranged to from complete state space model.

$$\begin{bmatrix} \Delta\dot{\mathrm{i}}_{\mathrm{l}_d} \\ \Delta\dot{\mathrm{i}}_{\mathrm{l}_q} \\ \Delta\dot{\mathrm{v}}_{\mathrm{o}_d} \\ \Delta\dot{\mathrm{v}}_{\mathrm{o}_q} \\ \Delta\dot{\mathrm{i}}_{\mathrm{o}_d} \\ \Delta\dot{\mathrm{i}}_{\mathrm{o}_q} \end{bmatrix} = \begin{bmatrix} \frac{1}{\mathrm{L_f}}(\Delta \mathrm{v}_{\mathrm{l}_d} - \Delta \mathrm{v}_{\mathrm{o}_d}) + \mathrm{I}_{\mathrm{l}_q}\Delta\omega + \omega\Delta \mathrm{i}_{\mathrm{l}_q} - \frac{\mathrm{r_f}}{\mathrm{L_f}}\Delta \mathrm{i}_{\mathrm{l}_d} \\ \frac{1}{\mathrm{L_f}}(\Delta \mathrm{v}_{\mathrm{l}_q} - \Delta \mathrm{v}_{\mathrm{o}_q}) - \mathrm{I}_{\mathrm{l}_d}\Delta\omega - \omega\Delta \mathrm{i}_{\mathrm{l}_d} - \frac{\mathrm{r_f}}{\mathrm{L_f}}\Delta \mathrm{i}_{\mathrm{l}_q} \\ \frac{1}{c_f}\left(\Delta i_{l_d} - \Delta i_{o_d}\right) + \mathrm{V}_{\mathrm{o}_q}\Delta\omega + \omega\Delta \mathrm{v}_{\mathrm{o}_q} \\ \frac{1}{c_f}\left(\Delta i_{l_q} - \Delta i_{o_q}\right) - \omega\Delta \mathrm{v}_{\mathrm{o}_d} - \mathrm{V}_{\mathrm{o}_d}\Delta\omega \\ \frac{1}{\mathrm{L_f}}(\Delta \mathrm{v}_{\mathrm{o}_d} - \Delta \mathrm{v}_{\mathrm{b}_d}) + \mathrm{I}_{\mathrm{o}_q}\Delta\omega + \omega\Delta \mathrm{i}_{\mathrm{o}_q} - \frac{\mathrm{r_c}}{\mathrm{L_c}}\Delta \mathrm{i}_{\mathrm{o}_d} \\ \frac{1}{\mathrm{L_f}}(\Delta \mathrm{v}_{\mathrm{o}_q} - \Delta \mathrm{v}_{\mathrm{b}_q}) - \mathrm{I}_{\mathrm{o}_d}\Delta\omega - \omega\Delta \mathrm{i}_{\mathrm{o}_d} - \frac{\mathrm{r_c}}{\mathrm{L_c}}\Delta \mathrm{i}_{\mathrm{o}_q} \end{bmatrix}$$

4.3 Complete Model of inverter

In case of multiple inverters, their inputs and outputs should be transformed to common reference frame as depicted in (4.5).

Output of an inverter: $i_{o\,dq}$

Input to an inverter: $v_{b\,dq}$

Converting inverter to common reference frame and its output $i_{o\,dq}$ and input $v_{b\,dq}$ are converted as shown in (4.5)

$$[f_{DQ}] = \begin{bmatrix} \cos\delta & -\sin\delta \\ \sin\delta & \cos\delta \end{bmatrix}[f_{dq}] \quad \textbf{(4.5)}$$

Here f_{DQ} is common reference frame and f_{dq} is individual frame and δ is angle between both frames, now applying small signal we get (4.6).

$$[\Delta f_{DQ}] = \begin{bmatrix} \cos\delta & -\sin\delta \\ \sin\delta & \cos\delta \end{bmatrix}[\Delta f_{dq}] + \begin{bmatrix} -\sin\delta & -\cos\delta \\ \cos\delta & -\sin\delta \end{bmatrix}[f_{dq}]\Delta\delta \quad \textbf{(4.6)}$$

Now converting output into common reference frame in (4.7).

$$\begin{bmatrix} \Delta i_{o_D} \\ \Delta i_{o_Q} \end{bmatrix} = \begin{bmatrix} \cos\delta & -\sin\delta \\ \sin\delta & \cos\delta \end{bmatrix}\begin{bmatrix} \Delta i_{o_d} \\ \Delta i_{o_q} \end{bmatrix} + \begin{bmatrix} -\sin\delta & -\cos\delta \\ \cos\delta & -\sin\delta \end{bmatrix}\begin{bmatrix} I_{o_d} \\ I_{o_q} \end{bmatrix}\Delta\delta$$

$$\begin{bmatrix}\Delta i_{o_{DQ}}\end{bmatrix} = \begin{bmatrix}\cos\delta & -\sin\delta \\ \sin\delta & \cos\delta\end{bmatrix}\begin{bmatrix}\Delta i_{o_{dq}}\end{bmatrix} + \begin{bmatrix}-\sin\delta & -\cos\delta \\ \cos\delta & -\sin\delta\end{bmatrix}\begin{bmatrix}I_{o_{dq}}\end{bmatrix}\Delta\delta \quad \textbf{(4.7)}$$

Also input needs to be converted into common reference frame and for that we use (4.8) and input in common reference frame is expressed in (4.9).

$$\begin{bmatrix}f_{dq}\end{bmatrix} = \begin{bmatrix}\cos\delta & -\sin\delta \\ \sin\delta & \cos\delta\end{bmatrix}^{-1}\begin{bmatrix}f_{DQ}\end{bmatrix}$$

$$\begin{bmatrix}\Delta f_{dq}\end{bmatrix} = \begin{bmatrix}\cos\delta & \sin\delta \\ -\sin\delta & \cos\delta\end{bmatrix}\begin{bmatrix}\Delta f_{DQ}\end{bmatrix} + \begin{bmatrix}-\sin\delta & \cos\delta \\ -\cos\delta & -\sin\delta\end{bmatrix}\begin{bmatrix}\Delta f_{DQ}\end{bmatrix}\Delta\delta \quad \textbf{(4.8)}$$

$$\begin{bmatrix}\Delta v_{b_d} \\ \Delta v_{b_q}\end{bmatrix} = \begin{bmatrix}\cos\delta & \sin\delta \\ -\sin\delta & \cos\delta\end{bmatrix}\begin{bmatrix}\Delta v_{b_D} \\ \Delta v_{b_Q}\end{bmatrix} + \begin{bmatrix}-\sin\delta & \cos\delta \\ -\cos\delta & -\sin\delta\end{bmatrix}\begin{bmatrix}V_{b_D} \\ V_{b_Q}\end{bmatrix}\Delta\delta \quad \textbf{(4.9)}$$

4.4 State space equations

Arranging derived equations into state space form, shown through equations (4.10)-(4.11).

$$\dot{x} = Ax + Bu \quad \textbf{(4.10)}$$

$$y = Cx + Du \quad \textbf{(4.11)}$$

Where u is input matrix, x is state vector matrix and y is output matrix.

4.4.1 Grid connected mode

a) PLL

$$\begin{bmatrix}\dot{\theta} \\ \dot{\Phi}_{PLL}\end{bmatrix} = \begin{bmatrix}0 & \mathrm{k_{i,PLL}} \\ 0 & 0\end{bmatrix}\begin{bmatrix}\theta \\ \Phi_{PLL}\end{bmatrix} + \begin{bmatrix}0 & \mathrm{k_{p,PLL}} \\ 0 & 1\end{bmatrix}\begin{bmatrix}\mathrm{V_{od}} \\ \mathrm{V_{oq}}\end{bmatrix} \quad \textbf{(4.12)}$$

b) Power controller

$$\begin{bmatrix}\dot{i_{ld}}^* \\ \dot{i_{lq}}^* \\ \dot{q_{3d}} \\ \dot{q_{3q}}\end{bmatrix} = \begin{bmatrix}-\sqrt{2}\omega_c & 0 & {\omega_c}^2 & 0 \\ 0 & -\sqrt{2}\omega_c & 0 & {\omega_c}^2 \\ -1 & 0 & 0 & 0 \\ 0 & -1 & 0 & 0\end{bmatrix}\begin{bmatrix}{i_{ld}}^* \\ {i_{lq}}^* \\ q_{3d} \\ q_{3q}\end{bmatrix} + \begin{bmatrix}0 \\ 0 \\ \frac{\mathrm{v_{od}}*\mathrm{P_{ref}}-\mathrm{v_{oq}}*\mathrm{Q_{ref}}}{{\mathrm{v_{od}}^2+\mathrm{v_{oq}}^2}} + i_{ld} - i_{od} \\ \frac{\mathrm{v_{oq}}*\mathrm{P_{ref}}+\mathrm{v_{od}}*\mathrm{Q_{ref}}}{{\mathrm{v_{od}}^2+\mathrm{v_{oq}}^2}} + i_{ld} - i_{od}\end{bmatrix} \quad \textbf{(4.13)}$$

Non linearity can clearly be seen here but through small signal analysis can be linearized.

c) Current controller

$$\begin{bmatrix} \dot{q}_d^{err} \\ \dot{q}_q^{err} \end{bmatrix} = \begin{bmatrix} 0 & 0 \\ 0 & 0 \end{bmatrix} \begin{bmatrix} q_d^{err} \\ q_q^{err} \end{bmatrix} + \begin{bmatrix} 1 & 0 & -1 & 0 & 0 & 0 & 0 \\ 0 & 1 & 0 & -1 & 0 & 0 & 0 \end{bmatrix} \begin{bmatrix} i_{ld}^{*} \\ i_{lq}^{*} \\ i_{ld} \\ i_{lq} \\ v_{od} \\ v_{oq} \\ \omega \end{bmatrix} \quad \textbf{(4.14)}$$

d) LCL filter

$$\begin{bmatrix} \Delta\dot{i}_{l_d} \\ \Delta\dot{i}_{l_q} \\ \Delta\dot{v}_{o_d} \\ \Delta\dot{v}_{o_q} \\ \Delta\dot{i}_{o_d} \\ \Delta\dot{i}_{o_q} \end{bmatrix} = \begin{bmatrix} -\frac{r_f}{L_f} & \omega & -\frac{1}{L_f} & 0 & 0 & 0 \\ -\omega & -\frac{r_f}{L_f} & 0 & -\frac{1}{L_f} & 0 & 0 \\ \frac{1}{c_f} & 0 & 0 & \omega & -\frac{1}{c_f} & 0 \\ 0 & \frac{1}{c_f} & -\omega & 0 & 0 & -\frac{1}{c_f} \\ 0 & 0 & \frac{1}{L_c} & 0 & -\frac{r_c}{L_c} & \omega \\ 0 & 0 & 0 & \frac{1}{L_c} & -\omega & -\frac{r_c}{L_c} \end{bmatrix} \begin{bmatrix} \Delta i_{ld} \\ \Delta i_{lq} \\ \Delta v_{od} \\ \Delta v_{oq} \\ \Delta i_{od} \\ \Delta i_{oq} \end{bmatrix} + \begin{bmatrix} 0 & 0 \\ 0 & 0 \\ 0 & 0 \\ 0 & 0 \\ -\frac{1}{L_c} & 0 \\ 0 & -\frac{1}{L_c} \end{bmatrix} \begin{bmatrix} \Delta v_{bd} \\ \Delta v_{bq} \end{bmatrix} + \begin{bmatrix} \frac{1}{L_f} & 0 \\ 0 & \frac{1}{L_f} \\ 0 & 0 \\ 0 & 0 \\ 0 & 0 \\ 0 & 0 \end{bmatrix} \begin{bmatrix} \Delta v_{ld} \\ \Delta v_{lq} \end{bmatrix} + \begin{bmatrix} I_{l_q} \\ -I_{l_d} \\ V_{o_q} \\ -V_{o_d} \\ I_{o_q} \\ -I_{o_d} \end{bmatrix} \Delta\omega \quad \textbf{(4.15)}$$

$$u = \begin{bmatrix} v_{od} \\ v_{oq} \\ P^* \\ Q^* \\ \omega \end{bmatrix}, \; x = \begin{bmatrix} x_1 \\ x_2 \\ x_3 \\ x_4 \\ x_5 \\ x_6 \end{bmatrix} \text{ and } y = \begin{bmatrix} i_{ld} \\ i_{lq} \\ i_{od} \\ i_{oq} \end{bmatrix} \quad \textbf{(4.16)}$$

Above equations are arranged and complete state space model is developed, alongwith individual state space equation. Combining all the equations, it is observed that 14 eigen values are there. Figure 4.6 shows the state variables of each subsystems, with developed model of CCI (current controlled inverter).

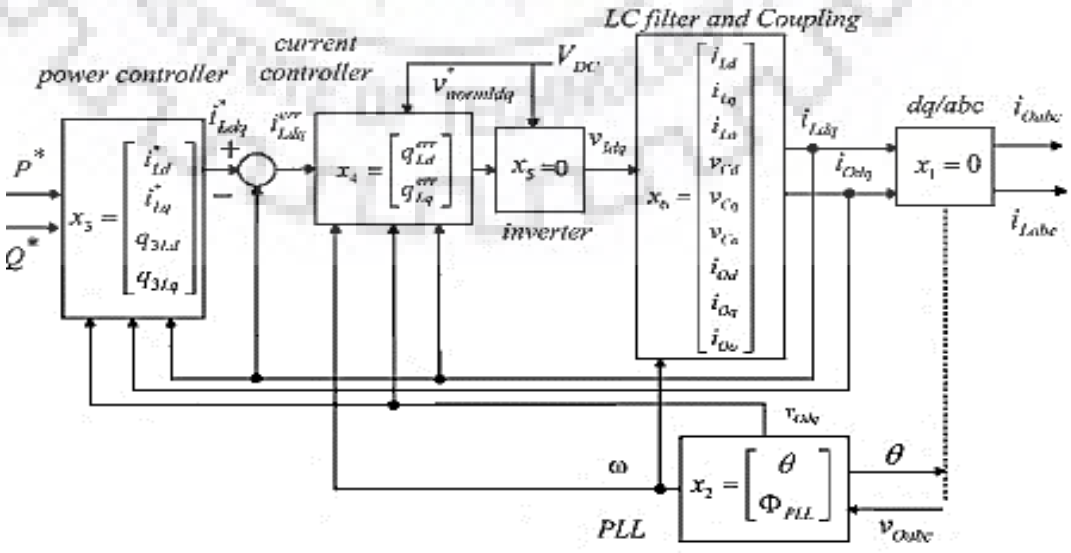

Figure 4. 6: Grid connected inverter model showing state vectors of each subsystem

System developed is of the form as described through (4.17), which is non-linear. For linearization purpose an operating point is found out by simulation. So for convenience purpose Simulink model developed has been used to find steady state value or stable operating point as shown in table 4.1.

$$\dot{x} = Ax + Bu + R(x, u) \quad \textbf{(4.17)}$$

Table 4. 1: Calculated operating point

Parameters	Value
v_{od}	*350*
v_{oq}	*0*
i_{od}	*19*
i_{oq}	*-10*
v_{bd}	*340*
v_{bq}	*-12*
i_{ld}	*20*
i_{lq}	*-9*
P_{ref}	*10000*
Q_{ref}	*5000*
v_{ld}	*400*
v_{lq}	*0*
v_{cd}	*350*
v_{cq}	*0*
ω	*314*

Here voltages are in volt and current in ampere and P_{ref} and Q_{ref} in watt and ω in rad/sec. Using the above values, equations are linearized as per taylor series **[48]**. Now we have A, B, C, D matrices which are used for further analysis.

4.4.2 Islanded mode

The inputs (u), outputs (y) and state variables (x) in this mode are shown in (4.18).

$$u = \begin{bmatrix} v_{b_d} \\ v_{b_q} \end{bmatrix}, x = \begin{bmatrix} \Delta\delta \\ \Delta P \\ \Delta Q \\ \Delta\varphi_d \\ \Delta\varphi_q \\ \Delta\gamma_d \\ \Delta\gamma_q \\ \Delta i_{l_d} \\ \Delta i_{l_q} \\ \Delta v_{o_d} \\ \Delta v_{o_q} \\ \Delta i_{o_d} \\ \Delta i_{o_q} \end{bmatrix} \text{ and } y = \begin{bmatrix} i_{o_d} \\ i_{o_q} \\ \omega \end{bmatrix} \quad \textbf{(4.18)}$$

a) Power Controller

Equations (3.94) derived in section 3.3.3, is now converted to state space form and expressed in (4.19) and (4.20).

$$\begin{bmatrix} \dot{\Delta\delta} \\ \dot{\Delta P} \\ \dot{\Delta Q} \end{bmatrix} = \begin{bmatrix} 0 & -k_p & 0 \\ 0 & -\omega_c & 0 \\ 0 & 0 & -\omega_c \end{bmatrix} \begin{bmatrix} \Delta\delta \\ \Delta P \\ \Delta Q \end{bmatrix} + \begin{bmatrix} 0 & 0 & 0 & 0 & 0 & 0 \\ 0 & 0 & \omega_c I_{od} & \omega_c I_{oq} & \omega_c V_{od} & \omega_c V_{oq} \\ 0 & 0 & \omega_c I_{oq} & -\omega_c I_{od} & -\omega_c V_{oq} & \omega_c V_{od} \end{bmatrix} \begin{bmatrix} \Delta i_{ld} \\ \Delta i_{lq} \\ \Delta v_{od} \\ \Delta v_{oq} \\ \Delta i_{od} \\ \Delta i_{oq} \end{bmatrix} + \begin{bmatrix} -1 \\ 0 \\ 0 \end{bmatrix} [\Delta\omega_{ref}] \quad \textbf{(4.19)}$$

$$\begin{bmatrix} \dot{\Delta\delta} \\ \dot{\Delta P} \\ \dot{\Delta Q} \end{bmatrix} = [A_p] \begin{bmatrix} \Delta\delta \\ \Delta P \\ \Delta Q \end{bmatrix} + [B_p] \begin{bmatrix} \Delta i_{ld} \\ \Delta i_{lq} \\ \Delta v_{od} \\ \Delta v_{oq} \\ \Delta i_{od} \\ \Delta i_{oq} \end{bmatrix} + \left[B_{p_{wcom}}\right] [\Delta\omega_{ref}] \quad \textbf{(4.20)}$$

In (4.20), variables used are defined below.

$$[A_p] = \begin{bmatrix} 0 & -k_p & 0 \\ 0 & -\omega_c & 0 \\ 0 & 0 & -\omega_c \end{bmatrix}, [B_p] = \begin{bmatrix} 0 & 0 & 0 & 0 & 0 & 0 \\ 0 & 0 & \omega_c I_{od} & \omega_c I_{oq} & \omega_c V_{od} & \omega_c V_{oq} \\ 0 & 0 & \omega_c I_{oq} & -\omega_c I_{od} & -\omega_c V_{oq} & \omega_c V_{od} \end{bmatrix}, \left[B_{p_{wcom}}\right] = \begin{bmatrix} -1 \\ 0 \\ 0 \end{bmatrix}$$

$\Delta\omega_{ref}$ is frequency deviation of common reference frame, used for connecting additional inverters. Output is also shown in (4.21) and (4.22) which is derived from (3.95).

$$\begin{bmatrix} \Delta\omega \\ \Delta v_{o_d}^* \\ \Delta v_{o_q}^* \end{bmatrix} = \begin{bmatrix} 0 & -k_p & 0 \\ 0 & 0 & -k_q \\ 0 & 0 & 0 \end{bmatrix} \begin{bmatrix} \Delta\delta \\ \Delta P \\ \Delta Q \end{bmatrix} \quad \textbf{(4.21)}$$

$$\begin{bmatrix} \Delta\omega \\ \Delta {v_o}_d^* \\ \Delta {v_o}_q^* \end{bmatrix} = \begin{bmatrix} C_{p_w} \\ C_{p_v} \\ 0 \end{bmatrix} \begin{bmatrix} \Delta\delta \\ \Delta P \\ \Delta Q \end{bmatrix} \quad \textbf{(4.22)}$$

Where, $\begin{bmatrix} C_{p_w} \\ C_{p_v} \\ 0 \end{bmatrix} = \begin{bmatrix} 0 & -k_p & 0 \\ 0 & 0 & -k_q \\ 0 & 0 & 0 \end{bmatrix}$

b) Voltage Controller

Equations (3.13) and (3.14) derived in section 3.3.3, are now converted to state space form and expressed in (4.23)-(4.26).

$$\begin{bmatrix} \Delta\dot{\varphi}_d \\ \Delta\dot{\varphi}_q \end{bmatrix} = [0] \begin{bmatrix} \Delta\varphi_d \\ \Delta\varphi_q \end{bmatrix} + \begin{bmatrix} 1 & 0 \\ 0 & 1 \end{bmatrix} \begin{bmatrix} \Delta {v_{od}}^* \\ \Delta {v_{oq}}^* \end{bmatrix} + \begin{bmatrix} -1 & 0 \\ 0 & -1 \end{bmatrix} \begin{bmatrix} \Delta v_{od} \\ \Delta v_{oq} \end{bmatrix} \quad \textbf{(4.23)}$$

$$\begin{bmatrix} \Delta\dot{\varphi}_d \\ \Delta\dot{\varphi}_q \end{bmatrix} = [0] \begin{bmatrix} \Delta\varphi_d \\ \Delta\varphi_q \end{bmatrix} + [B_{v1}] \begin{bmatrix} \Delta {v_{od}}^* \\ \Delta {v_{oq}}^* \end{bmatrix} + [B_{v2}] \begin{bmatrix} \Delta v_{od} \\ \Delta v_{oq} \end{bmatrix} \quad \textbf{(4.24)}$$

$$\begin{bmatrix} \Delta {i_{ld}}^* \\ \Delta {i_{lq}}^* \end{bmatrix} = \begin{bmatrix} k_{iv_d} & 0 \\ 0 & k_{iv_q} \end{bmatrix} \begin{bmatrix} \Delta\varphi_d \\ \Delta\varphi_q \end{bmatrix} + \begin{bmatrix} k_{pv_d} & 0 \\ 0 & k_{pv_q} \end{bmatrix} \begin{bmatrix} \Delta {v_{od}}^* \\ \Delta {v_{oq}}^* \end{bmatrix} + \begin{bmatrix} 0 & 0 & -k_{pv_d} & -\omega C_f & F & 0 \\ 0 & 0 & \omega C_f & -k_{pv_q} & 0 & F \end{bmatrix} \begin{bmatrix} \Delta i_{ld} \\ \Delta i_{lq} \\ \Delta v_{od} \\ \Delta v_{oq} \\ \Delta i_{od} \\ \Delta i_{oq} \end{bmatrix} \quad \textbf{(4.25)}$$

$$\begin{bmatrix} \Delta {i_{ld}}^* \\ \Delta {i_{lq}}^* \end{bmatrix} = [C_v] \begin{bmatrix} \Delta\varphi_d \\ \Delta\varphi_q \end{bmatrix} + [D_{v1}] \begin{bmatrix} \Delta {v_{od}}^* \\ \Delta {v_{oq}}^* \end{bmatrix} + [D_{v2}] \begin{bmatrix} \Delta i_{ld} \\ \Delta i_{lq} \\ \Delta v_{od} \\ \Delta v_{oq} \\ \Delta i_{od} \\ \Delta i_{oq} \end{bmatrix} \quad \textbf{(4.26)}$$

Variables used in (4.24) and (4.26) are defined as,

$$[B_{v1}] = \begin{bmatrix} 1 & 0 \\ 0 & 1 \end{bmatrix}, [B_{v2}] = \begin{bmatrix} -1 & 0 \\ 0 & -1 \end{bmatrix}, [C_v] = \begin{bmatrix} k_{iv_d} & 0 \\ 0 & k_{iv_q} \end{bmatrix}$$

$$[D_{v1}] = \begin{bmatrix} k_{pv_d} & 0 \\ 0 & k_{pv_q} \end{bmatrix}, [D_{v2}] = \begin{bmatrix} 0 & 0 & -k_{pv_d} & -\omega C_f & F & 0 \\ 0 & 0 & \omega C_f & -k_{pv_q} & 0 & F \end{bmatrix}$$

c) Current Controller

Equations (3.76) and (3.77) derived in section 3.3.3, are now converted to state space form and shown in (4.27)-(4.30). Here we have assumed that no feedforward loop is there and internal resistance of filter inductance i.e. r_f is zero.

$$\begin{bmatrix}\Delta\dot{\Upsilon}_d\\ \Delta\dot{\Upsilon}_q\end{bmatrix}=[0]\begin{bmatrix}\Delta\Upsilon_d\\ \Delta\Upsilon_q\end{bmatrix}+\begin{bmatrix}1 & 0\\ 0 & 1\end{bmatrix}\begin{bmatrix}\Delta i_{ld}{}^*\\ \Delta i_{lq}{}^*\end{bmatrix}+\begin{bmatrix}-1 & 0 & 0 & 0 & 0 & 0\\ 0 & -1 & 0 & 0 & 0 & 0\end{bmatrix}\begin{bmatrix}\Delta i_{ld}\\ \Delta i_{lq}\\ \Delta v_{od}\\ \Delta v_{oq}\\ \Delta i_{od}\\ \Delta i_{oq}\end{bmatrix} \quad \textbf{(4.27)}$$

$$\begin{bmatrix}\Delta\dot{\Upsilon}_d\\ \Delta\dot{\Upsilon}_q\end{bmatrix}=[0]\begin{bmatrix}\Delta\Upsilon_d\\ \Delta\Upsilon_q\end{bmatrix}+[B_{c1}]\begin{bmatrix}\Delta i_{ld}{}^*\\ \Delta i_{lq}{}^*\end{bmatrix}+[B_{c2}]\begin{bmatrix}\Delta i_{ld}\\ \Delta i_{lq}\\ \Delta v_{od}\\ \Delta v_{oq}\\ \Delta i_{od}\\ \Delta i_{oq}\end{bmatrix} \quad \textbf{(4.28)}$$

$$\begin{bmatrix}\Delta \mathrm{v}_{1_d}{}^*\\ \Delta \mathrm{v}_{1_q}{}^*\end{bmatrix}=\begin{bmatrix}k_{ic_d} & 0\\ 0 & k_{ic_q}\end{bmatrix}\begin{bmatrix}\Delta\Upsilon_d\\ \Delta\Upsilon_q\end{bmatrix}+\begin{bmatrix}k_{pc_d} & 0\\ 0 & k_{pc_q}\end{bmatrix}\begin{bmatrix}\Delta i_{ld}{}^*\\ \Delta i_{lq}{}^*\end{bmatrix}+\begin{bmatrix}-k_{pc_d} & -\omega L_f & 0 & 0 & 0 & 0\\ \omega L_f & -k_{pc_q} & 0 & 0 & 0 & 0\end{bmatrix}\begin{bmatrix}\Delta i_{ld}\\ \Delta i_{lq}\\ \Delta v_{od}\\ \Delta v_{oq}\\ \Delta i_{od}\\ \Delta i_{oq}\end{bmatrix} \quad \textbf{(4.29)}$$

$$\begin{bmatrix}\Delta \mathrm{v}_{1_d}{}^*\\ \Delta \mathrm{v}_{1_q}{}^*\end{bmatrix}=[C_c]\begin{bmatrix}\Delta\Upsilon_d\\ \Delta\Upsilon_q\end{bmatrix}+[D_{c1}]\begin{bmatrix}\Delta i_{ld}{}^*\\ \Delta i_{lq}{}^*\end{bmatrix}+[D_{c2}]\begin{bmatrix}\Delta i_{ld}\\ \Delta i_{lq}\\ \Delta v_{od}\\ \Delta v_{oq}\\ \Delta i_{od}\\ \Delta i_{oq}\end{bmatrix} \quad \textbf{(4.30)}$$

Variables used in (4.28) and (4.30) used are stated as,

$$[B_{c1}]=\begin{bmatrix}1 & 0\\ 0 & 1\end{bmatrix},[B_{c2}]=\begin{bmatrix}-1 & 0 & 0 & 0 & 0 & 0\\ 0 & -1 & 0 & 0 & 0 & 0\end{bmatrix},[C_c]=\begin{bmatrix}k_{ic_d} & 0\\ 0 & k_{ic_q}\end{bmatrix}$$

$$[D_{c1}]=\begin{bmatrix}k_{pc_d} & 0\\ 0 & k_{pc_q}\end{bmatrix},[D_{c2}]=\begin{bmatrix}-k_{pc_d} & -\omega L_f & 0 & 0 & 0 & 0\\ \omega L_f & -k_{pc_q} & 0 & 0 & 0 & 0\end{bmatrix}$$

d) LCL Filter

Equations (3.109) derived in section 3.3.3 is converted to state space form (4.31) and (4.32). Derived equations (4.22), (4.24), (4.26), (4.28), (4.30), (4.32), (4.20) are used to model the inverter and stability has been analysed in next section. Schematic diagram showing different controller blocks and filter block is shown in figure 4.7. It can clearly be observed that 13 states are there.

$$\begin{bmatrix} \Delta\dot{i}_{l_d} \\ \Delta\dot{i}_{l_q} \\ \Delta\dot{v}_{o_d} \\ \Delta\dot{v}_{o_q} \\ \Delta\dot{\imath}_{o_d} \\ \Delta\dot{\imath}_{o_q} \end{bmatrix} = \begin{bmatrix} -\frac{r_f}{L_f} & \omega & -\frac{1}{L_f} & 0 & 0 & 0 \\ -\omega & -\frac{r_f}{L_f} & 0 & -\frac{1}{L_f} & 0 & 0 \\ \frac{1}{c_f} & 0 & 0 & \omega & -\frac{1}{c_f} & 0 \\ 0 & \frac{1}{c_f} & -\omega & 0 & 0 & -\frac{1}{c_f} \\ 0 & 0 & \frac{1}{L_c} & 0 & -\frac{r_c}{L_c} & \omega \\ 0 & 0 & 0 & \frac{1}{L_c} & -\omega & -\frac{r_c}{L_c} \end{bmatrix} \begin{bmatrix} \Delta i_{ld} \\ \Delta i_{lq} \\ \Delta v_{od} \\ \Delta v_{oq} \\ \Delta i_{od} \\ \Delta i_{oq} \end{bmatrix} + \begin{bmatrix} 0 & 0 \\ 0 & 0 \\ 0 & 0 \\ 0 & 0 \\ -\frac{1}{L_c} & 0 \\ 0 & -\frac{1}{L_c} \end{bmatrix} \begin{bmatrix} \Delta v_{bd} \\ \Delta v_{bq} \end{bmatrix} + \begin{bmatrix} \frac{1}{L_f} & 0 \\ 0 & \frac{1}{L_f} \\ 0 & 0 \\ 0 & 0 \\ 0 & 0 \\ 0 & 0 \end{bmatrix} \begin{bmatrix} \Delta v_{ld} \\ \Delta v_{lq} \end{bmatrix} + \begin{bmatrix} I_{l_q} \\ -I_{l_d} \\ V_{o_q} \\ -V_{o_d} \\ I_{o_q} \\ -I_{o_d} \end{bmatrix} \Delta\omega \quad \textbf{(4.31)}$$

$$\begin{bmatrix} \Delta\dot{i}_{l_d} \\ \Delta\dot{i}_{l_q} \\ \Delta\dot{v}_{o_d} \\ \Delta\dot{v}_{o_q} \\ \Delta\dot{\imath}_{o_d} \\ \Delta\dot{\imath}_{o_q} \end{bmatrix} = [A_{LCL}] \begin{bmatrix} \Delta i_{ld} \\ \Delta i_{lq} \\ \Delta v_{od} \\ \Delta v_{oq} \\ \Delta i_{od} \\ \Delta i_{oq} \end{bmatrix} + [B_{LCL1}] \begin{bmatrix} \Delta v_{ld} \\ \Delta v_{lq} \end{bmatrix} + [B_{LCL2}] \begin{bmatrix} \Delta v_{bd} \\ \Delta v_{bq} \end{bmatrix} + [B_{LCL3}]\Delta\omega \quad \textbf{(4.32)}$$

Where,

$$[A_{LCL}] = \begin{bmatrix} -\frac{r_f}{L_f} & \omega & -\frac{1}{L_f} & 0 & 0 & 0 \\ -\omega & -\frac{r_f}{L_f} & 0 & -\frac{1}{L_f} & 0 & 0 \\ \frac{1}{c_f} & 0 & 0 & \omega & -\frac{1}{c_f} & 0 \\ 0 & \frac{1}{c_f} & -\omega & 0 & 0 & -\frac{1}{c_f} \\ 0 & 0 & \frac{1}{L_c} & 0 & -\frac{r_c}{L_c} & \omega \\ 0 & 0 & 0 & \frac{1}{L_c} & -\omega & -\frac{r_c}{L_c} \end{bmatrix}, [B_{LCL1}] = \begin{bmatrix} \frac{1}{L_f} & 0 \\ 0 & \frac{1}{L_f} \\ 0 & 0 \\ 0 & 0 \\ 0 & 0 \\ 0 & 0 \end{bmatrix}, [B_{LCL2}] = \begin{bmatrix} 0 & 0 \\ 0 & 0 \\ 0 & 0 \\ 0 & 0 \\ -\frac{1}{L_c} & 0 \\ 0 & -\frac{1}{L_c} \end{bmatrix}, [B_{LCL3}] = \begin{bmatrix} I_{l_q} \\ -I_{l_d} \\ V_{o_q} \\ -V_{o_d} \\ I_{o_q} \\ -I_{o_d} \end{bmatrix}$$

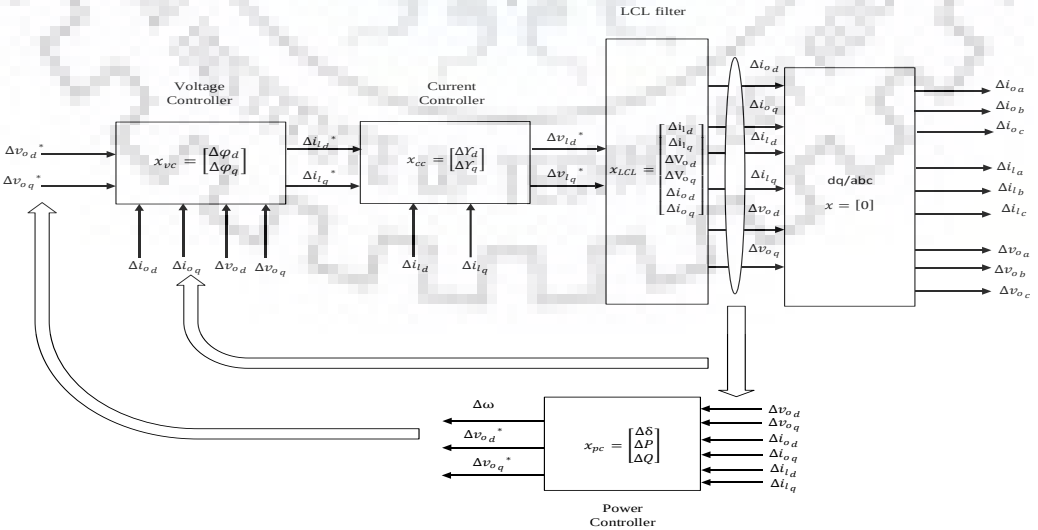

Figure 4. 7: Inverter model showing state vectors of each subsystem in autonomous mode

System is linearized around an operating point and tuning parameters are shown in table 4.3 calculated through simulation. Simulink model has been developed to find steady state value or stable operating point as shown in table 4.2.

Table 4. 2: Initial operating point

Parameters	Value
V_{od}	310.7
V_{oq}	-4.3
I_{od}	8.87
I_{oq}	-5.32
V_{bd}	265.9
V_{bq}	-159.85
I_{ld}	13.25
I_{lq}	-1.75

PI tuning has been done from method described in previous chapter and tuned values are shown in table 4.3. For simulation filter values and controller values are selected as shown in table 4.4 and 4.5 respectively.

Table 4. 3: Tuned values

Parameters	Value
k_{pv_d}	0.12589
k_{pv_q}	0.226
k_{iv_d}	199.52
k_{iv_q}	1369.632
k_{pc_d}	10.698
k_{pc_q}	1.1038
k_{ic_d}	41069.77
k_{ic_q}	176.197

Table 4. 4: LCL filter values

Parameters	Value
L_f	1.35 mH
R_f	0.1 Ω
L_c	0.35 mH
R_c	0.03 Ω
C_f	50 μF

Table 4. 5: Controller values

Parameters	Value
k_p	10^{-6}
k_q	$3.37 * 10^{-6}$
F	0.75
ω_c	30 rad/sec
ω	314 rad/sec
v_{DC}	810 volt

Here voltages are in volt and current in ampere and ω in rad/sec. Using the above values, equations are linearized as per taylor series as given in **[48]**. For eigen value analysis we need A matrix which is shown in (4.33).

$$\begin{bmatrix} \dot{\Delta\delta} \\ \Delta P \\ \Delta Q \\ \Delta\varphi_d \\ \Delta\varphi_q \\ \Delta Y_d \\ \Delta Y_q \\ \Delta i_{l_d} \\ \Delta i_{l_q} \\ \Delta v_{o_d} \\ \Delta v_{o_q} \\ \Delta i_{o_d} \\ \Delta i_{o_q} \end{bmatrix} = \begin{bmatrix} 0 & -k_p & 0 & 0 & 0 & 0 & 0 & 0 & 0 & 0 & 0 & 0 & 0 \\ 0 & -\omega_c & 0 & 0 & 0 & 0 & 0 & 0 & 0 & \omega_c I_{od} & \omega_c I_{oq} & \omega_c V_{od} & \omega_c V_{oq} \\ 0 & 0 & -\omega_c & 0 & 0 & 0 & 0 & 0 & 0 & -\omega_c I_{od} & -\omega_c I_{oq} & -\omega_c V_{oq} & \omega_c V_{od} \\ 0 & 0 & -k_q & 0 & 0 & 0 & 0 & 0 & 0 & -1 & 0 & 0 & 0 \\ 0 & 0 & 0 & 0 & 0 & 0 & 0 & 0 & 0 & 0 & -1 & 0 & 0 \\ 0 & 0 & -k_{pv_d} k_q & k_{iv_d} & 0 & 0 & 0 & -1 & 0 & -k_{pv_d} & -\omega C_f & 0 & 0 \\ 0 & 0 & 0 & 0 & k_{iv_q} & 0 & 0 & 0 & -1 & \omega C_f & k_{pv_q} & F & 0 \\ 0 & -k_p I_{l_q} & -\frac{k_q k_{pc_d} k_{pv_d}}{L_f} & \frac{k_{pc_d} k_{iv_d}}{L_f} & 0 & \frac{k_{ic_d}}{L_f} & 0 & -\frac{k_{pc_d}}{L_f} & 0 & -\frac{k_{pv_d} k_{pc_d}}{L_f} & -\frac{k_{pc_d} \omega C_f}{L_f} & \frac{F k_{pc_d}}{L_f} & 0 \\ 0 & k_p I_{l_d} & 0 & 0 & \frac{k_{pc_q} k_{iv_q}}{L_f} & 0 & \frac{k_{ic_q}}{L_f} & 0 & -\frac{k_{pc_q}}{L_f} & \frac{k_{pc_q} \omega C_f}{L_f} & -\frac{k_{pv_q} k_{pc_q}}{L_f} & 0 & \frac{F k_{pc_q}}{L_f} \\ 0 & -k_p V_{o_q} & 0 & 0 & 0 & 0 & 0 & \frac{1}{C_f} & 0 & 0 & 0 & -\frac{1}{C_f} & 0 \\ \frac{V_{b_D} \sin\delta - V_{b_Q} \cos\delta}{L_c} & k_p V_{o_d} & 0 & 0 & 0 & 0 & 0 & 0 & \frac{1}{C_f} & -\omega & 0 & 0 & -\frac{1}{C_f} \\ \frac{V_{b_D} \cos\delta + V_{b_Q} \sin\delta}{L_c} & -k_p I_{o_q} & 0 & 0 & 0 & 0 & 0 & 0 & 0 & 0 & -\frac{r_c}{L_c} & \omega & -\frac{r_c}{L_c} \\ & k_p I_{o_d} & 0 & 0 & 0 & 0 & 0 & 0 & 0 & \frac{1}{L_c} & \omega & -\frac{r_c}{L_c} & \omega \\ & & & & & & & & & 0 & \frac{1}{L_c} & 0 & \frac{1}{L_c} \end{bmatrix} \begin{bmatrix} \Delta\delta \\ \Delta P \\ \Delta Q \\ \Delta\varphi_d \\ \Delta\varphi_q \\ \Delta Y_d \\ \Delta Y_q \\ \Delta i_{l_d} \\ \Delta i_{l_q} \\ \Delta v_{o_d} \\ \Delta v_{o_q} \\ \Delta i_{o_d} \\ \Delta i_{o_q} \end{bmatrix} \quad \textbf{(4.33)}$$

Hence we have A matrix but we classify it into more generalised and easy form as shown in (4.35).

$$\begin{bmatrix} \dot{\Delta\delta} \\ \Delta P \\ \Delta Q \\ \Delta\varphi_d \\ \Delta\varphi_q \\ \Delta Y_d \\ \Delta Y_q \\ \Delta\imath_{l_d} \\ \Delta\imath_{l_q} \\ \Delta v_{o_d} \\ \Delta v_{o_q} \\ \Delta\imath_{o_d} \\ \Delta\imath_{o_q} \end{bmatrix} = \begin{bmatrix} [A_p]_{3X3} & [0]_{3X2} & [0]_{3X2} & [B_p]_{3X3} \\ [B_{v1}C_{P_v}]_{2X3} & [0]_{2X2} & [0]_{2X2} & [B_{v2}]_{2X6} \\ [B_{c1}D_{v1}C_{P_v}]_{2X3} & [B_{c1}C_v]_{2X2} & [0]_{2X2} & [B_{c1}D_{v2} + B_{c2}]_{2X6} \\ \begin{bmatrix} B_{LCL1}D_{C1}D_{v1}C_{P_v} + \\ B_{LCL2}[T_v{}^{-1} \quad 0 \quad 0] + \\ B_{LCL3}C_{pw} \end{bmatrix}_{6X3} & [B_{LCL1}D_{C1}C_v]_{6X2} & [B_{LCL1}C_C]_{6X2} & \begin{bmatrix} A_{LCL} + \\ B_{LCL1}(D_{c1}D_{v2} + D_{c2}) \end{bmatrix}_{6X6} \end{bmatrix} \begin{bmatrix} \Delta\delta \\ \Delta P \\ \Delta Q \\ \Delta\varphi_d \\ \Delta\varphi_q \\ \Delta Y_d \\ \Delta Y_q \\ \Delta i_{l_d} \\ \Delta i_{l_q} \\ \Delta v_{o_d} \\ \Delta v_{o_q} \\ \Delta i_{o_d} \\ \Delta i_{o_q} \end{bmatrix} \quad \textbf{(4.34)}$$

$$A = \begin{bmatrix} [A_p]_{3X3} & [0]_{3X2} & [0]_{3X2} & [B_p]_{3X3} \\ [B_{v1}C_{P_v}]_{2X3} & [0]_{2X2} & [0]_{2X2} & [B_{v2}]_{2X6} \\ [B_{c1}D_{v1}C_{P_v}]_{2X3} & [B_{c1}C_v]_{2X2} & [0]_{2X2} & [B_{c1}D_{v2} + B_{c2}]_{2X6} \\ \begin{bmatrix} B_{LCL1}D_{C1}D_{v1}C_{P_v} + \\ B_{LCL2}[T_v{}^{-1} \quad 0 \quad 0] + \\ B_{LCL3}C_{pw} \end{bmatrix}_{6X3} & [B_{LCL1}D_{C1}C_v]_{6X2} & [B_{LCL1}C_C]_{6X2} & \begin{bmatrix} A_{LCL} + \\ B_{LCL1}(D_{c1}D_{v2} + D_{c2}) \end{bmatrix}_{6X6} \end{bmatrix} \quad \textbf{(4.35)}$$

Here symbol used are initialised in previous equations.Now we have A,B,C,D matrices and hence they can be used for further analysis as shown in**[4]**.Now this A matrix can be converted into s-domain and used for calculation of eigen values based on above operating points.

Poles of open loop system = $|(sI - A)^{-1}|$.

Through which equation formed and can be solved, another method is using matlab function eig(A) which gives eigen values and if plotted correctly, gives location of eigen values as shown in next chapter.

CHAPTER – 5
RESULTS AND DISCUSSION

5.1 P/Q CONTROL VALIDATION

To validate the feasibility of the P/Q control, the micro-grid with P/Q control operating in the grid-connected mode is simulated. The active and reactive power of the load in the micro-grid are varied. Firstly, the load is varied and variation of output power is plotted.

i) At t = 0 sec, P_{ref} = 10 KW and Q_{ref} = 5KVar.

ii) At t = 0.15 sec, P_{ref} is increased by 2KW and Q_{ref} increased by 2KVar.

i) At t = 0.25 sec, P_{ref} is decreased by 5KW and Q_{ref} decreased by 5KVar.

ii) At t = 0.4 sec, P_{ref} is increased by 3KW and Q_{ref} increased by 3KVar.

P_{ref} is the active power of the load in the main grid

Q_{ref} is the reactive power of load in the main grid

- **Active Power variation**

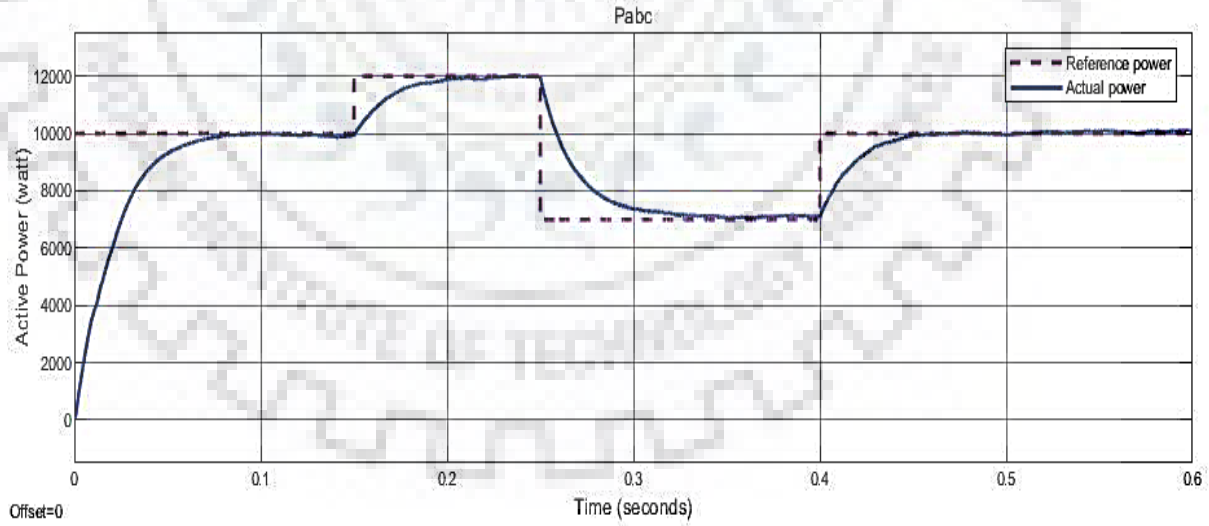

Figure 5. 1: Variation of reference and actual active power

From figure 5.1, it is observed that as the load power changes, generation of inverter also changes in proportion to the load.

- **Reactive Power variation**

From figure 5.2, it can be seen that inverter output changes as quickly as load changes. Though there is a little delay, that's because every element has been modelled practically.

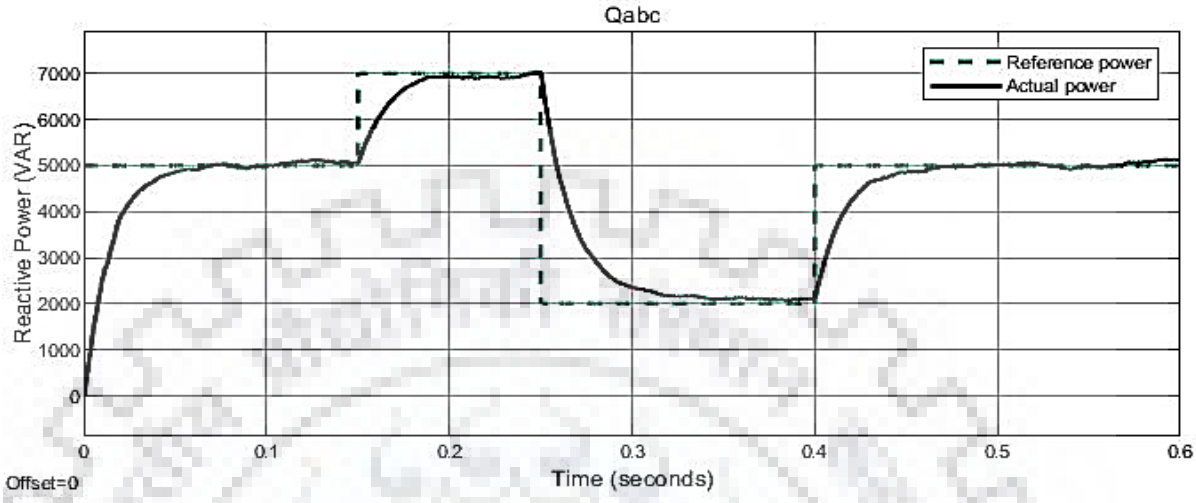

Figure 5. 2: Variation of reference and actual reactive power

- **Voltage and current variation (PCC)**

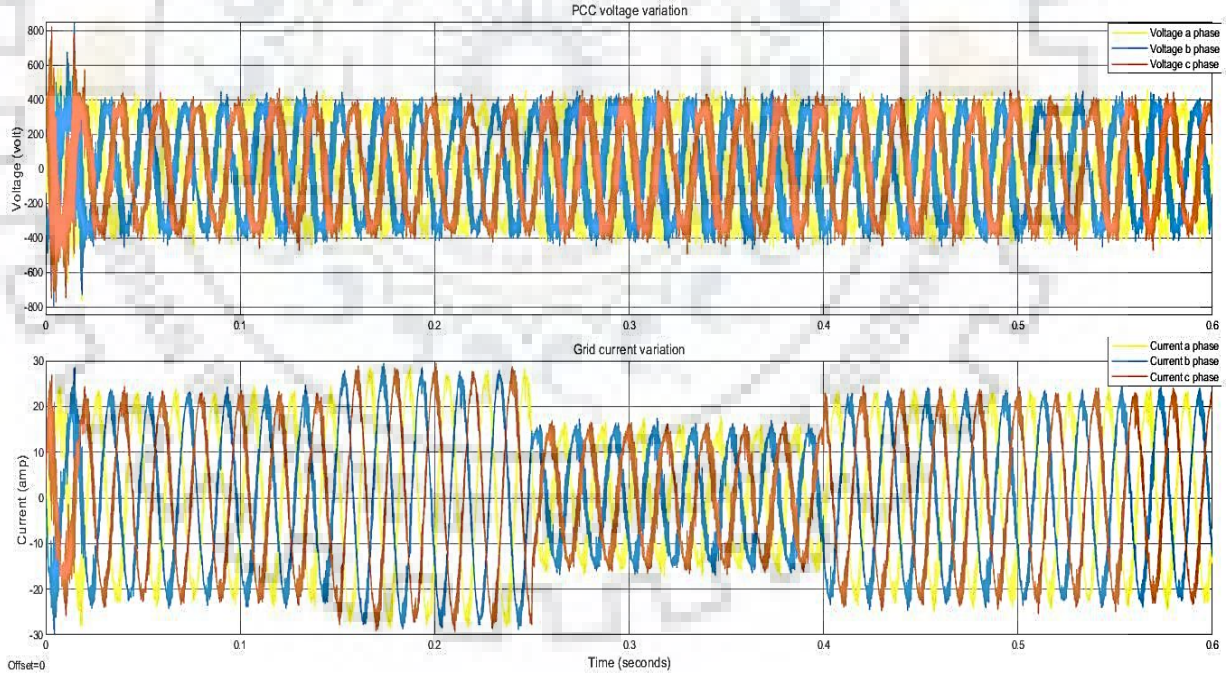

Figure 5. 3: Grid voltage and current variation

From figure 5.3, it is observed that when load changes load current changes correspondingly, At t=0.15 sec load increase and hence load current also increase to compensate load increment and same goes at every other point. Moreover PCC point voltage is almost sine and hence very less fluctuation can be observed.

- **Frequency variation**

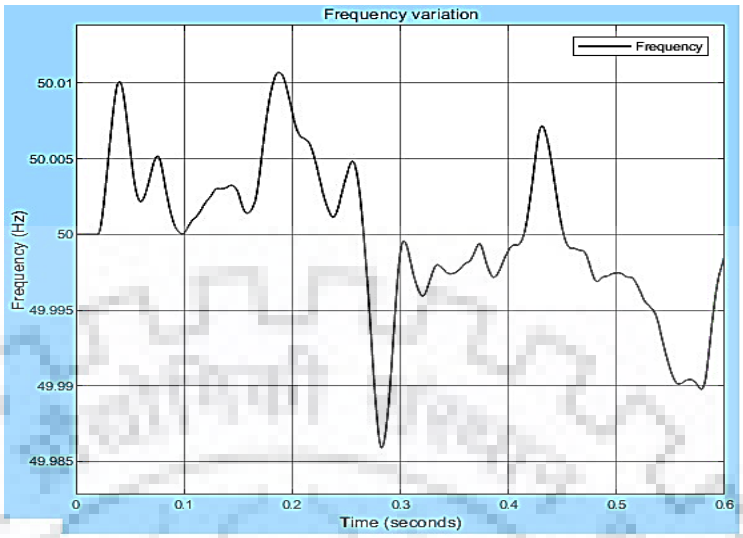

Figure 5. 4: Grid frequency variation

From figure 5.4, it can be deduced that the grid frequency is almost same, very less variations are there and that is in proportion to load i.e. if load changes frequency changes correspondingly.

- **Grid Voltage**

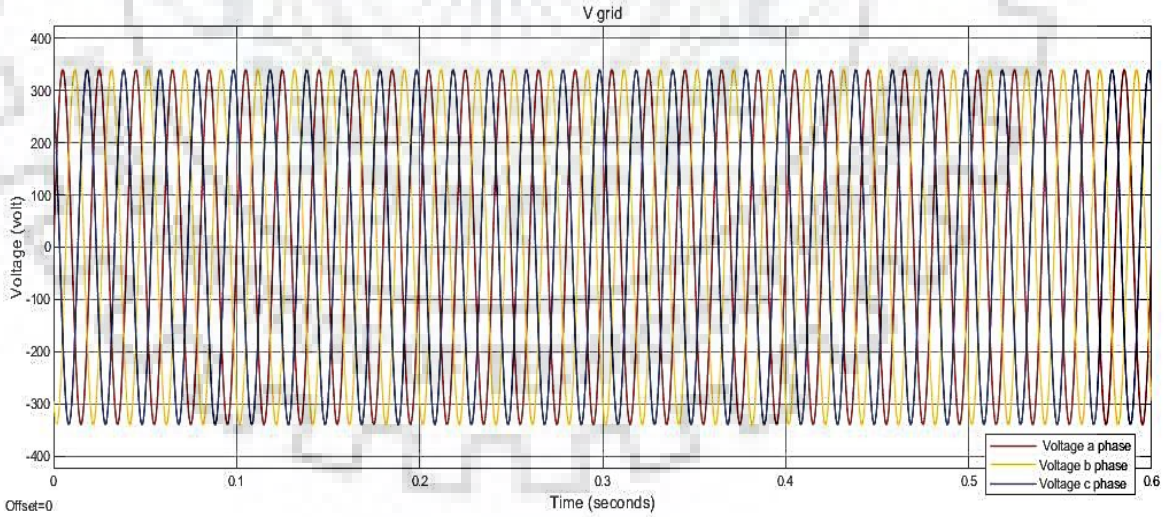

Figure 5. 5: Grid voltage

We can see that the main grid bears the fluctuation of the frequency and the power in the micro-grid system, and the output power of the DG is constant with the P/Q control. From figure 5.5, we can see that the frequency variation is small and THD is 14%. The simulation results validate the feasibility of the P/Q control.

5.1.1 STABILITY ANALYSIS OF DEVELOPED MODEL

Now with developed model vary any 1 quantity and observe the eigen value and hence we can comment on stability i.e. if eigen value goes to right side system is tending towards unstability. Some of the plots are shown:

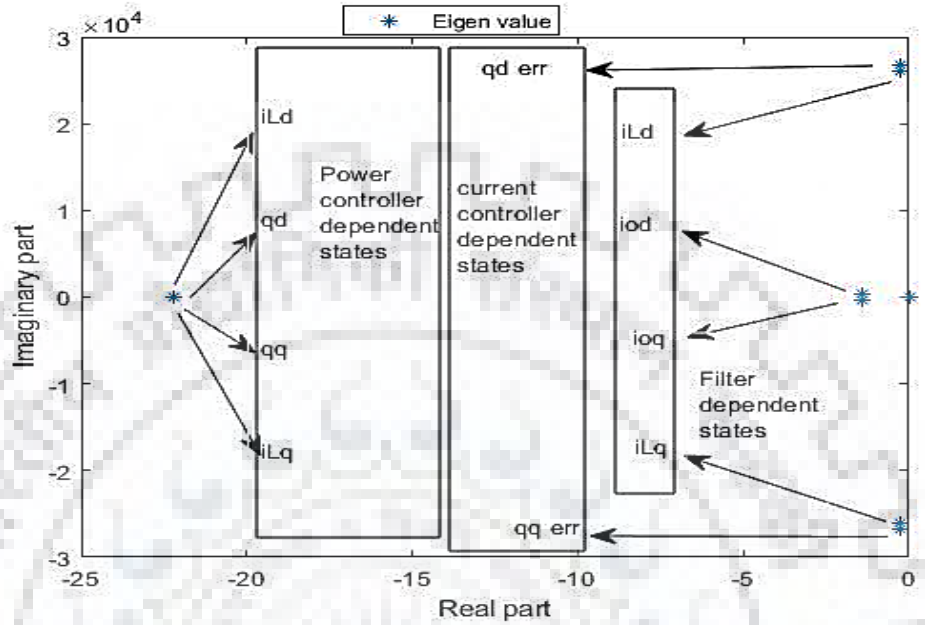

Figure 5. 6: Eigen values of whole system

Eigen values of each sub-model is shown in figure 5.6. Location of eigen values are shown in figure 5.7, all lying on left hand side so system is stable.

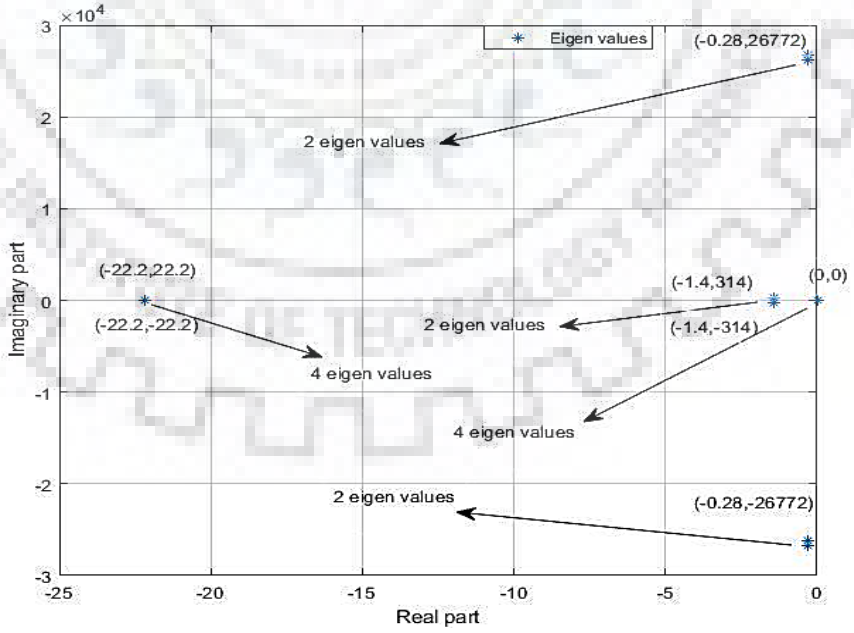

Figure 5. 7: Location of eigen values

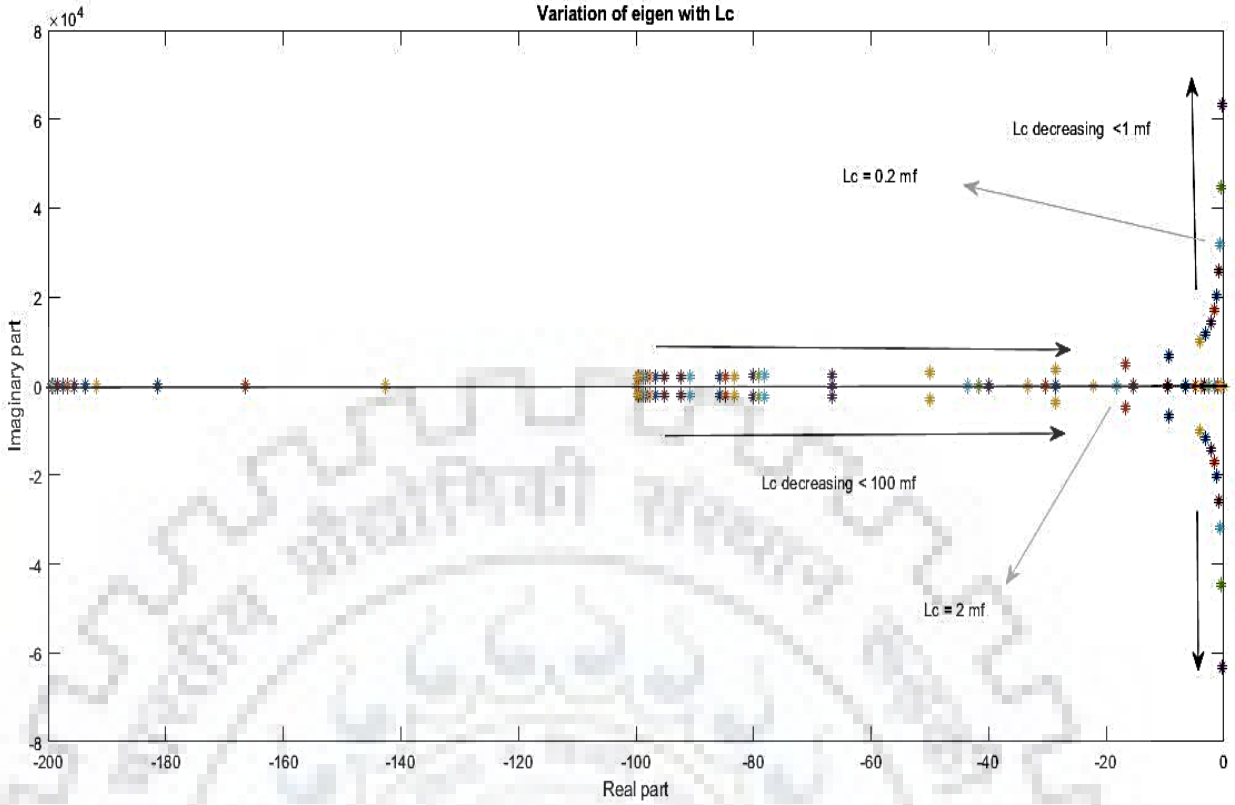

Figure 5. 8: Variation of eigen values with coupling inductance

Initially L_c was small and we observe eigen value shifted to jω axis and when L_c becomes more than 2 mH we get eigen values moving to left hand side with decreased oscillation but again if L_c becomes more than 10 mH eigen value start moving right side as shown in figure 5.8. So for analysis 2 mH is selected.

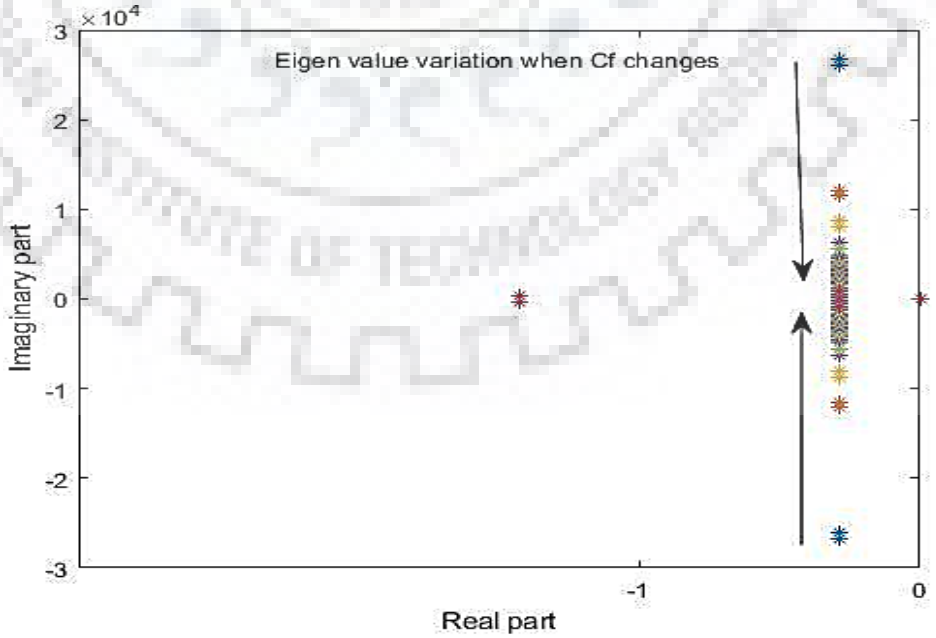

Figure 5. 9: Variation of eigen values with filter capacitance

In figure 5.9, range of values of C_f can be find out. Initially capacitance value was 1µf but osciallation was very large, as the capacitance values exceed 30µf oscillation become less and after 50µf oscillation slowly decrease. So C_f is taken as 50µf.

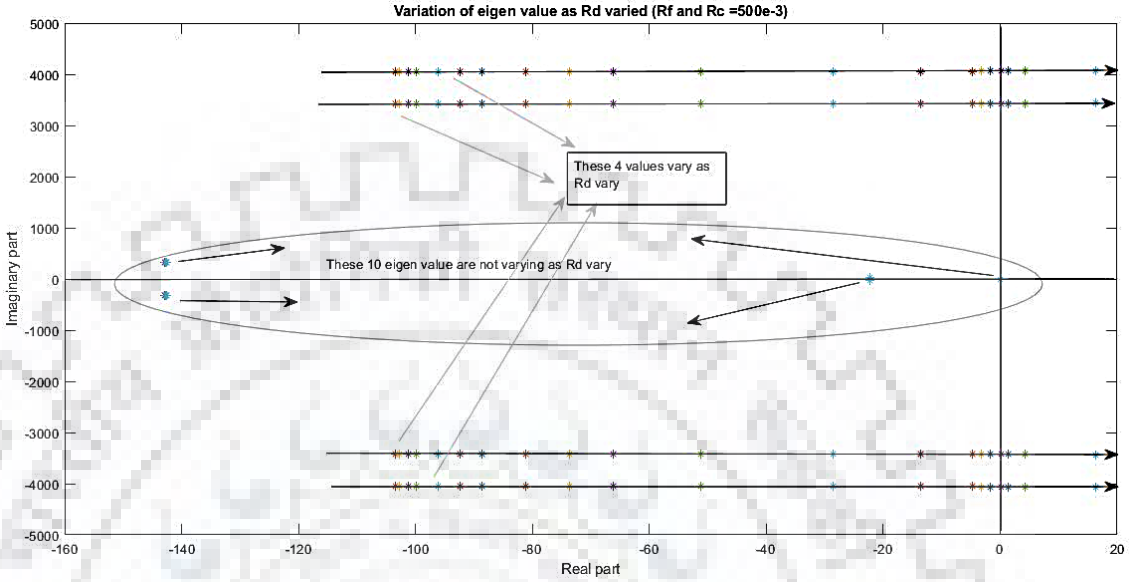

Figure 5. 10: Variation of eigen value with damping resistor

Variation of R_d is shown in figure 5.10, initially with small values shows high damping but as R_d increases then system start shifting right hand side and is stable till $R_d = 800e-3$ Ω. So for analysis $R_d = 500e-3$ Ω is selected.

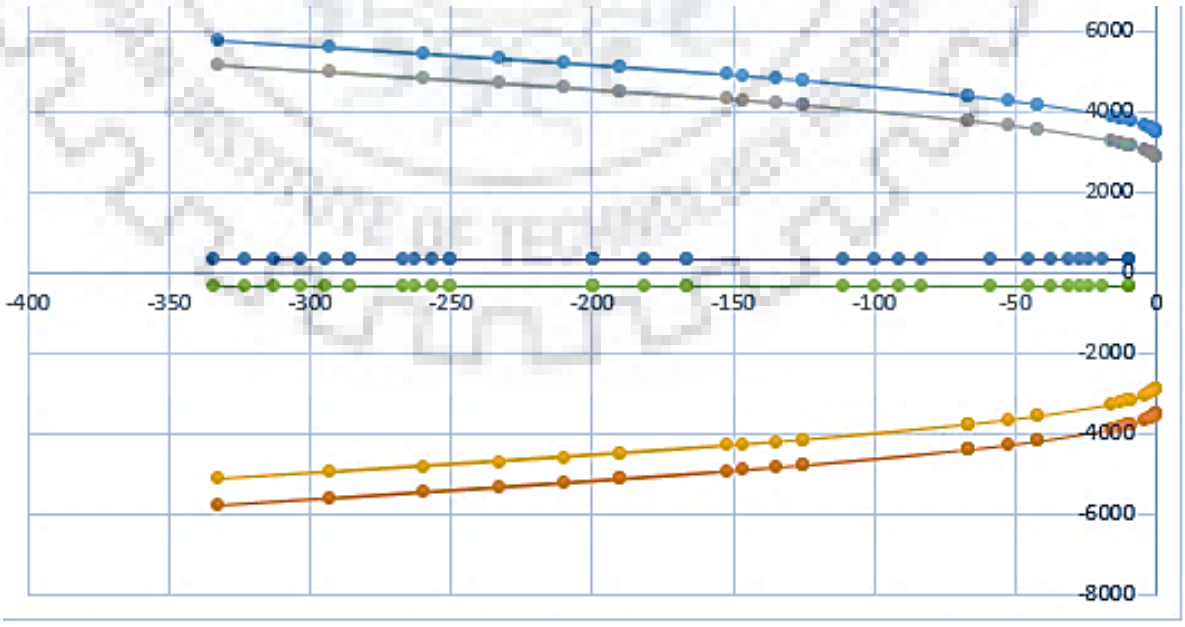

Figure 5. 11: Variation of eigen value with filter inductance

Here as L_f varies from 0.5 mH, initially very high oscillation frequency is there and as $L_f$increased beyond 1 mH damping increases and oscillation decrease but as L_f approaches 30 mH again it becomes close to jω axis as shown in figure 5.11. So for analysis L_f = 5 mH.

Change in root loci is analysed and is seen that some eigen values are close to imaginary axis with decreased damping. Furthermore sensitivity analyses of each critical mode can be done for each parameter and concluded as to which parameter is more effective on stability of grid connected microgrid stability.In the grid-connected mode, controller parameters and filter parameters are the key factors of microgrid stability. Generally, careful selection of the controller, filter, and power sharing parameters maintains power quality within the regulated range and enhance the system performance against load changes and disturbances. These values are shown in table 5.1-5.3.

Table 5. 1: LCL filter parameters range for stable region

Parameter	Range
L_c	2 mH to 10 mH
L_f	1 mH to 30 mH
R_d	5 mΩ to 800 mΩ
C_f	30 μF to 100 μF
R_f,R_c	5 mΩ to 800 mΩ

Table 5. 2: LCL filter paramaters range for stable region

Parameter	Range
L_c	2 mH to 10 mH
L_f	1 mH to 30 mH
R_d	5 mΩ to 800 mΩ
C_f	30 μF to 100 μF
R_f,R_c	5 mΩ to 800 mΩ

Values shown in table are valid only for proposed system and they vary for different systems based on parameter values.

Table 5. 3: Considered system parameters

Parameter	Value
V_{DC}	800 volt
V_{grid}	340 volt
$K_{p_{PLL}}$	180
$K_{i_{PLL}}$	3200
$K_{p_{PI}}$	30
$K_{i_{PI}}$	95
ω_c	30

Different approaches to select the controller parameters and control strategies have been reported in the literature **[18]**–**[20]**.

5.2 V/f CONTROL VALIDATION

To validate the feasibility of the V/f control, the micro-grid operating in the isolated mode is simulated as shown in figure 5.12.The reference voltages are shown :

$$v_{o_d} = 310 \text{ Volt}$$

$$v_{o_q} = 0 \text{ Volt}$$

$$v_{o_a} = 220 * \sqrt{2}\sin(\omega t)$$

$$v_{o_b} = 220 * \sqrt{2}\sin(\omega t - 120^o)$$

$$v_{o_c} = 220 * \sqrt{2}\sin(\omega t + 120^o)$$

The output power of inverter is analysed by varying load at various intervals. It is seen that inverter responds very quickly and accurately.

j) At t = 0 sec, load resistance = 50 Ω/phase.

ii) At t=0.1sec, additional load of 80 Ω/phase is added.

iii) At t = 0.2 sec, again an additional load of 100 Ω/phase is added.

iv) At t = 0.3 sec, another load of 150 Ω/phase is added.

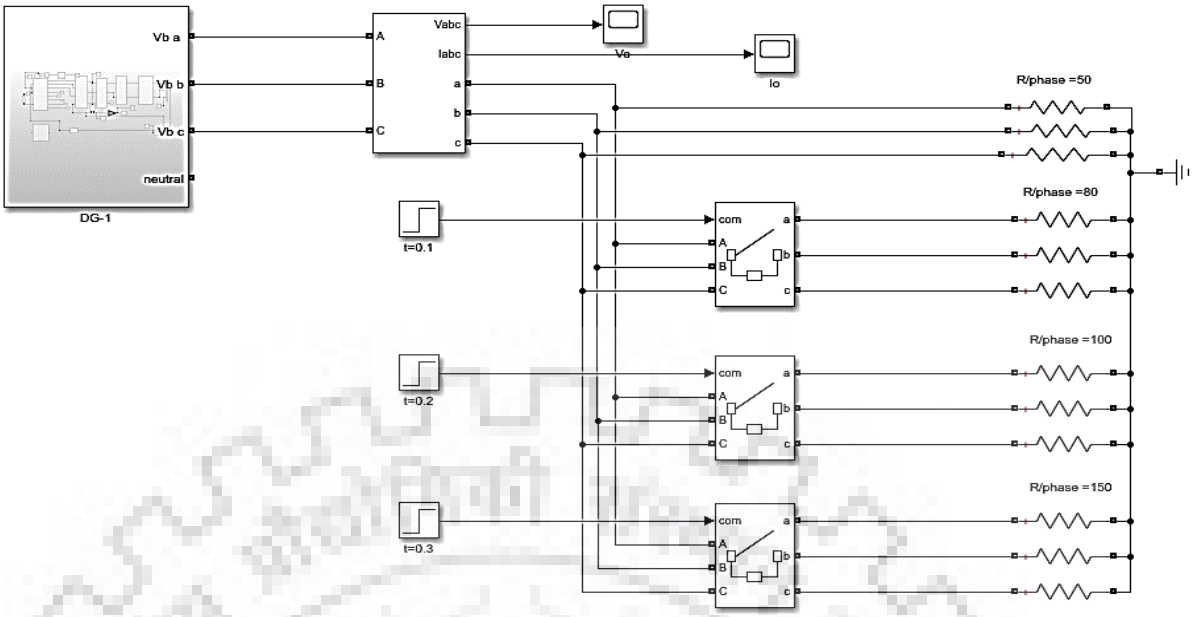

Figure 5. 12: Simulink model developed for validation of V/f control

- **Active Power variation**

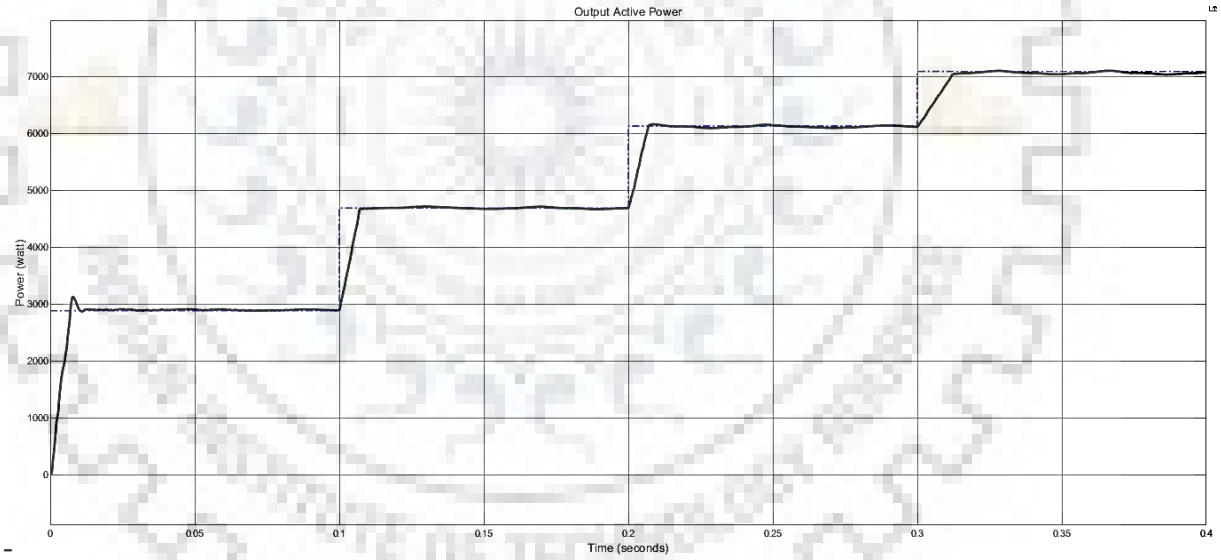

Figure 5. 13: Variation of reference and actual active power

From figure 5.13, it is observed that load power changes very quickly and in response to that inverter power also generates which is in response to load.

- Initially power across load of 50 Ω/phase, power delivered is defined as below

  Power = 3 X $\frac{\left(\frac{310}{\sqrt{2}}\right)^2}{50} = 2883$ watt

- At t=0.1 additional load of 80 Ω/phase connected, power is delivered as shown:

Power = 3 X $\frac{\left(\frac{310}{\sqrt{2}}\right)^2}{80} = 1801.875$ watt,

Total power = 4684.875 watt

- At t=0.2 additional load of 100 Ω/phase connected, power delivered as shown

Power = 3 X $\frac{\left(\frac{310}{\sqrt{2}}\right)^2}{100} = 1441.5$ watt,

Total power = 6126.375 watt

- At t=0.3 additional load of 150 Ω/phase connected, power delivered as shown

Power = 3 X $\frac{\left(\frac{310}{\sqrt{2}}\right)^2}{150} = 961$ watt,

Total power = 7087.375 watt

Hence we can conclude that inverter response is fast, maintaining reliability and quality as it it supplying power as required by load.

- **Reactive Power variation**

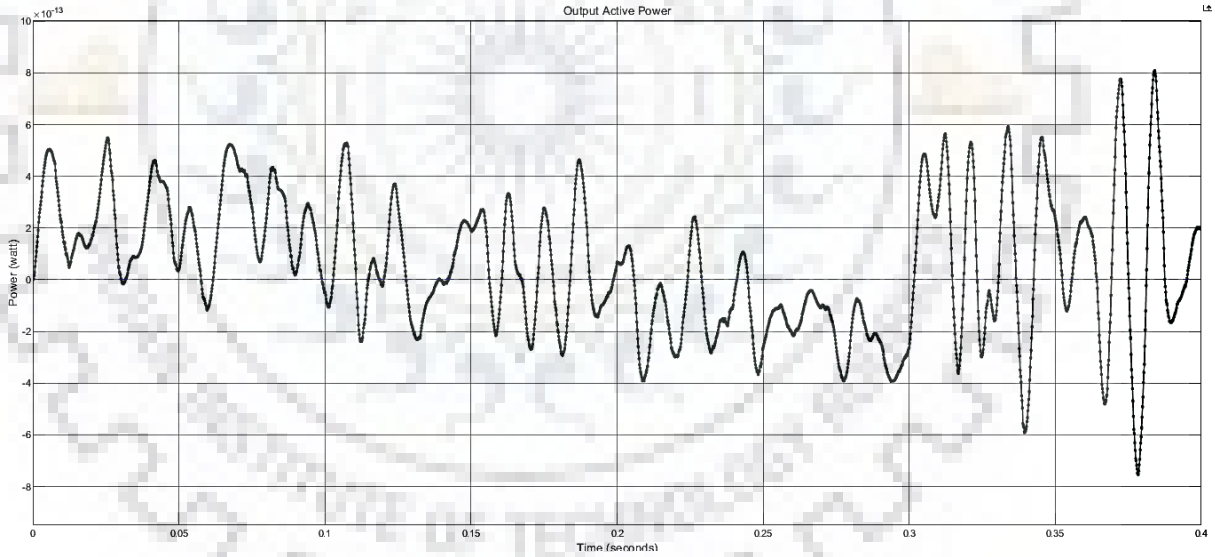

Figure 5. 14: Variation of reference and actual reactive power

From figure 5.14 it can be seen that inverter output changes as quickly as load changes, though there is a little delay, that's because every element has been modelled practically. Now load consume only active power since only resistance is considered but due to non-linear nature of power electronic devices it has certain harmonics in current and voltage and hence reactive power is small but negligible as seen from above figure.

- **Voltage variation (PCC)**

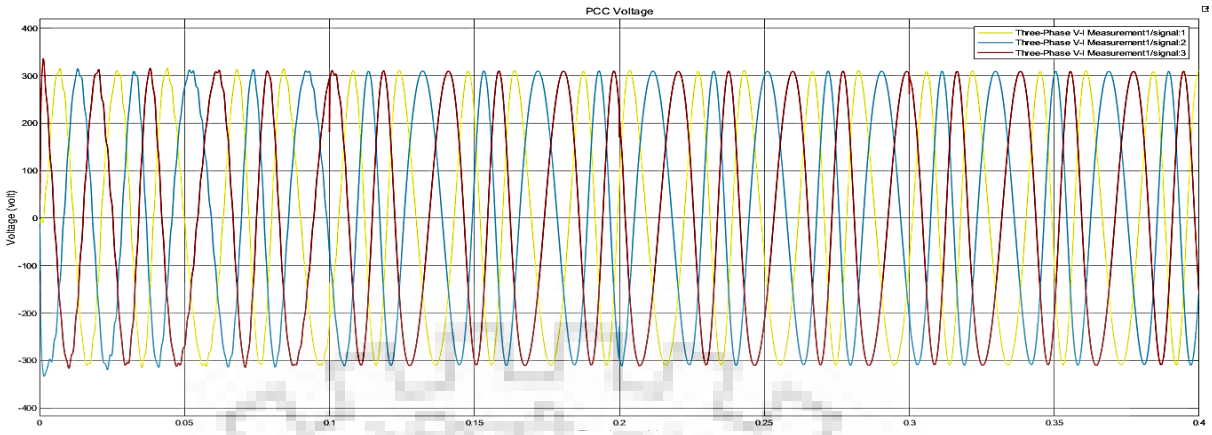

Figure 5. 15: PCC voltage variation

From figure 5.15, it is observed that when load changes load current changes correspondingly, At t=0.1, 0.2, 0.3 sec load increase and but PCC point voltage is almost sine and hence very less fluctuation can be observed.

- **Vod**

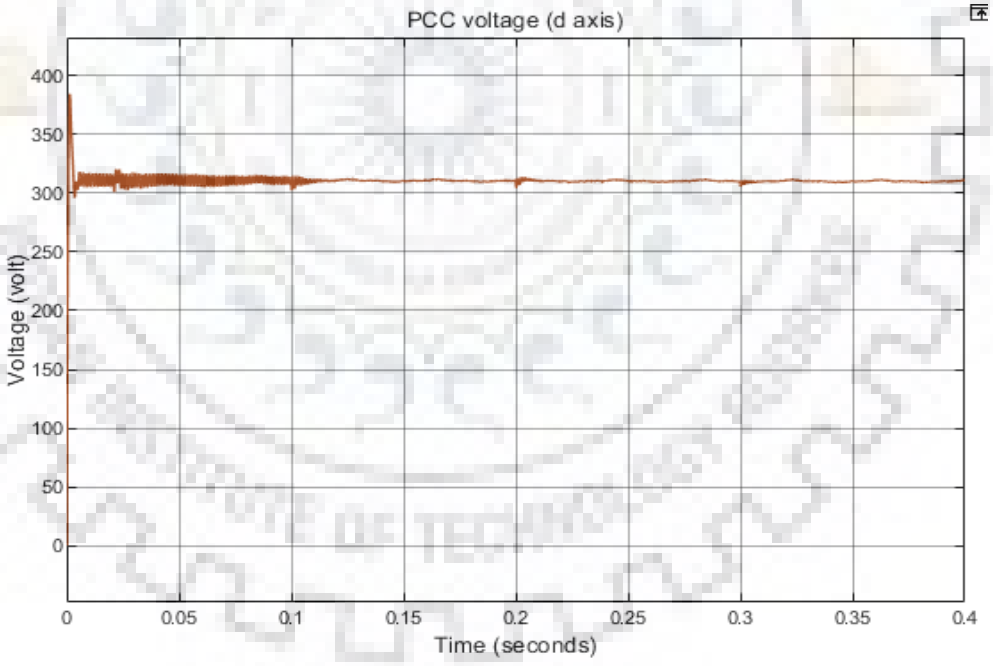

Figure 5. 16: Variation of output d-axis voltage

In figure 5.16 we can see that d component of output voltage is giving magnitude of output voltage in abc frame as described in previous chapter and this magnitude is nearly constant which makes inverter control viable.

- **Voq**

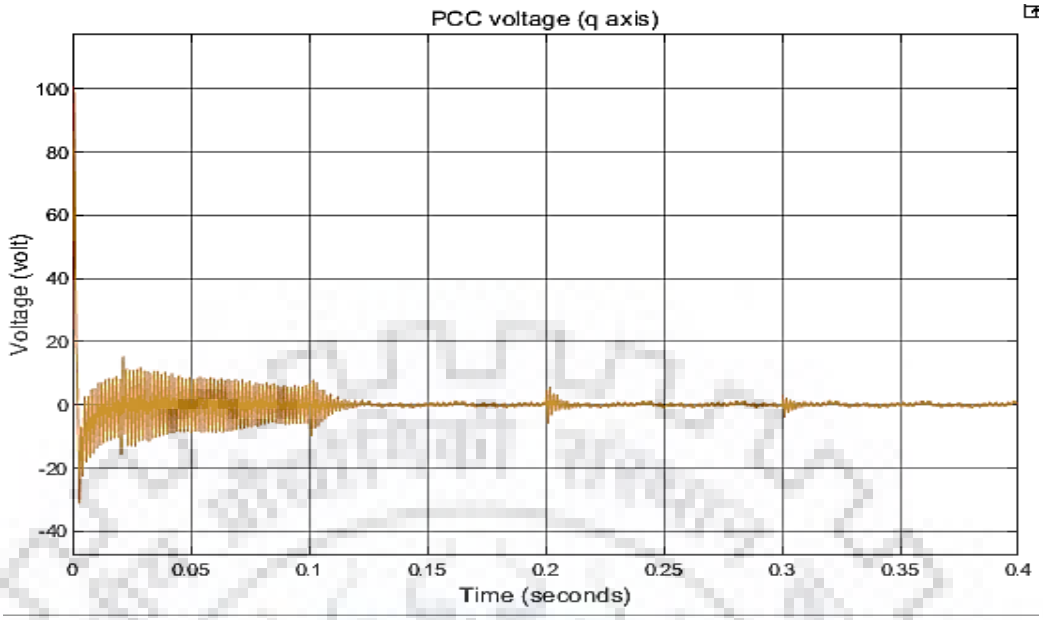

Figure 5. 17: Variation of q-axis output voltage

Q component of output voltage should be 0 as described in previous chapter for proper working of PLL. Figure 5.17 verifies that theory and hence we can say that PLL operation is successful but still some deviations can be observed in frequency which makes it more practical.

- **Current variation (PCC)**

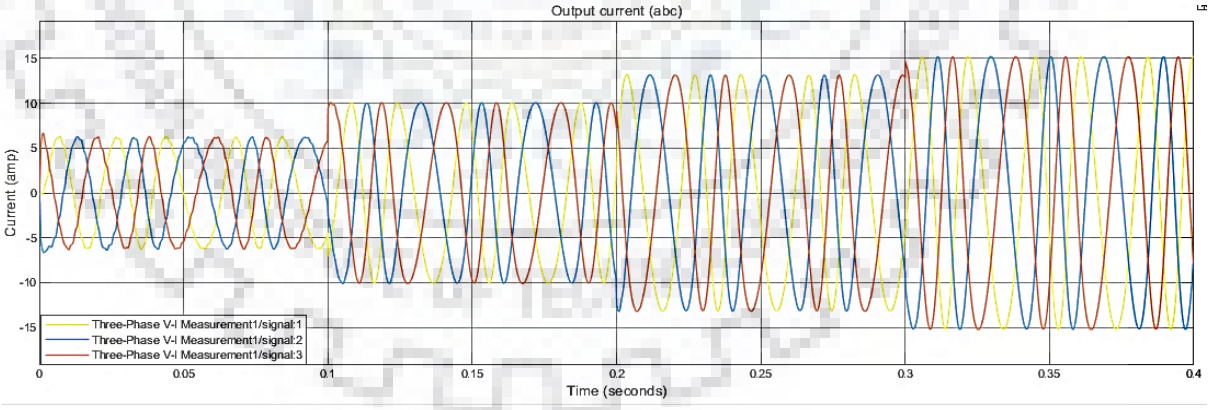

Figure 5. 18: Output current variation in abc frame

As previously mentioned load increase at each interval of 0.1 sec and it can be observed that current increase proportionally to supply load as clearly observed in figure 5.18.

- **Iod**

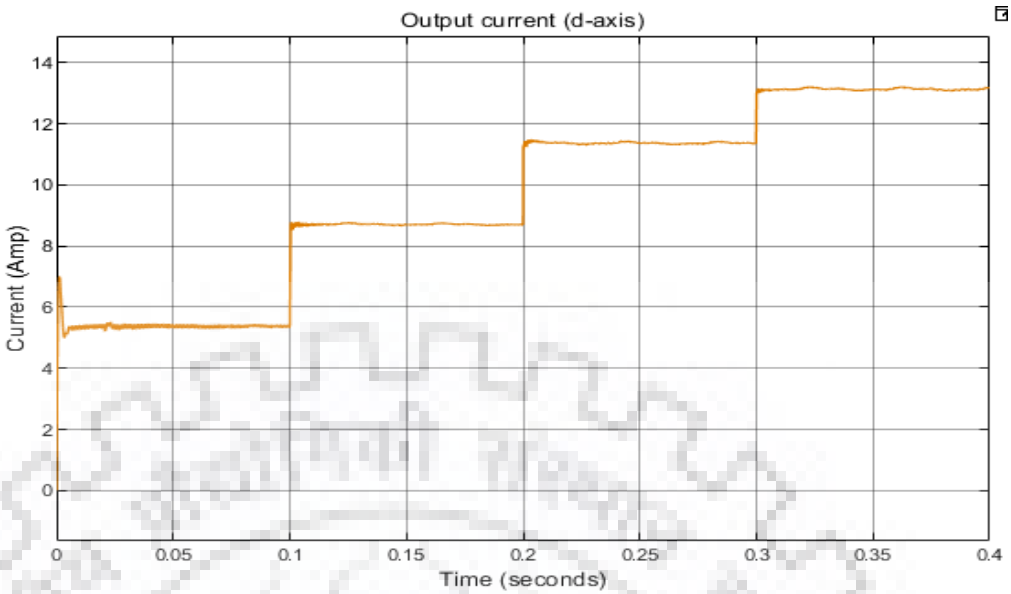

Figure 5. 19: Output d-axis current variation

D axis component of current gives peak value of current magnitude in abc frame as shown in figure 5.19 which can be verified by calculation also.

- **Ioq**

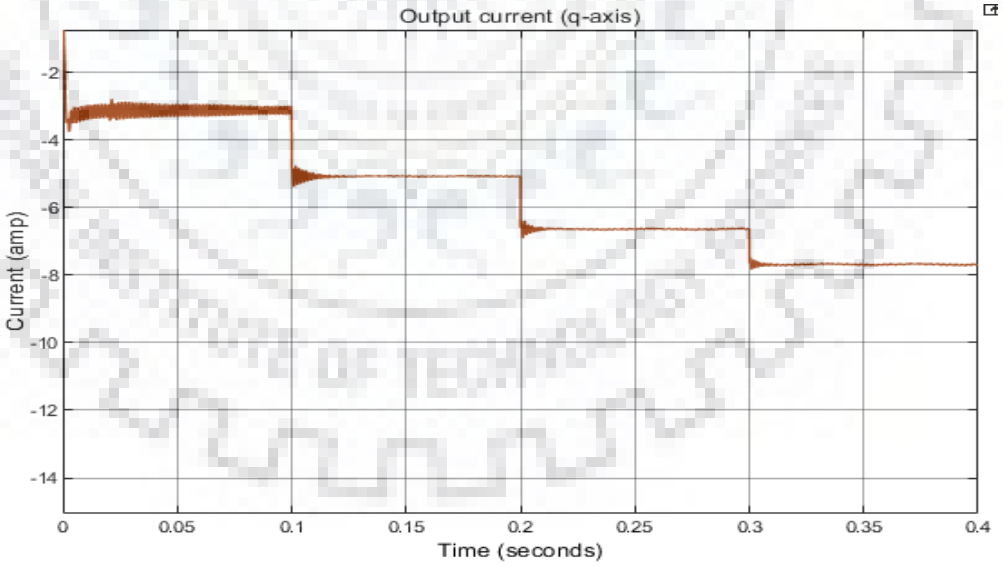

Figure 5. 20: Output q-axis current variation

Q component of current is also very less and such deviations are negligible as shown in figure 5.20.

- **Frequency variation**

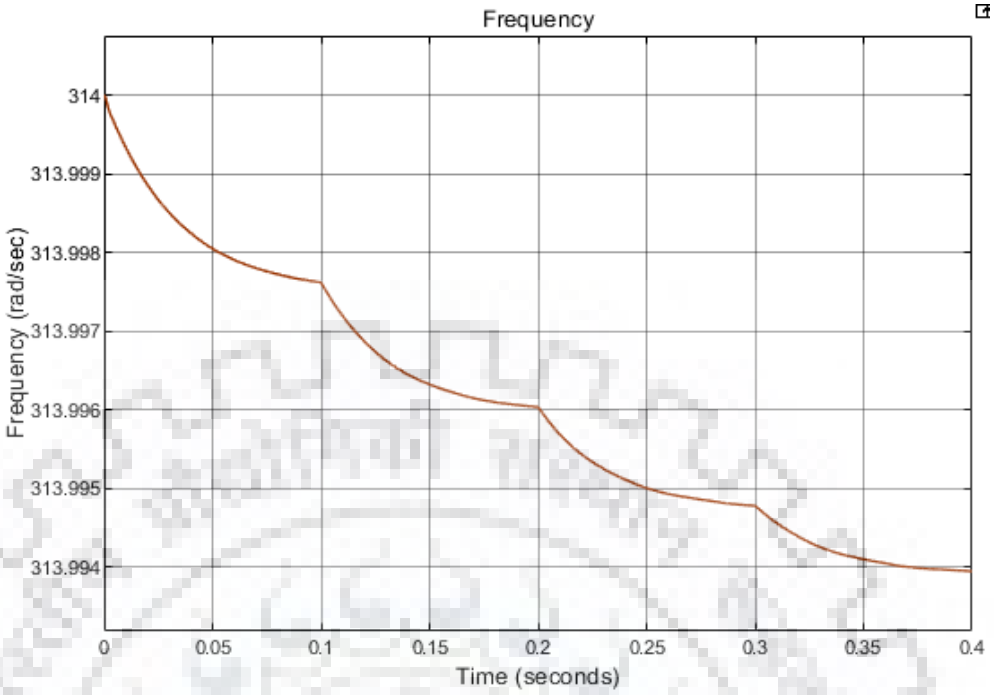

Figure 5. 21: Inverter frequency variation

From figure 5.21 the frequency is almost same, very less variations are there and that is in proportion to load i.e if load increases frequency decrease and vice-verse.

We can see that the fluctuation of the frequency and the power in the micro-grid system are very less and the output power of the DG is proportional to load with the V/f control. The simulation results validate the feasibility of the V/f control.

5.2.1STABILITY ANALYSIS OF DEVELOPED MODEL

Now with developed model vary any 1 quantity and observe the eigen value and hence we can comment on stability i.e if eigen value goes to right side system is tending towards unstability. Some of the plots are shown in next 6 sections.

- **Eigen value plot**

Location of eigen value are required to comment on stability, since whole system is non linear so it is difficult to calculated eigen values. So system is first linearised around operating points which are calculated in simulation after system achieved steady state and then again linear state space matrix is form and now matrix A is calculated as explained in previous chapter and then using matlab function “eig()” eigen values are found out.

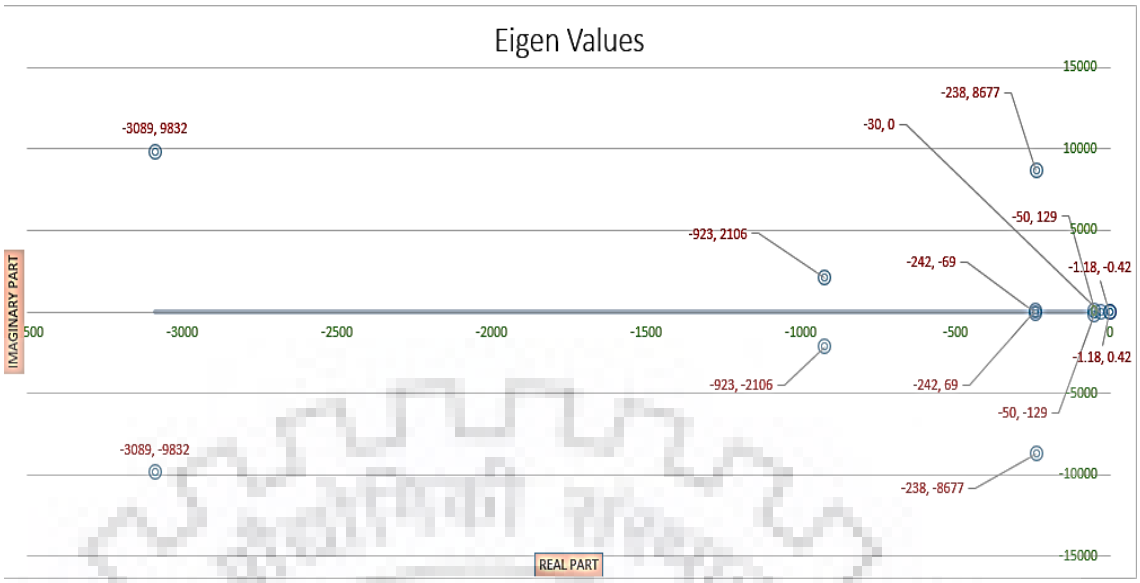

Figure 5. 22: Location of eigen values

It can clearly be seen that each eigen value shown in figure 5.22, with values lie on left hand side so system is stable. Hence parameters selected in obtaining this represent a stable system. Hence system is stable and analysis done is for small signal.

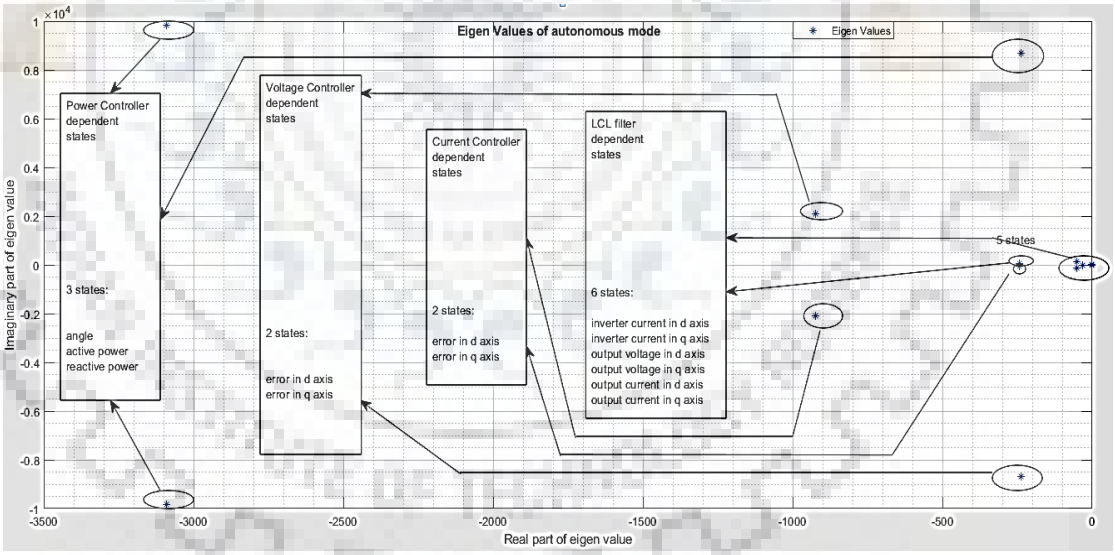

Figure 5. 23: Eigen values of whole system

Now these values correspond to each selected state. We have 4 subsystems, all contributing to stability of an inverter and combining them all we get 13 eigen values which are shown in figure. Here each component is shown along with its contributing states as shown in figure 5.23. We can see that LCL filter states are sensitive so filter needs to be properly design as small change can lead to its unstable states which will affect stability of whole DG.

- **Root locus by varying coupling inductance (L_c)**

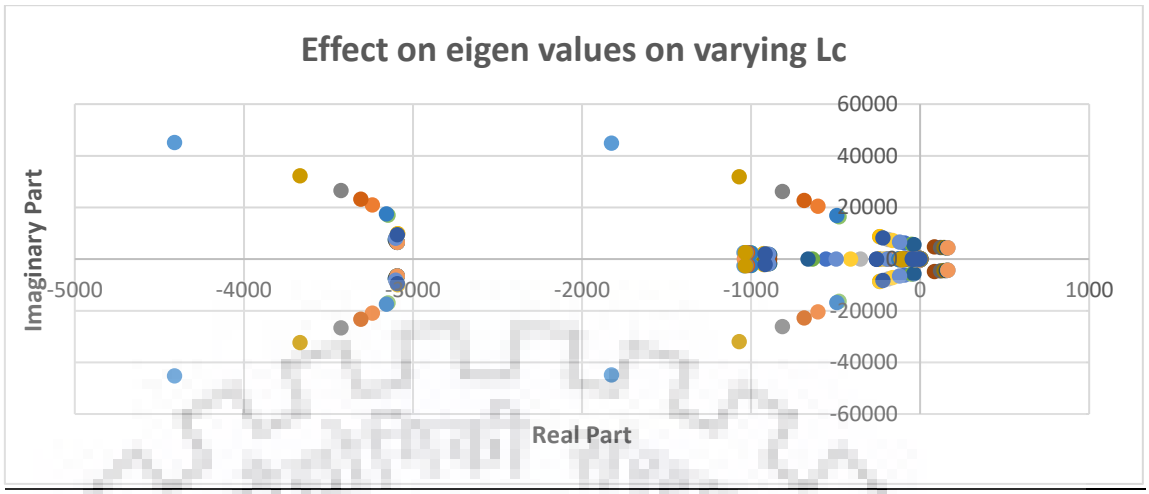

Figure 5. 24: Variation of eigen values with coupling inductance

- Initially L_c was small and we observe eigen value shifted to jω axis and when L_c becomes 0.4mHi.e at the boundary of stability, if L_c increases beyond this then it moves locus towards right hand side denoting unstability in LCL filter selection. So for stablilty consideration $L_c$value is selected as 0.35 mH. If value goes beyond 0.1 mH then also system move towards unstability as shown in figure 5.24.
- However it should be noted that in autonomous mode L_c is not necessary as we are not interfacing grid here so if $L_c = 0$ is taken then also system will remain stable.
- So optimal range is 0.2 mH to 0.4 mH, so we have considered$L_c = 0.35\ mH$.

- **Root locus by varying filter capacitance (C_f)**

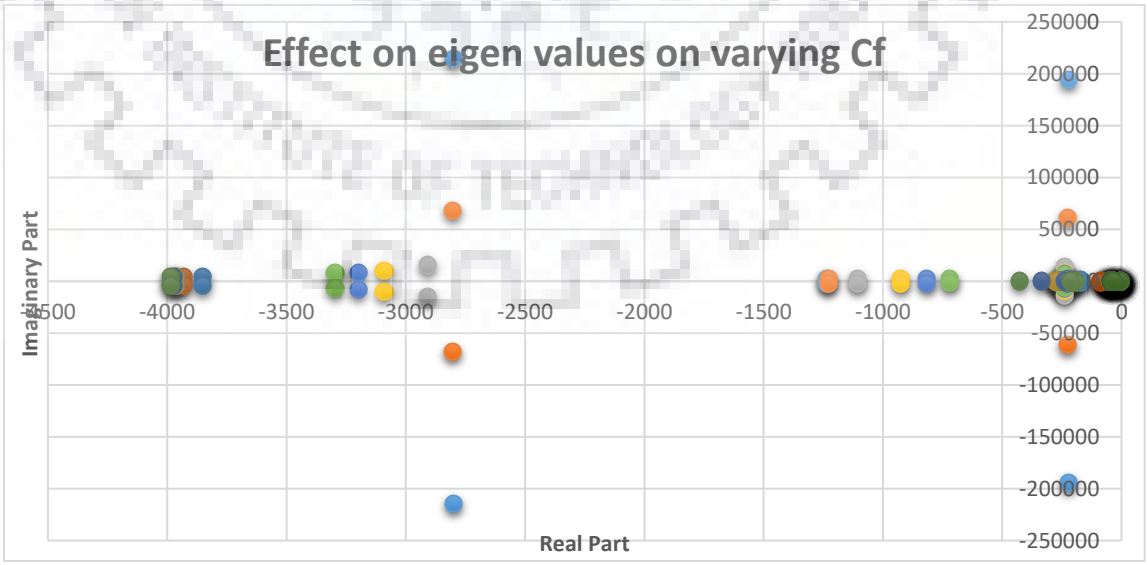

Figure 5. 25: Variation of eigen values with filter capacitance

- In figure 5.25, range of values of C_f can be find out. Initially capacitance value was 1μf but osciallation was very large, as the capacitance values exceed 20μf oscillation become less and after 50μf oscillation slowly decrease. So C_f is taken as 50μf.
- If value of C_f goes beyond 50μf then states move slightly towards unstability.
- If value of C_f is less than 20μf, then power controller eigen values become less stable
- Hence range of C_f is 20μf to 50μf. But for low distortion and low resonance frequency C_f is chosen as 50μf.

- **Root locus by varying filter inductance (L_f)**

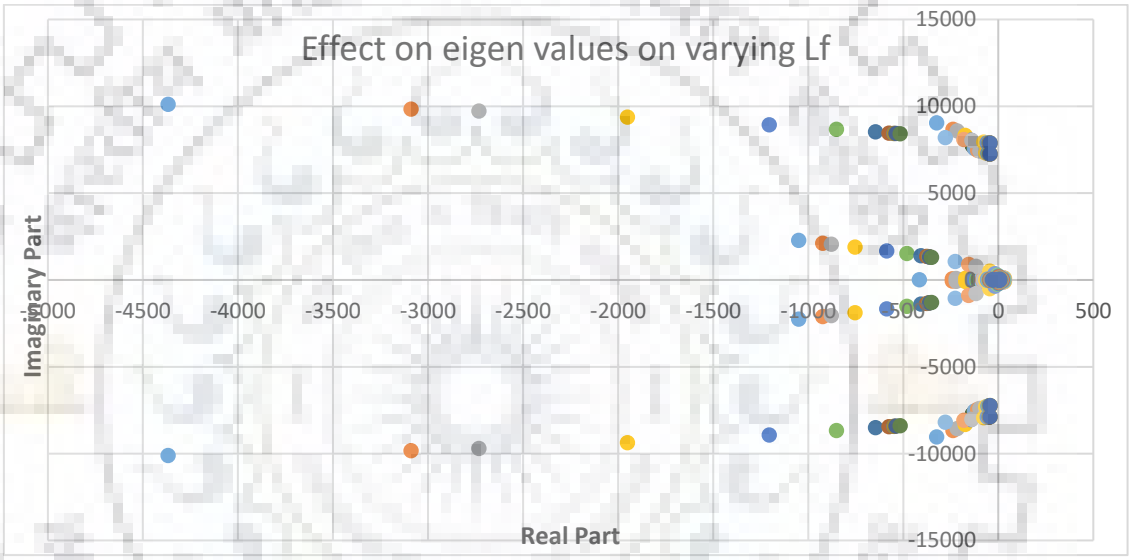

Figure 5. 26: Variation of eigen value with filter inductance

- Here as L_f varies from 1mH to 10 H, initially oscillations are the not there and as $L_f$increased beyond 3 mH damping decreases and oscillation increase as shown in figure 5.26.
- At $L_f = 5.7$ mH locus intersect jw axis i.e eigen value of LCL filter is at jw axis.
- As L_f increase beyond instability increase and at $L_f = 0.315$ H we get eigen values of current and voltage controllers at jw axis.
- So optimum value of L_f selected is 1.35 mH.

- **Root locus by varying active power-frequency droop coefficient (k_p)**

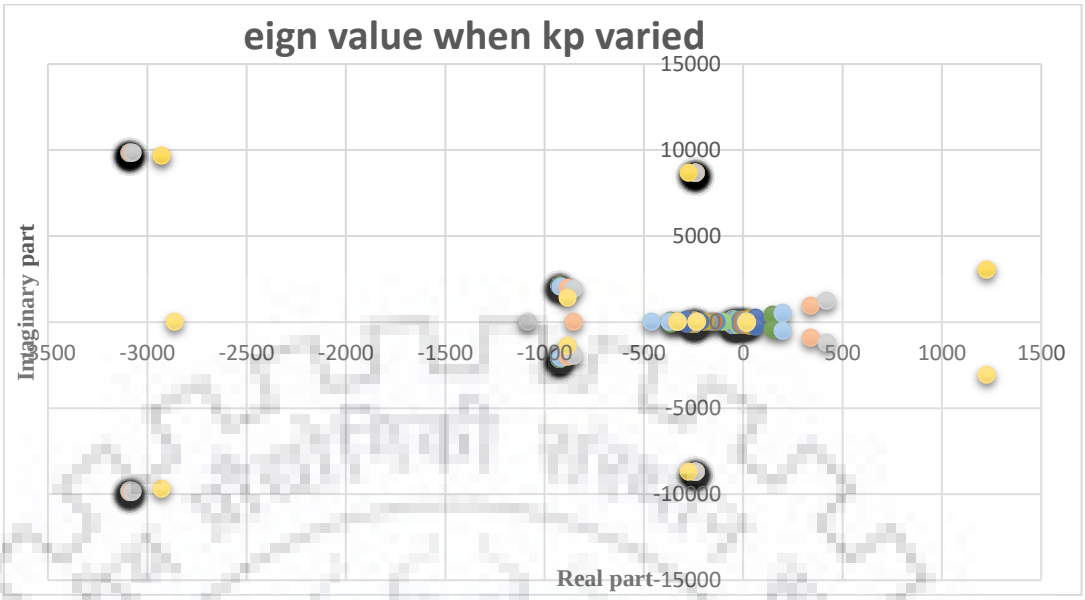

Figure 5. 27: Variation of eigen values if active power frequency droop coefficient is varied

$k_p$is varied from $10^{-7}$to 10 and the root locus is plotted as shown in figure. Now with increased value of k_p it is observed that LCL filter parameter values are moving towards unstability as shown in figure 5.27.

- When k_p is 90 X 10^{-6} locus cut jw axis and we can say verge of unstability is achieved, now if k_p is further increased root locus move towards right hand side and system leads to unstability.
- So range of k_p is $10^{-7}$to 90 X 10^{-5}, and value of k_p selected is 10^{-6}.

- **Root locus by varying reactive power-voltage droop coefficient (k_q)**

- $k_q$is varied from $10^{-2}$to 10 and the root locus is plotted as shown in figure. Now with increased value of k_p it is observed that LCL filter parameter values are moving towards unstability as shown in figure 5.28.
- When k_q is 3.76 X 10^{-4} locus cuts jw axis and we can say verge of unstability is achieved, now if k_q is further increased root locus move towards right hand side and system leads to unstability.
- So range of k_q is 1 X $10^{-3}$to 3.7 X 10^{-4}, and value of k_q selected is 3.37 X 10^{-4}.

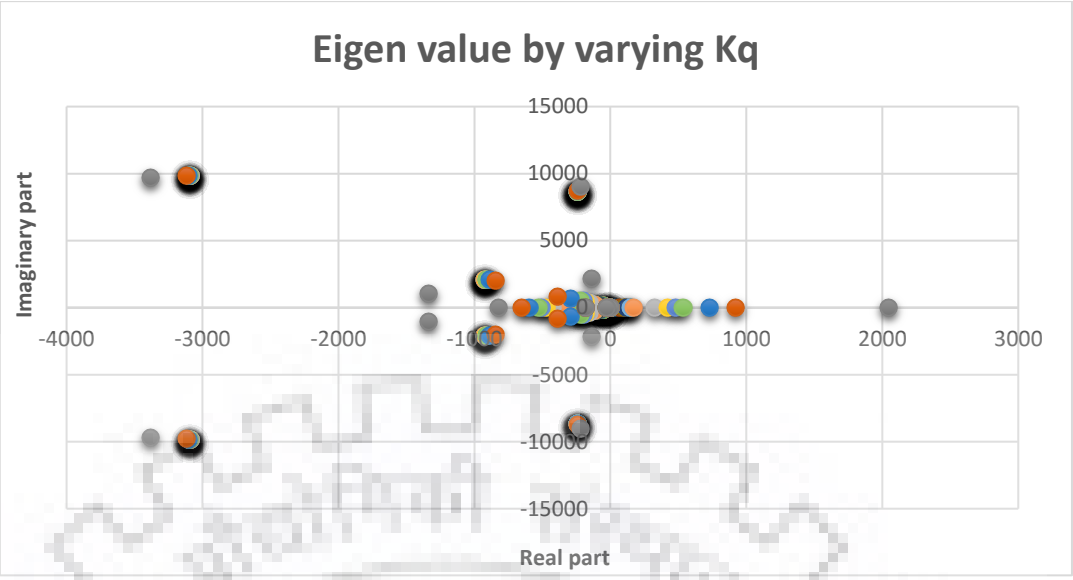

Figure 5. 28: Variation of eigen values if reactive power voltage droop coefficient is varied

Change in root loci is analysed and is seen that some eigen values are close to imaginary axis with decreased damping. Furthermore, sensitivity analyses of each critical mode can be done for each parameter and concluded as to which parameter is more effective on stability of grid connected microgrid stability. In the autonomous mode, controller parameters and filter parameters are the key factors of microgrid stability. Generally, careful selection of the controller, filter, and power sharing parameters maintains power quality within the regulated range and enhance the system performance against load changes and disturbances. These values are shown in table 5.4-5.6.

Table 5. 4: LCL filter paramaters range for stable region

Parameter	Range
L_c	0.2 mH to 0.4 mH
L_f	1 mH to 3 mH
C_f	20 µF to 100 µF
k_p	10^{-7} to 90 X 10^{-5}
k_q	10^{-2} to 3.7 X 10^{-4}
R_f,R_c	30 mΩ to 100 mΩ

Table 5. 5: LCL filter paramaters value for stable region

Parameter	Selected value
L_c	0.35 mH
L_f	1.35 mH
C_f	50 µF
k_p	10^{-6}
k_q	3.37 X 10^{-4}
R_f	100 mΩ
R_c	30 mΩ

These values are valid for the proposed system values which are shown in table 5.6.

Table 5. 6: Considered system parameters

Parameter	Value
V_{DC}	800 volt
V_{grid}	340 volt
$K_{p_{PLL}}$	180
$K_{i_{PLL}}$	3200
$K_{p_{PI}}$	30
$K_{i_{PI}}$	95
ω_c	30

Different approaches to select the controller parameters and control strategies have been reported in the literature **[14], [25]** and **[20]**.

CHAPTER - 6

MULTIPLE PARALLEL CONNECTED INVERTERS IN ISLANDED MODE

Since microgrid comprises of large no of power electronic devices, hence their dynamic stability is more prominent. Through small signal analysis we can know the response of system to a large no of variations. Small signal analysis is done at an operating point and often investigate the interactions among several converters and also done for stability issues of whole system**[16]**.Small signal analysis also allows us to select control and system parameters through frequency domain analysis by knowing eigen values. In this report small signal model of VSI has been done, control loop is designed and stability of system is studied. Such system is shown in figure 6.1.

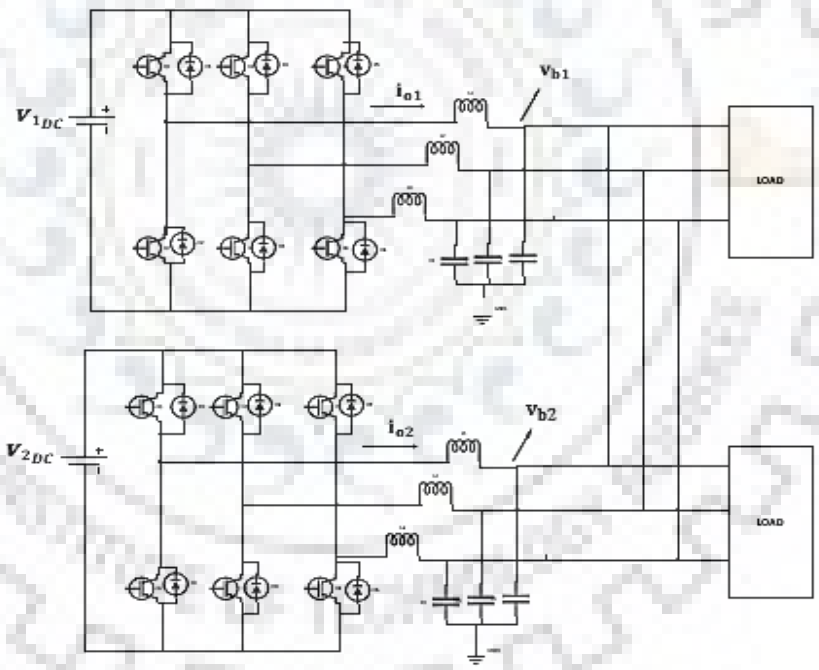

Figure 6. 1: Two 3Ø inverter with difference DC sources

6.1 CONTROL BLOCK OF MULTIPLE PARALLEL CONNECTED INVERTERS

We have formed state space equation and model of single inverter in previous chapter and now lets extend our concept to multiple inverters. The state space equation of single inverter was shown in previous chapter, now same concept is carry forwarded in finding state space equation of multiple inverters. The A matrix derived previously can be called as A_{inv1}as it

contain only 1 inverter, but here we refer it as A_{inv} as shown in (6.1).Hence state space equation of 2 inverter are formed as shown below:

$$A_{INV} = \begin{bmatrix} A_{INV1} + B_{1wcom}C_{INVw1} & 0 \\ 0 & A_{INV2} + B_{2wcom}C_{INVw2} \end{bmatrix} \quad \textbf{(6.1)}$$

The outer loop (Voltage controller block) is used for voltage regulation purposes and gives current reference as output which serve as input for inner loop (Current controller block), here output and input are in d-q form and this hence is termed as voltage control mode.

In autonomous mode, inner loop (Current controller block) also regulate d-q axis current references and outer loop (Power controller block) maintain P and Q at given setpoint and generate d-q axis reference current as input for inner loop for power sharing control among microsources. These are explain in detail in **[16]**and shown in figure 6.2.

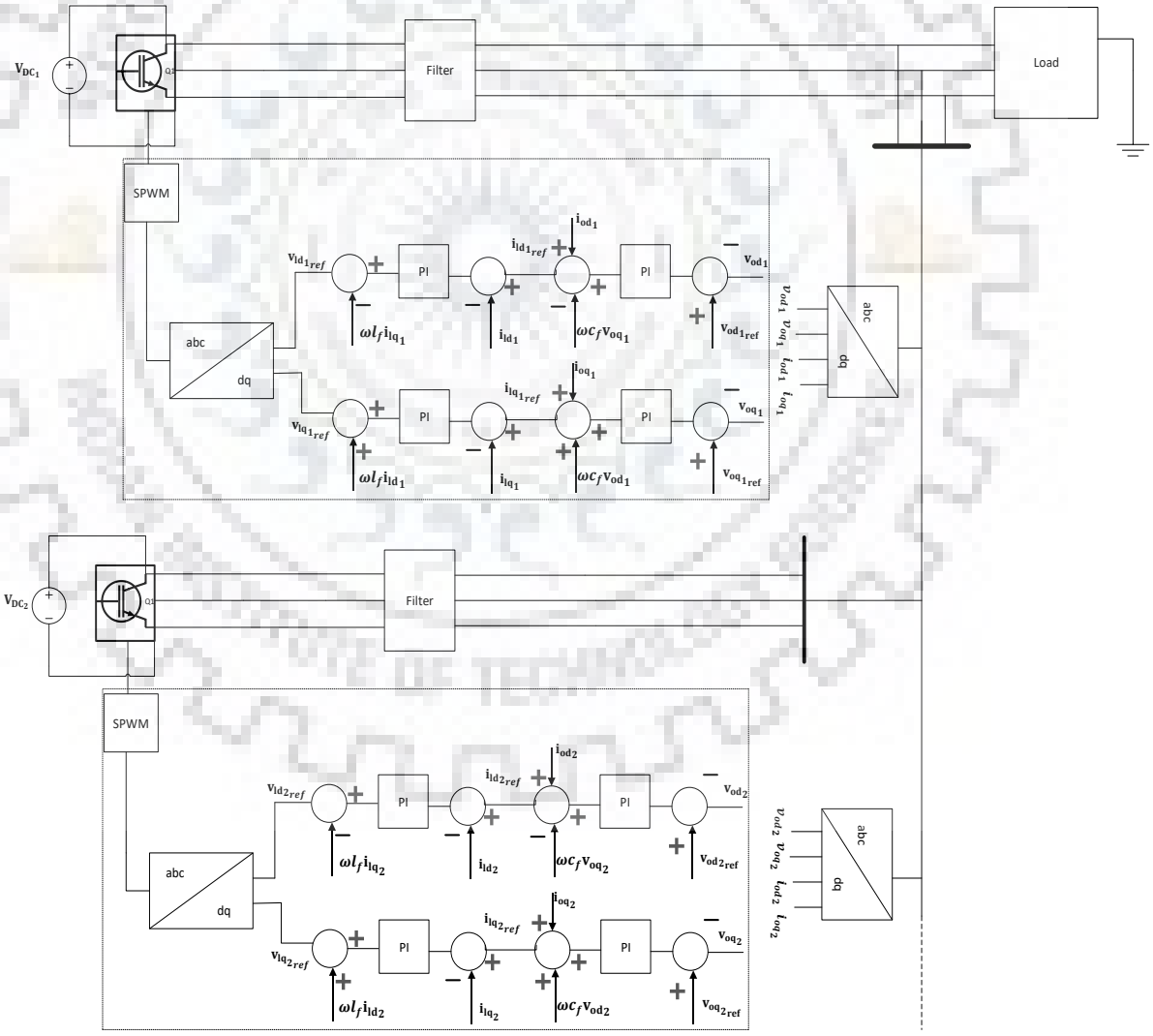

Figure 6. 2: Control strategy of two inverters connected from PCC point

6.2 Simulating 2 sources in autonomous mode

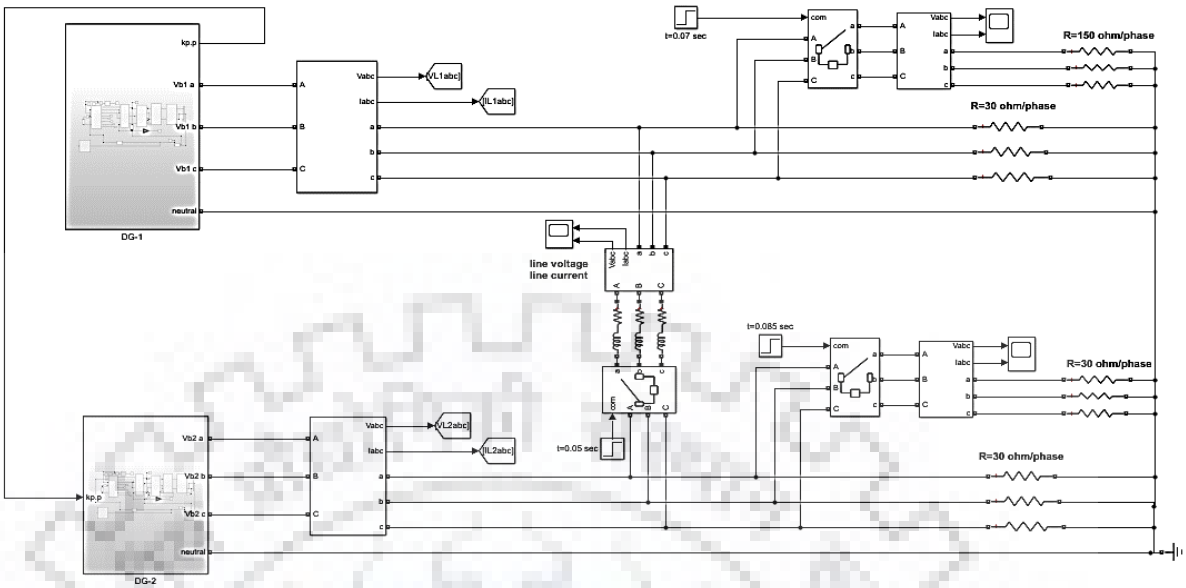

Figure 6. 3: Simulation system considered for load sharing

- In figure 6.3, 2 DGs are there each one with same local load of 30Ω/phase and both DG areactivated at t=0 and allowed to achieve steady state.
- At t=0.05 sec, line connecting both DGs is activated and hence both DGs are now connected through one point and this point is PCC.
- At t=0.07 sec, load of 150Ω/phase near DG1 is switched on.
- At t=0.085 sec, load of 30Ω/phase near DG2 is switched on.

6.3 Theory for interconnection of 2 DGs

In previous chapters, power controller equations are derived considering frequency deviation in reference inverter should affect in others and therefore the term Δω should be added to other inverters. Here we have assumed DG1 as reference inverter and hence its frequency deviations should reflect in other DGs. Droop equation is shown below in which ω isoperating frequencyand ω_{ref} is reference frequency or nominal frequency or frequency set point, k_p is droop coefficient and P is max power delivered by DG.

$$\omega = \omega_{ref} - k_p * P \quad \textbf{(6.2)}$$

$$\omega_1 = \omega_{ref} - k_{p1} P_1 \quad \textbf{(6.3)}$$

$$\omega_2 = \omega_{ref} - k_{p2} P_2 \quad \textbf{(6.4)}$$

Individual droop equation for each inverter is shown in (6.3) and (6.4) where ω_1 and ω_2 are operating frequency of individual inverter, k_{p1} and k_{p2} are droop coefficient of individual

inverter and finally P_1 and P_2 are max power outputs of inverters. For inverter connected together, operating frequency should be same so $\omega_1 = \omega_2$ and ω_{ref} is same 314 rad/sec, so (6.5) can be observed.

$$k_{p1}P_1 = k_{p2}P_2 \tag{6.5}$$

Now in this case it has been assumed that max power DG1 can supply is 6500 watt, and remaining power is supplied by DG2. If we consider load then local load of DG1 consume 4805 watt and same with DG2. Additional load near DG1 consume 961 watt and that of DG2 consume 4805 watt which gives total load of 15376 watt.

6.3.1 Load sharing in multiple DG

$$\text{Droop coefficient } (k_p) = \frac{\Delta\omega}{P} \tag{6.6}$$

$\Delta\omega$is deviation in frequency in rad/sec and P is max power supplied by unit in watt and droop coefficient can be given by (6.6).

6.3.1.1 When droop coefficients are equal

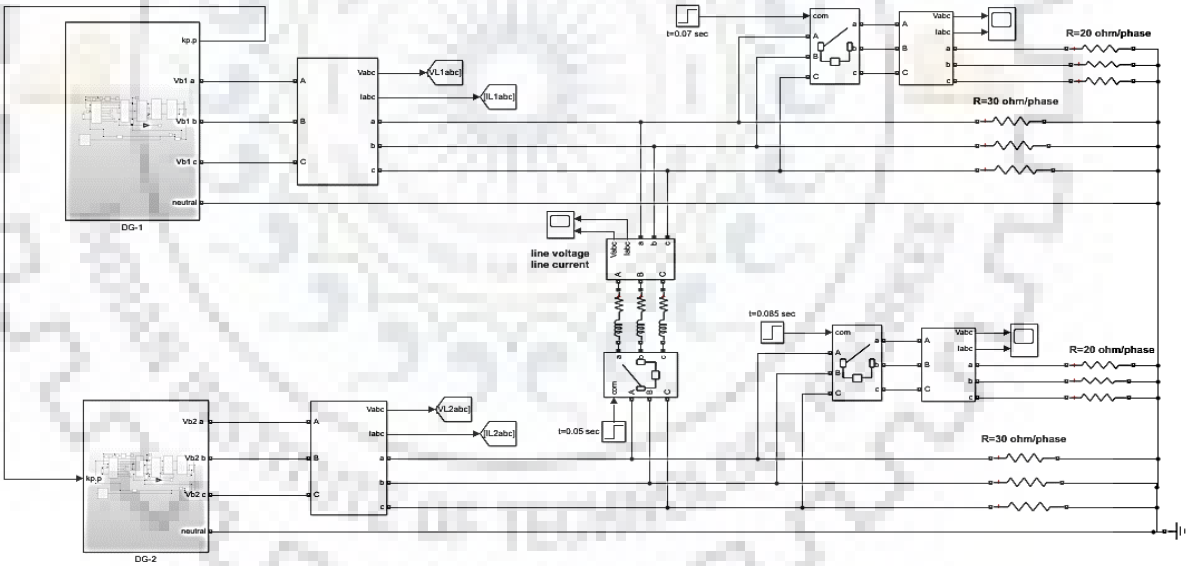

Figure 6. 4: Simulation of 2 DGs in autonomous mode with equal droop gain

We have assumed that both DG are of capacity 10KVA but resistive load is considered only as sown in figure 6.4. As given in theory above and verified with root locus we have considered $k_{p1} = k_{p2} = 10^{-6}$.Now since operating frequency (ω) is same as both are operating in same system and reference frequency (ω_{ref}) is same for both so it can be deduced from equation that$k_{p1}P_1 = k_{p2}P_2$. Using these relations, (6.7) can be deduced.

$$k_{p1} = k_{p2} \text{ , so } P_1 = P_2 \tag{6.7}$$

Total load = 4805+4805+7207+7207=24025 watt

At steady state each DG should supply load equally at 12012.5 watt.

- **Active power of both DGs**

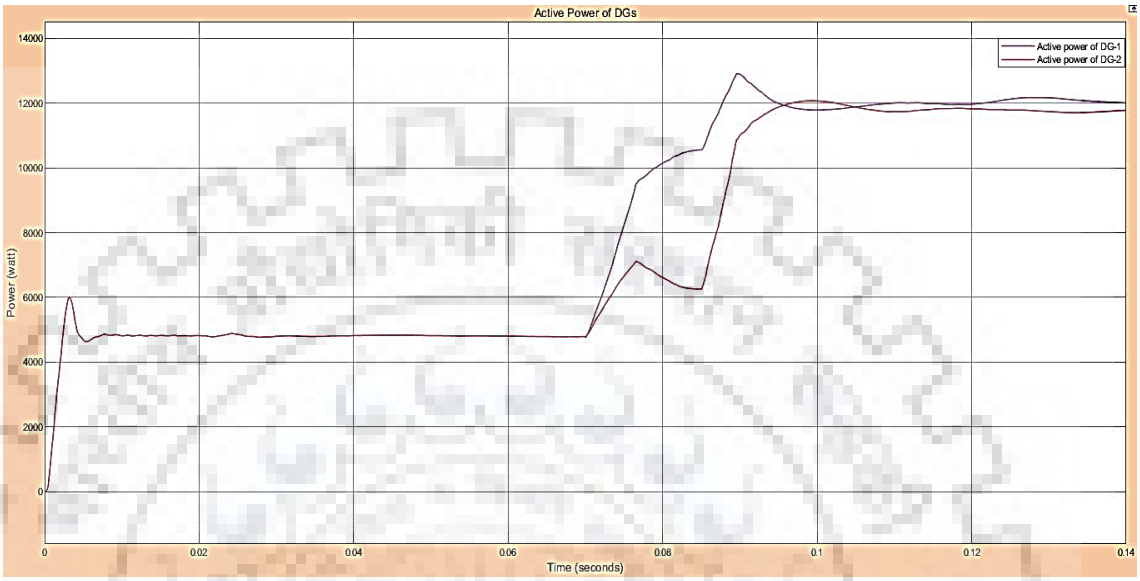

Figure 6. 5: Active power variation of 2 DGs operating in autonomous mode

- It can be seen in figure 6.5, that initially both DG were supplying their local load of 4805 watt.
- At t=0.07sec load near to DG1 is on and hence it quickly respond to load change, however DG2 take some time and respond but since DG1 supplied the load it reduces its output.
- At t=0.085 sec load near to DG2 is on and this time it supply load quickly and quickly they share load in proportion to their coefficient.

- **Reactive power of both DGs**
  - In figure 6.6, initially reactive power is very less but as load switched on at t=0.07 sec some fluctuations occur as now current change instantly even though voltage remains same so now current is not in phase with voltage and hence reactive power comes into picture.
  - System even though quickly start returning to stablility but again at t=0.085 sec load changed instantly and hence fluctuations appear. But after moment system start coming back to stability.

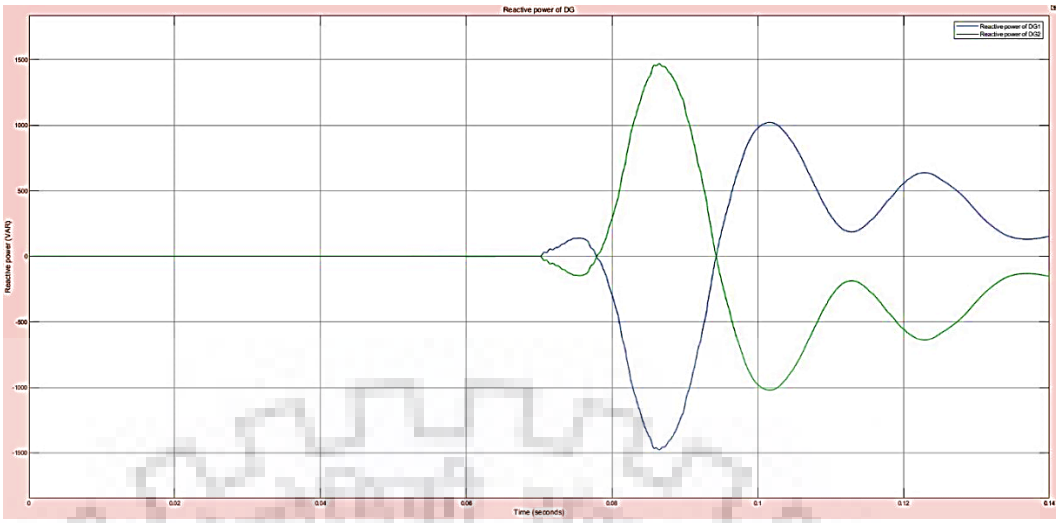

Figure 6. 6: Reactive power of 2 DGs in autonomous mode

- **Voltage at PCC**

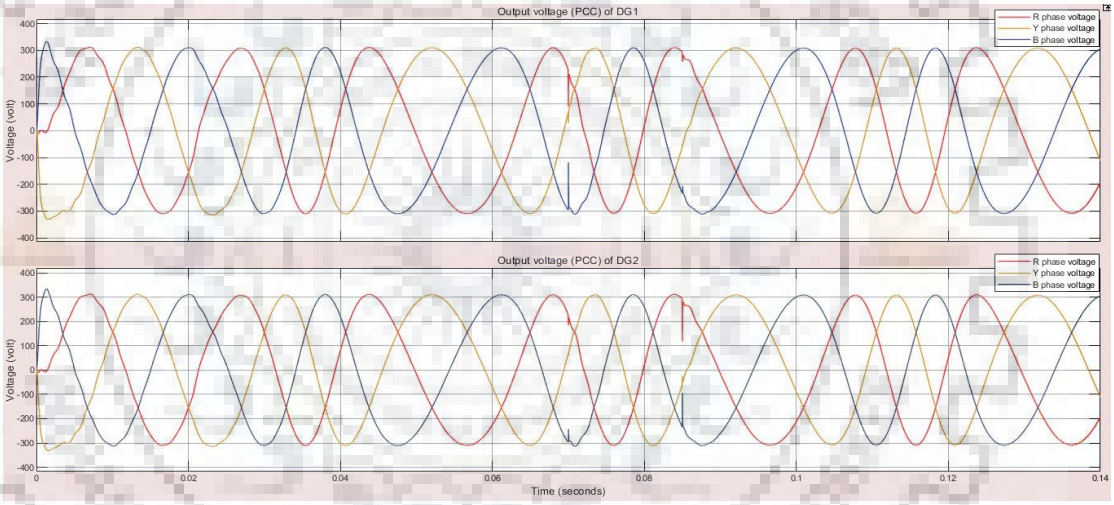

Figure 6. 7: Output voltage (PCC) variation

- Output voltage is in sync with required value even though load change instantly.
- Few disturbance can be observed when load are changed instantly but these quickly settle down and almost no deviation can be seen in voltage at PCC point as shown in figure 6.8.

- **Frequency deviation**

- Deviations in both the DGs are increased with the increase in load on both DGs. Their frequency decreases as per droop equation which can easily be observed in figure 6.7.
- Now frequency of both DG decrease at instant load increases but still the deviation in frequency is within permissible limits.

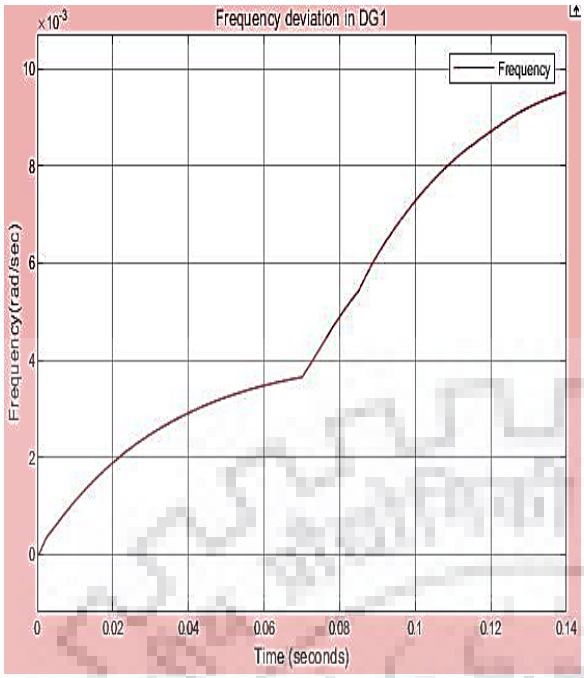

(a)

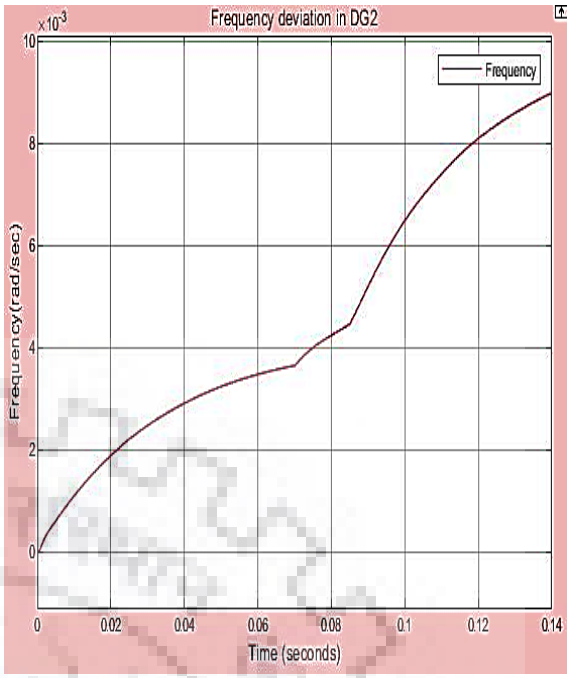

(c)

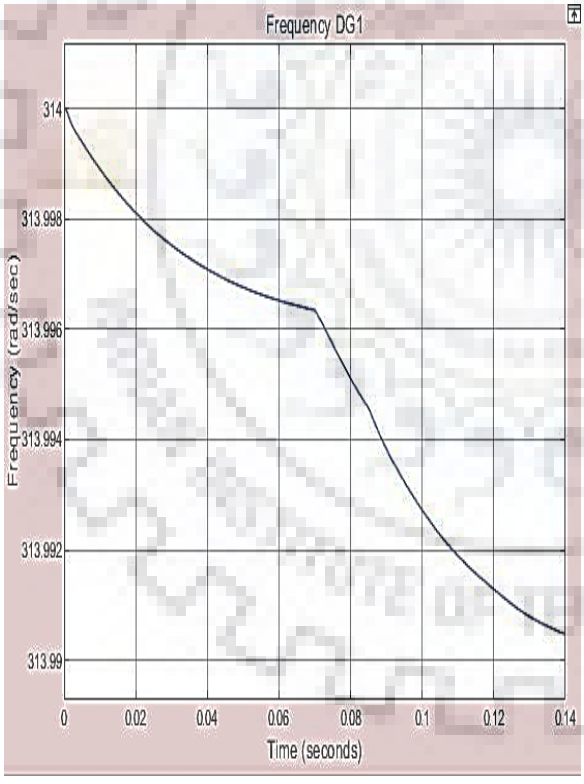

(b)

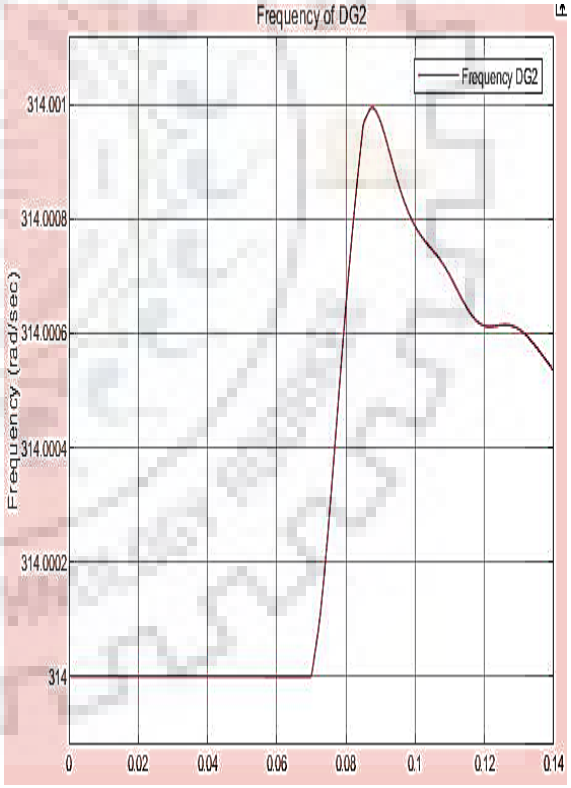

(d)

Figure 6. 8: Frequency under equal droop gain

(a) Frequency deviation in DG1, **(b)**Frequency of DG1

(c) Frequency deviation in DG1, **(d)** Frequency of DG2

- **Current at PCC**

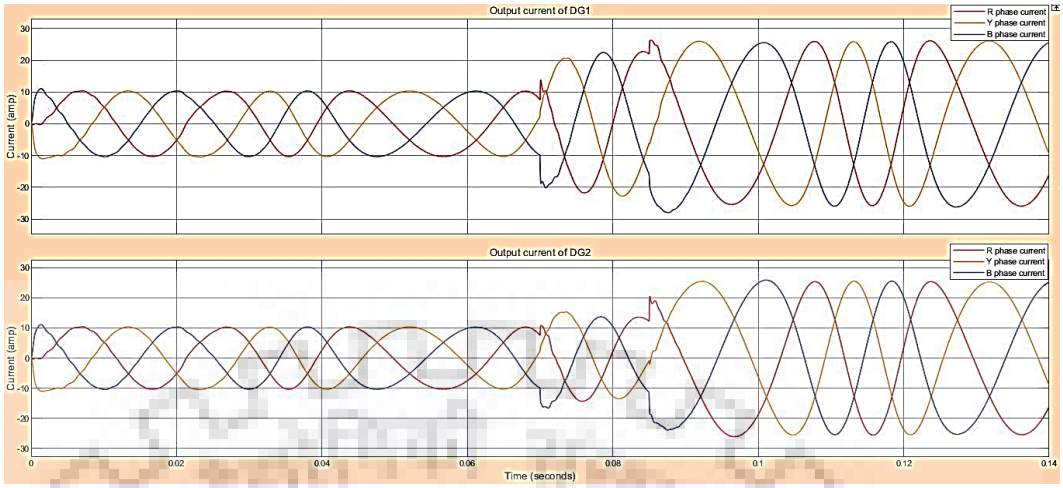

Figure 6. 9: Output current variation of DG1 and DG2

- Current depends on output voltage and load which change at 2 instants.
- Current initially take very less time to settle down and again when both DG connect through same point their frequency matched and now at t=0.07 sec load near DG1 is switched and increase in current is in proportion to load. Since DG1 is near to load so it supply more as compared to DG2.
- At t=0.085 sec load near DG2 is switched and hence its current increase to supply load which in proportion to total load.
- Finally both load shared depending on droop coefficient and current also shared depending on coefficient which is equal so both share equal current which clearly by observed in figure 6.9.

- **Line voltage and current**

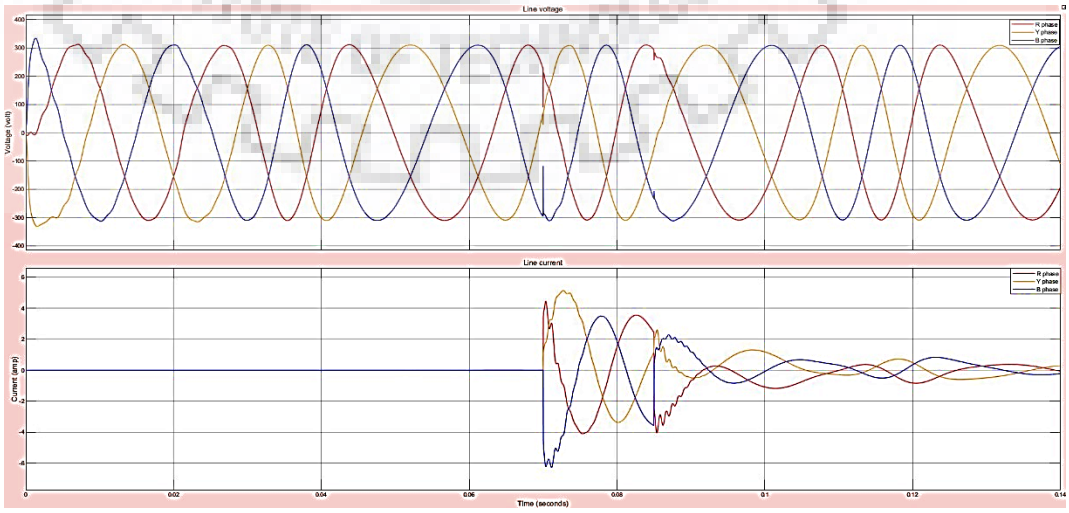

Figure 6. 10: Line voltage and current variation connected between both DGs

- Line current and voltage at PCC side is shown and it can be observed that when load switched on shared power is such that required power flows through line and at both the times this power is transferred from line.
- Later on after sharing is done current through line is decided to maintain shared power and that can be observed in figure 6.10.

- **Load voltage and current**

- It can be seen from figure 6.11 as when load near DG1 switched at t=0.07 sec its voltage and current changes as depicted in figure. This current is in proportion to load when voltage is decided.
- It can be seen from figure 6.12 that as load near DG2 switched at t=0.085 sec voltage and current changes in proportion to load.

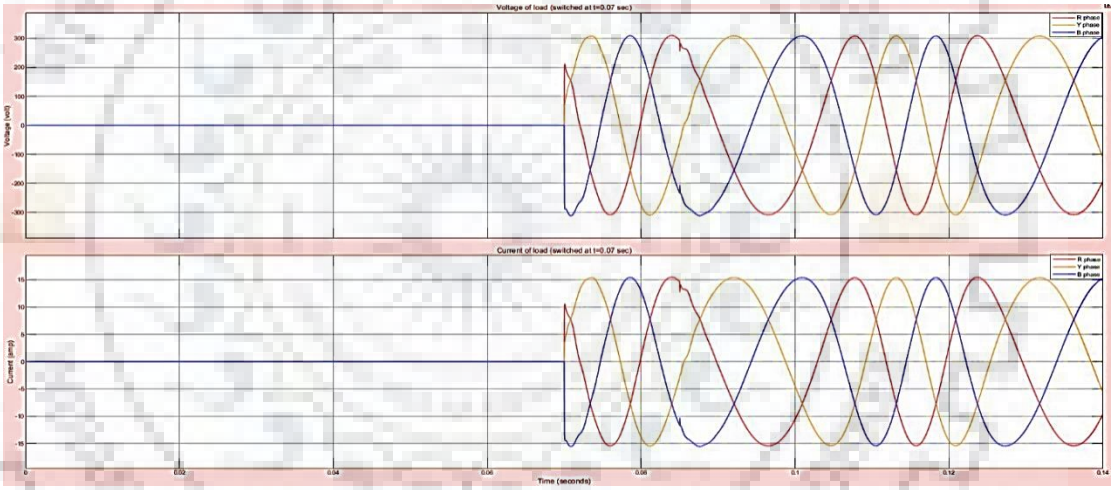

Figure 6. 11: Voltage and current variation of load switched at t=0.07 sec

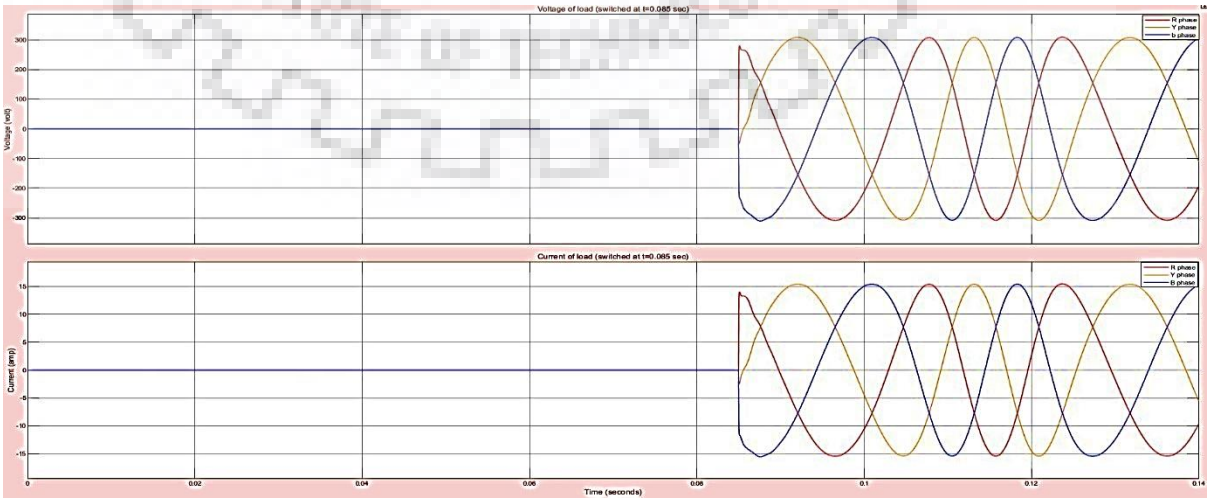

Figure 6. 12: Voltage and current variation of load switched at t=0.085 sec

6.3.1.2 When droop coefficients are different

Observing frequency deviation we get,

$$\Delta\omega_1 = \Delta\omega_2 = 0.45\ rad/sec$$

$$P_1 = 6500\ W$$

$$P_2 = 8800\ W$$

$$P_1 + P_2 = 15300\ \text{W}$$

Now for load sharing we select droop coefficient:

$$k_{p1} = \frac{0.45}{6500} = 6.875\ \text{X}\ 10^{-5}$$

$$k_{p2} = \frac{0.45}{8800} = 4.88\ \text{X}\ 10^{-5}$$

As previously described, these values lie in stability range of value selection as given in table so system should be stable. Using these values, previous mentioned model is simulated and results obtained as shown:

i. <u>Simulation</u>

a) **Frequency deviation**

- Deviations in both the DGs are to be increased as load is increasing on both DG so their frequency should decrease as per droop equation which can easily be observed in figure 6.13.
- Now frequency of both DG decreases at instant load increases but the deviation in frequency is within permissible limits.

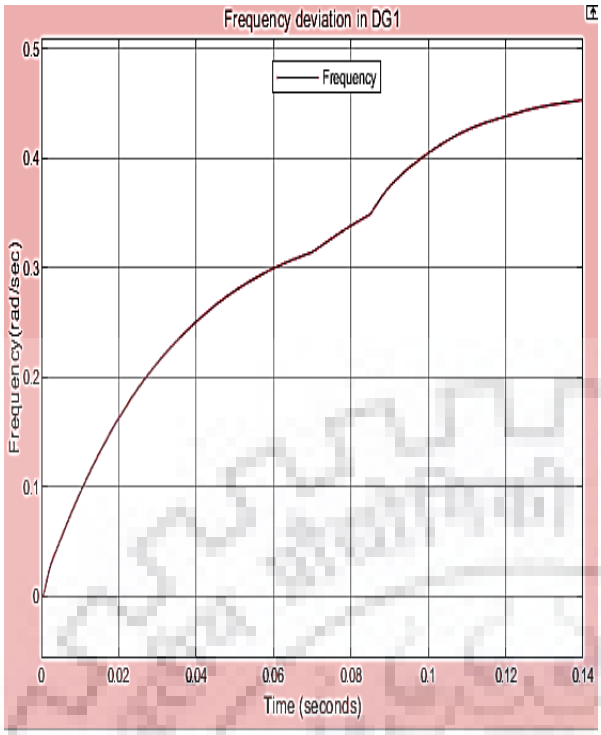

(a)

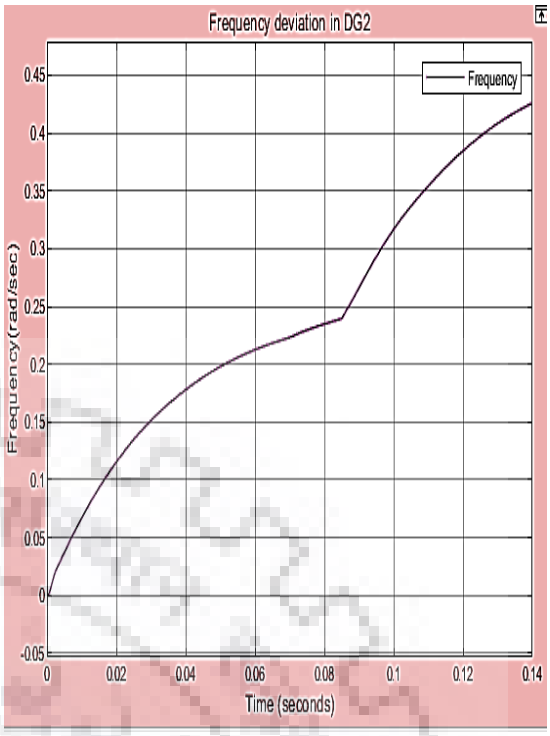

(c)

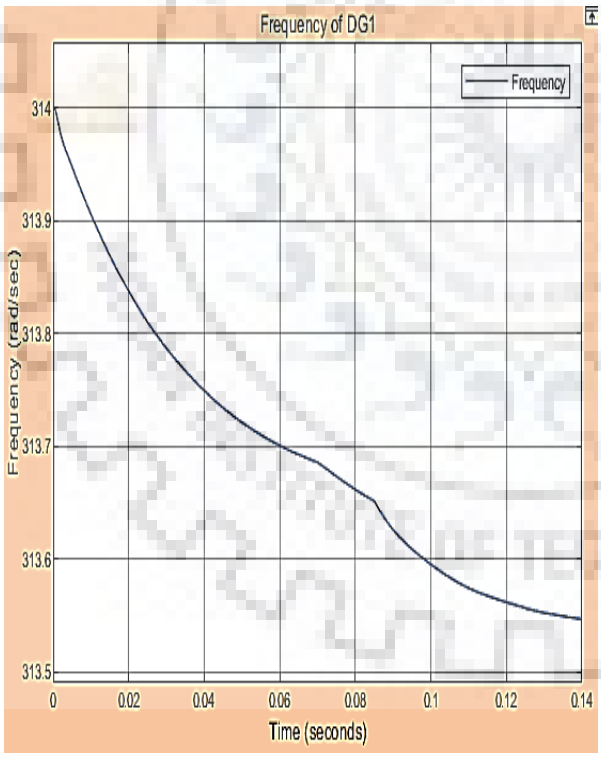

(b)

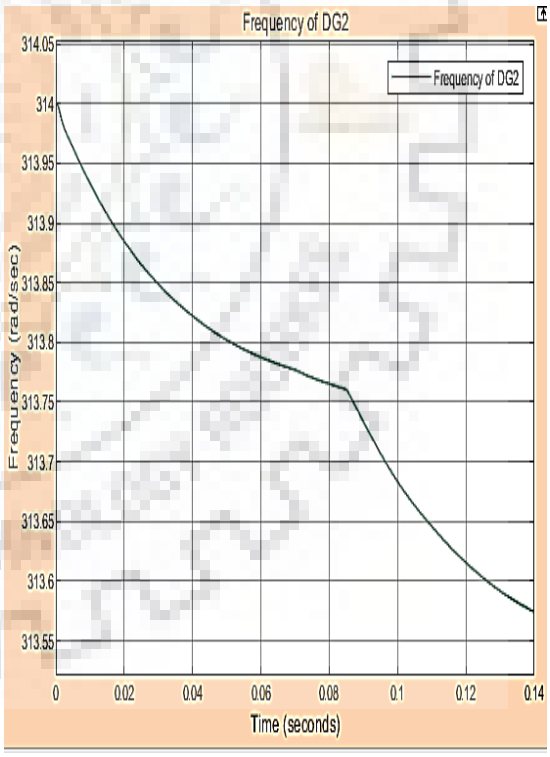

(d)

Figure 6. 13: Frequency under unequal droop gain

(a) Frequency deviation in DG1, **(b)** Frequency of DG1

(c) Frequency deviation in DG1, **(d)** Frequency of DG2

b) **Active power**

Figure 6. 14: Active power variation of DG1 and DG2

- It is derived by calculation that DG1 is delivering power of 6383W and it can be observed in graph that it is delivering power of 6370W. Such difference is negligible and is due to certain assumptions which are not exact in practical circuit like operating frequency of both DG is not exactly same, also frequency deviation is not exactly same. There are differences in decimal values and moreover line impedance also plays part in consuming certain power.
- For DG2 it is derived that power of 8992 should be supplied but in simulation it can be observed supplying 8950W and such difference is negligible and reason is explained above. These inferences can be observed in figure 6.14.

c) **Reactive power**

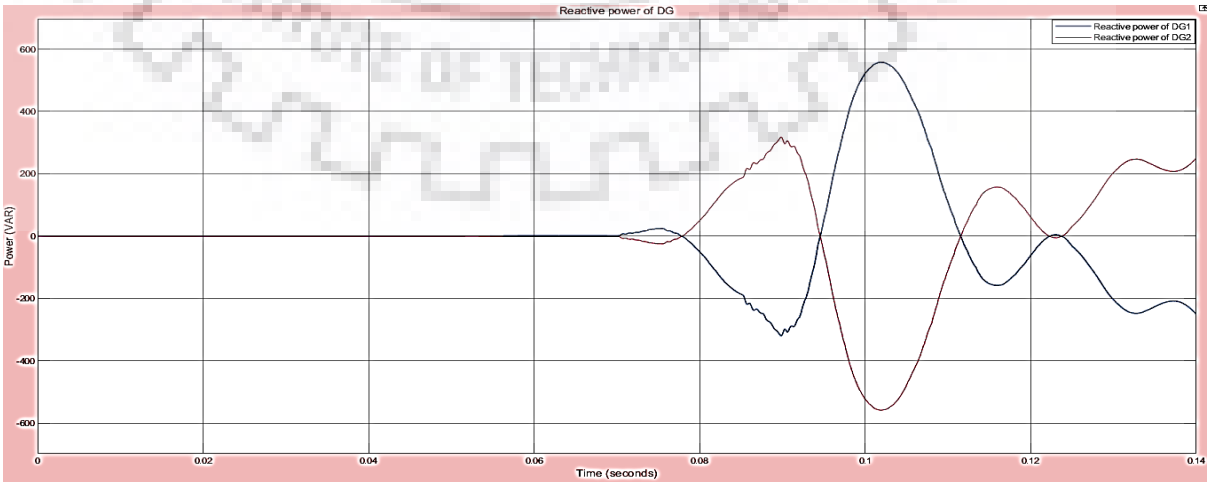

Figure 6. 15: Reactive power variation of DG1 and DG2

- Initially reactive power is very less but as load switched on at t=0.07 sec some fluctuations occur as now current change instantly even though voltage remains same so now current is not in phase with voltage and hence reactive power comes into picture.
- System even though quickly start returning to stability but again at t=0.085 sec load changed instantly and hence fluctuations appear. But after moment system start coming back to stability which clearly can be observed in figure 6.15.

d) **Output Voltage**

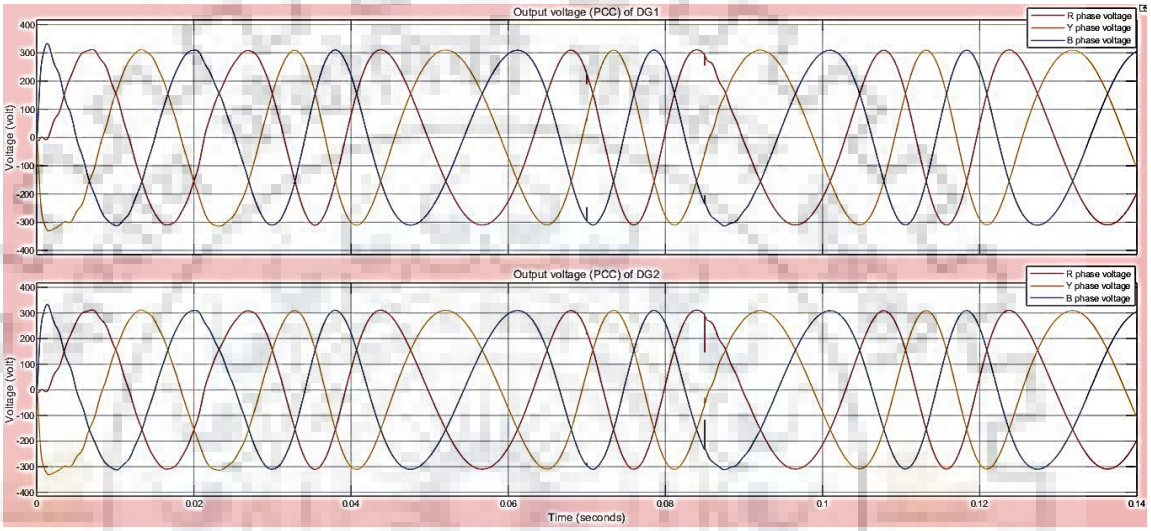

Figure 6. 16: Output voltage variation of DG1 and DG2

- Output voltage is in sync with required value even though load change instantly.
- Few disturbance can be seen in figure 6.16 when load are changed instantly but these quickly settle down and almost no deviation can be seen in voltage at PCC point.

e) **Output Current**

- Current depends on output voltage and load which change at 2 instants.
- Current initially take very less time to settle down and again when both DG connect through same point their frequency matched and now at t=0.07 sec load near DG1 is switched and increase in current is in proportion to load. Since DG1 is near to load so it supply more as compared to DG2.
- At t=0.085 sec load near DG2 is switched and hence its current increase to supply load which in proportion to total load.

- Finally both load shared depending on droop coefficient and current also shared depending on coefficient which is equal so both share equal current as seen from figure 6.17.

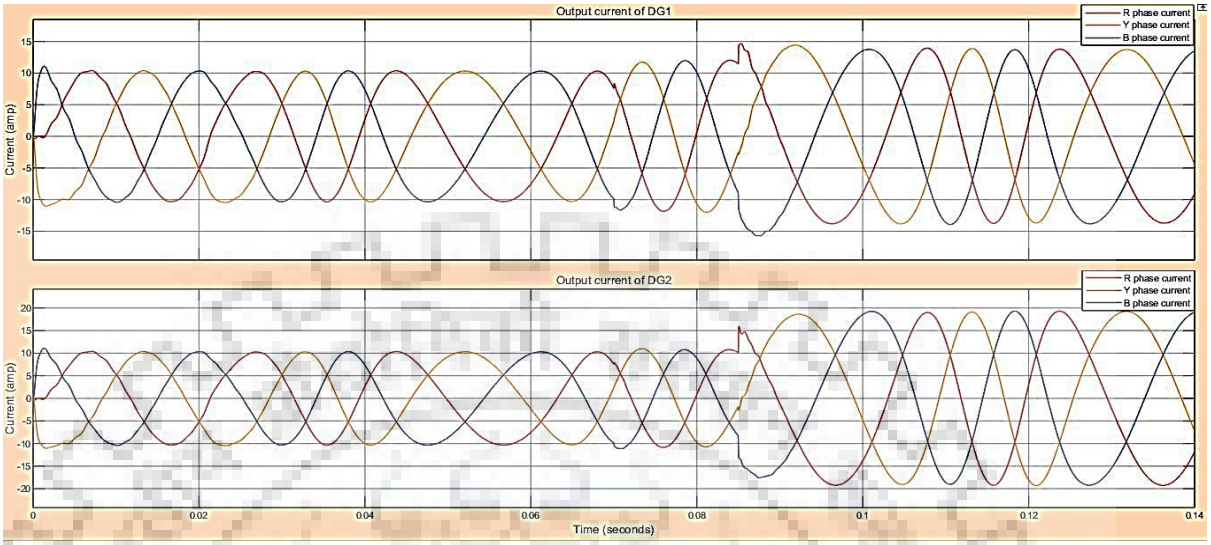

Figure 6. 17: Output current variation of DG1 and DG2

f) **Load voltage and current**

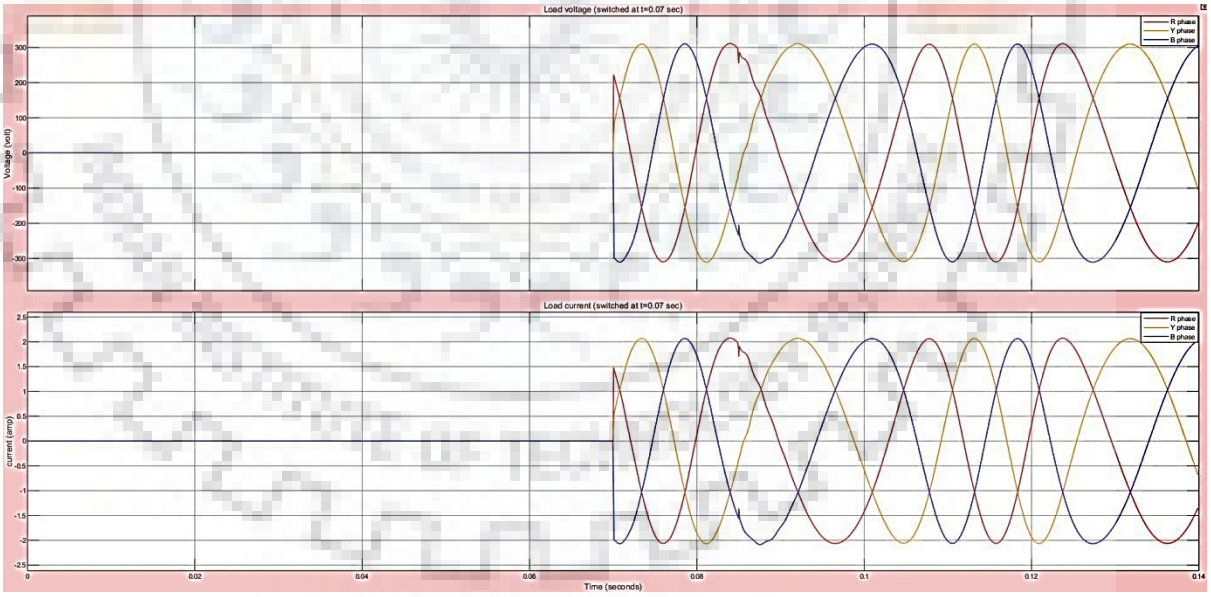

Figure 6. 18: Voltage and current of load switched at t=0.07 sec

- It can be seen as when load near DG1 switched at t=0.07 sec its voltage and current changes and this current is in proportion to load when voltage is decided which can be seen from figure 6.18.

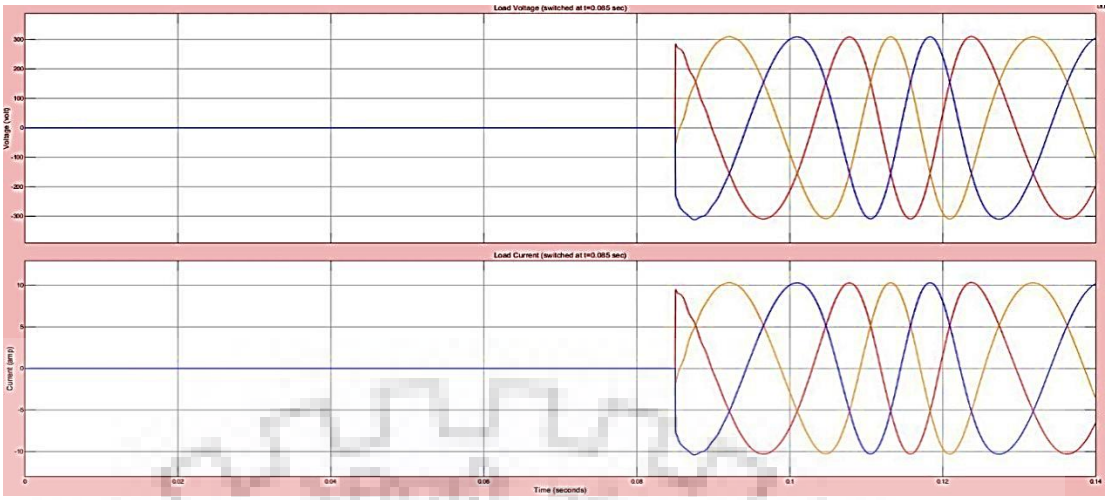

Figure 6. 19: Voltage and current of load switched at t=0.085 sec

- When load near DG2 switched at t=0.085 sec voltage and current changes and this current is in proportion to load when voltage is decided as seen from figure 6.19.

g) **Line voltage and current**

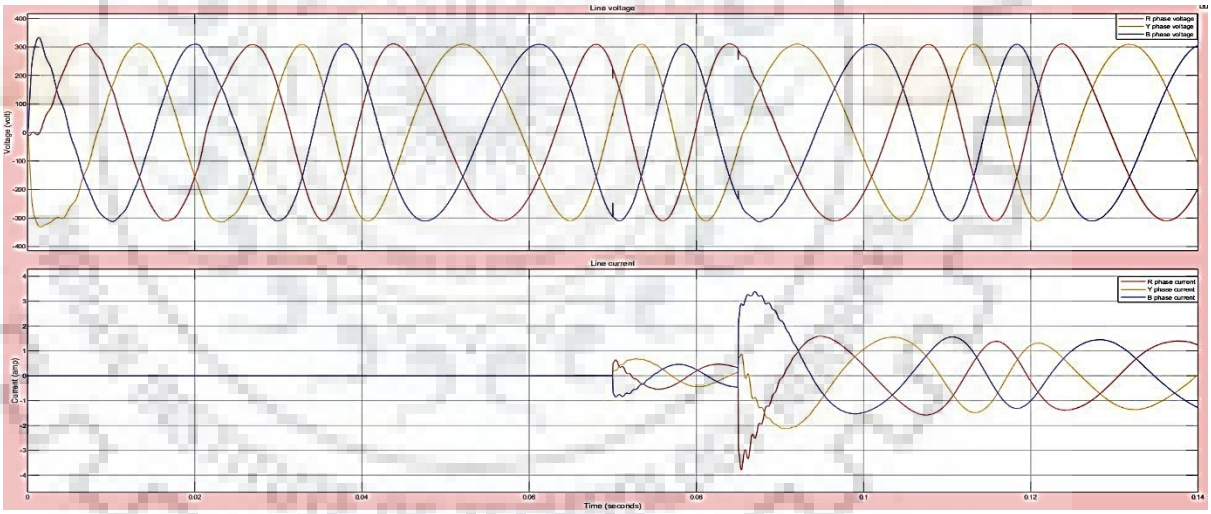

Figure 6. 20: Voltage and current of line connected between DGs

- Line current and voltage at PCC side is shown and it can be observed that when load switched on shared power is such that required power flows through line and at both the times this power is transferred from line.
- Later on after sharing is done current through line is decided to maintain shared power and that can be observed in figure 6.20.

ii. Calculation

We have already established that $k_{p1}P_1 = k_{p2}P_2$, so following can be deduced.

$$\frac{P_1}{P_2} = \frac{k_{p2}}{k_{p1}} = \frac{4.88}{6.875} = 0.7098$$

$$\frac{P_2}{P_1} = 1.4088$$

$$P_1 + P_2 = 15376$$

Solving them we get,

$$P_1 = 6383\ watt$$

$$P_2 = 8992\ watt$$

$$\Delta\omega = k_{p1}P_1 = k_{p2}P_2 = 0.438 \text{ rad/sec}$$

Hence we can see that simulation verifies mathematical calculations as there is negligible error in frequency and power output. Hence this concept can be used in load sharing among multiple DGs.

CHAPTER - 7
CONCLUSION

The mathematical process and structure for the development of micro-grid model are presented in a general form and can be expanded to include additional DG units, loads and controllers as desired. The developed model includes the PLL model to dynamically synchronise the electronically interfaced DG unit with the network frequency. Frequency restoration in isolated mode is carried out by the droop equation which makes it behave as the governor of the synchronous machine. Applications of the model to

(i) Investigate dynamics of the micro-grid

(ii) Design/optimise controllers of the electronically interfaced DG unit during grid-connected and isolated modes of operation are presented here.

Simulation results show that the fast control action of the electronically interfaced DG unit can be exploited to meet changes in power demand, maintain voltage and frequency stability and quality during the autonomous mode. The proposed strategy is validated both by fast response and by concluding that PLL works perfectly fine i.e. V_{oq}= 0.

Then state space equation form of overall system in both modes are linearized around operating point mentioned in table 4.1 and eigen values are plotted as shown in figure 5.6 and 5.7. Further analysis is done on finding optimum value for filter parameter for stable system through eigen value plot as shown in figure 5.8-figure 5.11. Hence we can say that it captures the important dynamics of the passive output filter, the current controllers and the filter in the power reference to current reference conversion.

Lastly it is shown how load is shared in isolated mode among DGs based on droop coefficient, which provides the base for connecting multiple DGs of different ratings to microgrid. This has also been verified mathematically.

REFERENCES

[1] A. Yazdani, "Control of an islanded Distributed Energy Resource unit with load compensating feed-forward," *2008 IEEE Power and Energy Society General Meeting - Conversion and Delivery of Electrical Energy in the 21st Century*, Pittsburgh, PA, 2008, pp. 1-7.

[2] B. Kroposki, C. Pink, R. DeBlasio, H. Thomas, M. Simoes and P. K. Sen, "Benefits of power electronic interfaces for distributed energy systems," *2006 IEEE Power Engineering Society General Meeting*, Montreal, Que., 2006, pp. 8.

[3] M. Hossain, H. Pota and W. Issa, "Overview of AC Microgrid Controls with Inverter-Interfaced Generations," *Energies*, vol. 10, no. 9, p. 1300, Aug. 2017.

[4] N. Pogaku, M. Prodanović, and T. C. Green, "Modeling, analysis and testing of autonomous operation of an inverter-based microgrid," *IEEE Trans. Power Electron.*, vol. 22, no. 2, pp. 613–625, 2007.

[5] P. Piagi and R. H. Lasseter, "Autonomous control of microgrids," *2006 IEEE Power Engineering Society General Meeting*, Montreal, Que., 2006, pp. 8

[6] S. Barsali, M. Ceraolo, P. Pelacchi and D. Poli, "Control techniques of Dispersed Generators to improve the continuity of electricity supply," *2002 IEEE Power Engineering Society Winter Meeting. Conference Proceedings (Cat. No.02CH37309)*, New York, NY, USA, 2002, vol.2, pp. 789-794.

[7] M. Rasheduzzaman, J. A. Mueller and J. W. Kimball, "Reduced-Order Small-Signal Model of Microgrid Systems," in *IEEE Transactions on Sustainable Energy*, vol. 6, no. 4, pp. 1292-1305, Oct. 2015.

[8] C. K. Sao and P. W. Lehn, "Intentional islanded operation of converter fed microgrids," *2006 IEEE Power Engineering Society General Meeting*, Montreal, Que., 2006, pp. 6

[9] Ionel Vechiu, Octavian Curea, Alvaro Llaria, Haritza Camblong, (2011) "Control of power converters for microgrids", COMPEL - The international journal for computation and mathematics in electrical and electronic engineering, Vol. 30 Issue: 1, pp.300-309

[10] V. Blasko and V. Kaura, "A new mathematical model and control of a three-phase AC-DC voltage source converter," in *IEEE Transactions on Power Electronics*, vol. 12, no. 1, pp. 116-123, Jan. 1997.

[11] P. Kundur, *Power System Stability and Control*, New York, McGraw-Hill, 1994, pp. 699-822.

[12] M. C. Chandorkar, D. M. Divan and R. Adapa, "Control of parallel connected inverters in standalone AC supply systems," in *IEEE Transactions on Industry Applications*, vol. 29, no. 1, pp. 136-143, Jan.-Feb. 1993.

[13] M. Yazdanian and A. Mehrizi-Sani, "Case Studies on Cascade Voltage Control of Islanded Microgrids Based on the Internal Model Control," *IFAC-PapersOnLine*, vol. 48, no. 30, pp. 578–582, Jan. 2015.

[14] N. Abdel-Rahim and J. E. Quaicoe, "Small-signal model and analysis of a multiple feedback control scheme for three-phase voltage-source UPS inverters," *PESC Record.*

27th Annual IEEE Power Electronics Specialists Conference, Baveno, Italy, 1996, pp. 188-194 vol.1.

[15] T. Green and M. Prodanovi´c, "Control of inverter-based micro-grids," Electric Power Systems Research, vol. 77, no. 9, pp. 1204–1213, Jul. 2007.

[16] Yu Zhang, Zhenhua Jiang and Xunwei Yu, "Small-signal modeling and analysis of parallel-connected voltage source inverters," *2009 IEEE 6th International Power Electronics and Motion Control Conference*, Wuhan, 2009, pp. 377-383.

[17] Shuya Wang, Jianhui Su, Xiangzhen Yang, Yan Du, Yong Tu and Huadian Xu, "A review on the small signal stability of microgrid," *2016 IEEE 8th International Power Electronics and Motion Control Conference (IPEMC-ECCE Asia)*, Hefei, 2016, pp. 1793-1798.

[18] Z. H. Zheng J, Li X , Wang Y, Zhu S, Wang X, "Small signal Stability Analysis of a Microgrid Switching to Islanded Mode," *Dianli Xitong Zidonghua/Automation Electr. Power Syst.*, vol. 36, no. 15, pp. 25–32, 2012.

[19] R. Majumder, "Some Aspects of Stability in Microgrids," in *IEEE Transactions on Power Systems*, vol. 28, no. 3, pp. 3243-3252, Aug. 2013.

[20] Michael Angelo Pedrasa, Ted Spooner, "A Survey of Techniques Used to Control Microgrid Generation and Storage during Island Operation." AUPEC2006.

[21] M. Rasheduzzaman, J. A. Mueller and J. W. Kimball, "An Accurate Small-Signal Model of Inverter- Dominated Islanded Microgrids Using dq Reference Frame," in *IEEE Journal of Emerging and Selected Topics in Power Electronics*, vol. 2, no. 4, pp. 1070-1080, Dec. 2014.

[22] S. Leitner, M. Yazdanian, A. Mehrizi-Sani and A. Muetze, "Small-Signal Stability Analysis of an Inverter-Based Microgrid With Internal Model-Based Controllers," in *IEEE Transactions on Smart Grid*, vol. 9, no. 5, pp. 5393-5402, Sept. 2018.

[23] N. Pogaku, M. Prodanovic and T. C. Green, "Inverter-based microgrids: small-signal modelling and testing," *The 3rd IET International Conference on Power Electronics, Machines and Drives, 2006. PEMD 2006*, 2006, pp. 499-504.

[24] M. A. Hassan and M. A. Abido, "Optimal Design of Microgrids in Autonomous and Grid-Connected Modes Using Particle Swarm Optimization," in *IEEE Transactions on Power Electronics*, vol. 26, no. 3, pp. 755-769, March 2011.

[25] F. Katiraei, M. R. Iravani and P. W. Lehn, "Small-signal dynamic model of a micro-grid including conventional and electronically interfaced distributed resources," in *IET Generation, Transmission & Distribution*, vol. 1, no. 3, pp. 369-378, May 2007.

[26] N. Kroutikova, C. a. Hernandez-Aramburo and T. C. Green, "State-space model of grid-connected inverters under current control mode," in *IET Electric Power Applications*, vol. 1, no. 3, pp. 329-338, May 2007.

[27] K. H. Ahmed, S. J. Finney and B. W. Williams, "Passive Filter Design for Three-Phase Inverter Interfacing in Distributed Generation," *2007 Compatibility in Power Electronics*, Gdansk, 2007, pp. 1-9.

[28] Tusar Kumar Dash and B. ChittiBabu, "A novel small signal modeling of three phase grid connected inverter system". *Researchgate.net*[Online]. Available: https://www.researchgate.net/publication/236735931_Small_signal_modelling_of_three_phase_grid_connected_inverter. [Accessed: 10-May-2019].

[29] R. H. Lasseter, "MicroGrids," *2002 IEEE Power Engineering Society Winter Meeting. Conference Proceedings (Cat. No.02CH37309)*, New York, NY, USA, 2002, pp. 305-308 vol.1.

[30] M. Barnes *et al.*, "Real-World MicroGrids-An Overview," *2007 IEEE International Conference on System of Systems Engineering*, San Antonio, TX, 2007, pp. 1-8.

[31] R. H. Lasseter, "Certs Microgrid," *2007 IEEE International Conference on System of Systems Engineering*, San Antonio, TX, 2007, pp. 1-5.

[32] S. Chen and H. Yu, "A Review on Overvoltages in Microgrid," *2010 Asia-Pacific Power and Energy Engineering Conference*, Chengdu, 2010, pp. 1-4.

[33] P. Basak, A. K. Saha, S. Chowdhury and S. P. Chowdhury, "Microgrid: Control techniques and modeling," *2009 44th International Universities Power Engineering Conference (UPEC)*, Glasgow, 2009, pp. 1-5.

[34] E. Perea, J. M. Oyarzabal, and R. Rodríguez, "Definition, evolution, applications and barriers for deployment of microgrids in the energy sector," *e &iElektrotechnik und Informationstechnik*, vol. 125, no. 12, pp. 432–437, Dec. 2008.

[35] M. Smith and D. Ton, "Key Connections: The U.S. Department of Energy's Microgrid Initiative," in *IEEE Power and Energy Magazine*, vol. 11, no. 4, pp. 22-27, July-Aug. 2013.

[36] J. A. P. Lopes *et al.*, "Control strategies for microgrids emergency operation," *2005 International Conference on Future Power Systems*, Amsterdam, 2005, pp. 6 pp.-6.

[37] F. Katiraei, M. R. Iravani and P. Lehn, "Microgrid autonomous operation during and subsequent to islanding process," *IEEE Power Engineering Society General Meeting, 2004.*, Denver, CO, 2004, pp. 2175 Vol.2.

[38] H. Liu, K. Li, H. Gao, Y. Sun, K. Sun and W. Lee, "Control and simulation of grid-connected micro-grid," *2012 IEEE Power and Energy Society General Meeting*, San Diego, CA, 2012, pp. 1-6

[39] R. Lasseter and P. Piagi, "Providing premium power through distributed resources," *Proceedings of the 33rd Annual Hawaii International Conference on System Sciences*, Maui, HI, USA, 2000, pp. 1-9, 2000.

[40] S. M. Amelian and R. Hooshmand, "Small signal stability analysis of microgrids considering comprehensive load models - A sensitivity based approach," *2013 Smart Grid Conference (SGC)*, Tehran, 2013, pp. 143-149.

[41] DuanYubing, Gong Yulei, Li Qingmin and Wang Hui, "Modelling and simulation of the microsources within a microgrid," *2008 International Conference on Electrical Machines and Systems*, Wuhan, 2008, pp. 2667-2671.

[42] Faridaddin. Katiraei, "Dynamic Analysis and Control of Distributed Energy Resources in a Micro-Grid," Ph.D. dissertation, University of Toronto, Univ Toronto, Canada, 2006. Accessed on: May, 10, 2019. [Online]. http://research.iaun.ac.ir/pd/bahador.fani/pdfs/UploadFile_6286.pdf

[43] R. J. Vijayan, S. Ch and R. Roy, "Dynamic modeling of microgrid for grid connected and intentional islanding operation," *2012 International Conference on Advances in Power Conversion and Energy Technologies (APCET)*, Mylavaram, Andhra Pradesh, 2012, pp. 1-6.

[44] L. N. Arruda, S. M. Silva and B. J. C. Filho, "PLL structures for utility connected systems," *Conference Record of the 2001 IEEE Industry Applications Conference. 36th IAS Annual Meeting (Cat. No.01CH37248)*, Chicago, IL, USA, 2001, pp. 2655-2660 vol.4.

[45] A. DehghanBanadaki, F. D. Mohammadi and A. Feliachi, "State space modeling of inverter based microgrids considering distributed secondary voltage control," *2017 North American Power Symposium (NAPS)*, Morgantown, WV, 2017, pp. 1-6.

[46] J. Sun and R. M. Bass, "Modeling and practical design issues for average current control," *APEC '99. Fourteenth Annual Applied Power Electronics Conference and Exposition. 1999 Conference Proceedings (Cat. No.99CH36285)*, Dallas, TX, USA, 1999, pp. 980-986 vol.2

[47] J. A. P. Lopes, C. L. Moreira and A. G. Madureira, "Defining control strategies for MicroGrids islanded operation," in *IEEE Transactions on Power Systems*, vol. 21, no. 2, pp. 916-924, May 2006.

[48] R.W. Erickson, *Fundamental of Power Electronics*. Norwell, 2nd ed. Norwell, Massachusetts: Kluwer Academic, 2001, pp-187-250.